JACS Au
AN OPEN ACCESS JOURNAL OF THE AMERICAN CHEMICAL SOCIETY

pubs.acs.org/jacsau
Perspective

Decarboxylation in Natural Products Biosynthesis

Nguyet A. Nguyen, Jacob H. Forstater, and John A. McIntosh*

Cite This: JACS Au 2024, 4, 2715−2745
Read Online

ACCESS | Metrics & More | Article Recommendations

ABSTRACT: Decarboxylation reactions are frequently found in the biosynthesis of primary and secondary metabolites. Decarboxylase enzymes responsible for these transformations operate via diverse mechanisms and act on a large variety of substrates, making them appealing in terms of biotechnological applications. This Perspective focuses on the occurrence of decarboxylation reactions in natural product biosynthesis and provides a perspective on their applications in biocatalysis for fine chemicals and pharmaceuticals.

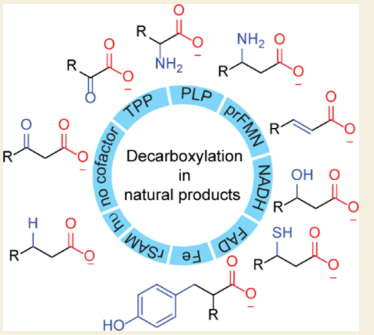

KEYWORDS: *decarboxylation, natural product, biosynthesis, thiamine pyrophosphate, pyridoxal 5′-phosphate, prenylated FMN, homolytic decarboxylation, oxidative decarboxylation, photodecarboxylase, cofactor-independent decarboxylase*

1. INTRODUCTION

Decarboxylation is a fundamental biochemical process involving the removal of a carboxylic acid, resulting in the release of carbon dioxide. It plays a critical role in various metabolic pathways, including the decarboxylation of α- and β-keto acids and amino acids; it is central to the biosynthesis of alkaloids, cholesterol, heme, and the catabolism of aromatic compounds.[1−4] While decarboxylation is thermodynamically favorable, the uncatalyzed reaction kinetics are slow, leading to the evolution of numerous enzymes that catalyze these reactions on diverse substrates. Given the ubiquity of decarboxylation reactions in primary metabolism, it is unsurprising that nature has repurposed many of these enzyme classes for the biosynthesis of natural products, which we review herein (Table 1).

Among the biosynthetic pathways described here, decarboxylases can be grouped into heterolytic and homolytic C-CO_2^- bond-breaking groups.[4] In heterolytic decarboxylation, a carbanion is formed at the α-carbon center where the C-CO_2^- bond is broken. Stabilization of the carbanion requires an electron sink, often in the form of a cofactor like thiamine pyrophosphate (TPP),[5] pyridoxal 5′-phosphate (PLP),[6] or functional groups on the substrate that can stabilize the carbanion through conjugation such as ketone, thial, or p-quinone methide. While most decarboxylases follow a heterolytic route, some enzymes break the C-CO_2^- bond homolytically, resulting in radical intermediates during decarboxylation.

Numerous reviews have been published to cover the diverse mechanisms of decarboxylation.[4,7] There are also reviews that focus on specific subsets of decarboxylases based on their cofactors, such as TPP-dependent decarboxylases,[8,9] PLP-dependent decarboxylases,[10,11] P450 fatty acid decarboxylases,[12] and prFMN-dependent decarboxylases.[13] Additionally, there are reviews that delve into the specific mechanisms of decarboxylation, including oxidative[14] and nonoxidative decarboxylation.[15]

This Perspective focuses on decarboxylases involved in the biosynthesis of secondary metabolites. These enzymes often exhibit relaxed substrate tolerance, making these enzymes promising functional starting points to evolve for activity on novel substrates. The biosynthesis of natural products provides a diverse set of substrates with chemical features that may be absent from primary metabolism, allowing for the study of novel and unexpected enzyme chemistry. In this Perspective, we explore decarboxylases based on their mechanism and cofactor, providing specific examples of each reaction type within the context of natural product biosynthesis. Our aim is to shed light on the interplay between decarboxylases and secondary metabolite biosynthesis and highlight the impact of decarboxylation on the pharmacological properties of bioactive natural products.

Received: May 13, 2024
Revised: July 1, 2024
Accepted: July 5, 2024
Published: July 25, 2024

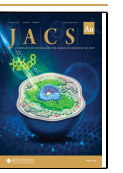

https://doi.org/10.1021/jacsau.4c00425
JACS Au 2024, 4, 2715−2745

Table 1. Summary of Types of Cofactor-Dependent and Independent Decarboxylases in Natural Product Biosynthesis

Cofactor	Substrate	Example enzyme	Example compound
TPP	α-keto acid	Phosphonopyruvate decarboxylase	Fosfomycin
PLP	α-amino acid	Ornithine decarboxylase	Loline
	β-amino acid	Aspartate aminotransferase	Incednine
prFMN	α, β-unsaturated acid	prFMN-dependent decarboxylase	9-Methylstreptimidone
NAD	UDP-glucuronic acid	UDP-glucuronic acid decarboxylase	Everninomicin
	β-hydroxy acid	Short-chain dehydrogenase/reductase	Micrococcin
FAD	β-hydroxyphenyl acid	Vanillyl alcohol phenyl oxidase/p-cresol methyl hydroxylase	Chondrochlorens
	β-sulfhydryl acid	Homo-oligomeric flavin-containing Cys decarboxylase	Epidermin
	7-carboxy-K252c	RebC	Rebeccamycin
rSAM	Peptide C-terminal acid	rSAM-SPASM	Mycofactocin
heme	Carboxythiazoline	P450 decarboxylase	Bottromycin A2
	Fatty acid	P450 peroxygenase	Olefin
mononuclear nonheme iron	Isocyanopropanic acid	Fe(II)/α-KG decarboxylase	Ambiguine
	3-((carboxymethyl)amino)butanoic acid	Fe(II)/α-KG decarboxylase	SF2768
multinuclear nonheme iron	Carboxy thiazoline	Nonheme diiron oxygenase/decarboxylase	Barbamide
	Fatty acid	Nonheme diiron oxygenase/decarboxylase	Olefins
	Peptide C-terminal Asp	Multinuclear nonheme iron-dependent oxidative enzyme	Aminopyruvatides
FAD, hν	Fatty acid	Fatty acid photodecarboxylase	Alkane
cofactor independent	Malonyl-ACP	Ketosynthase-like domain KS^{Q}	FD-891
	Methylmalonyl-CoA	Bifunctional acyltransferase/decarboxylase	Curacins
	Carboxylated β-branch-ACP	ECH2 domain	Bacillaene

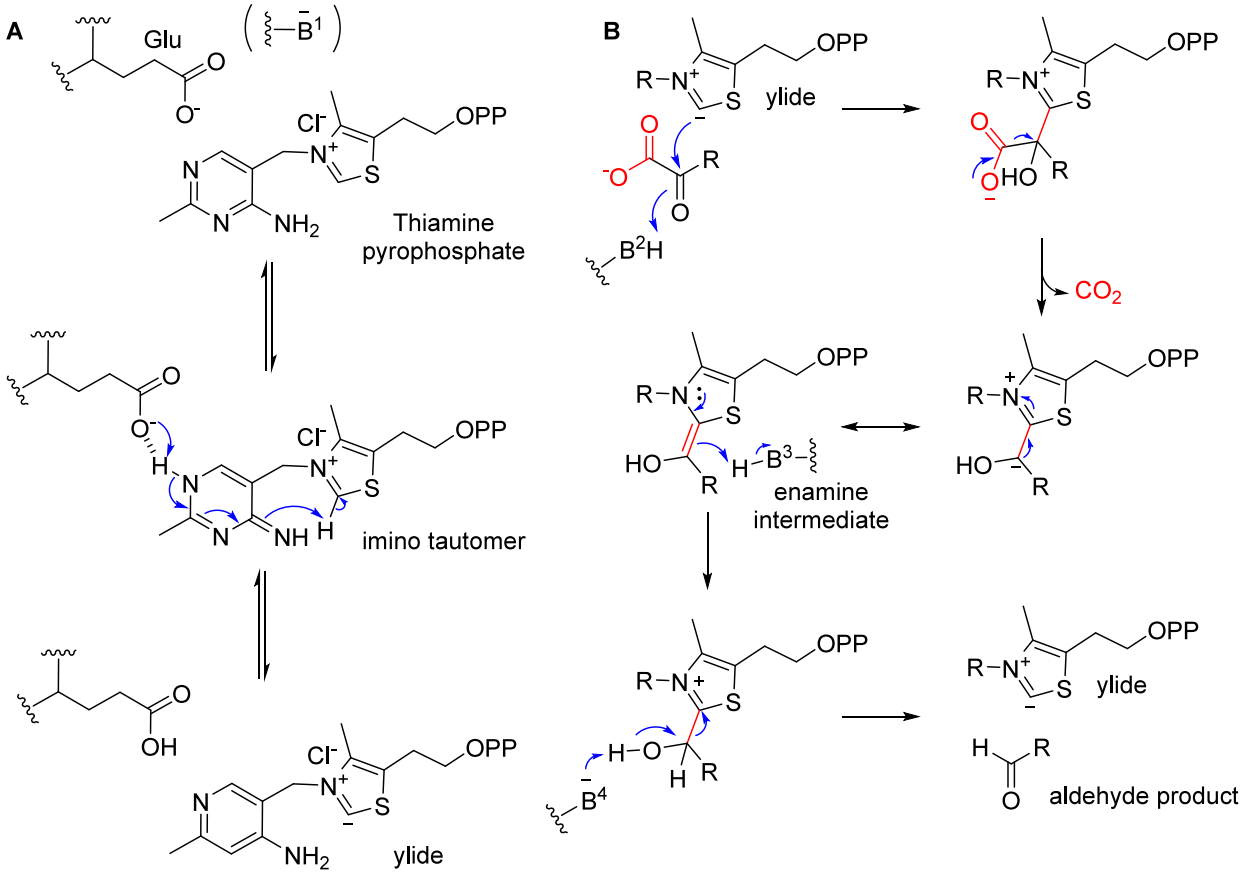

Figure 1. (A) Formation and stabilization of the ylide species. (B) General catalytic mechanism of TPP-dependent decarboxylases. Due to significant variations in domain organization among various TPP-dependent decarboxylase superfamilies, the specific placement of the catalytic Glu residue is not illustrated, and general bases are utilized in the mechanism. For a more extensive understanding of the structural and catalytic features of TPP-dependent decarboxylases, we suggest referring to comprehensive review articles.[5,8]

https://doi.org/10.1021/jacsau.4c00425
JACS Au 2024, 4, 2715−2745

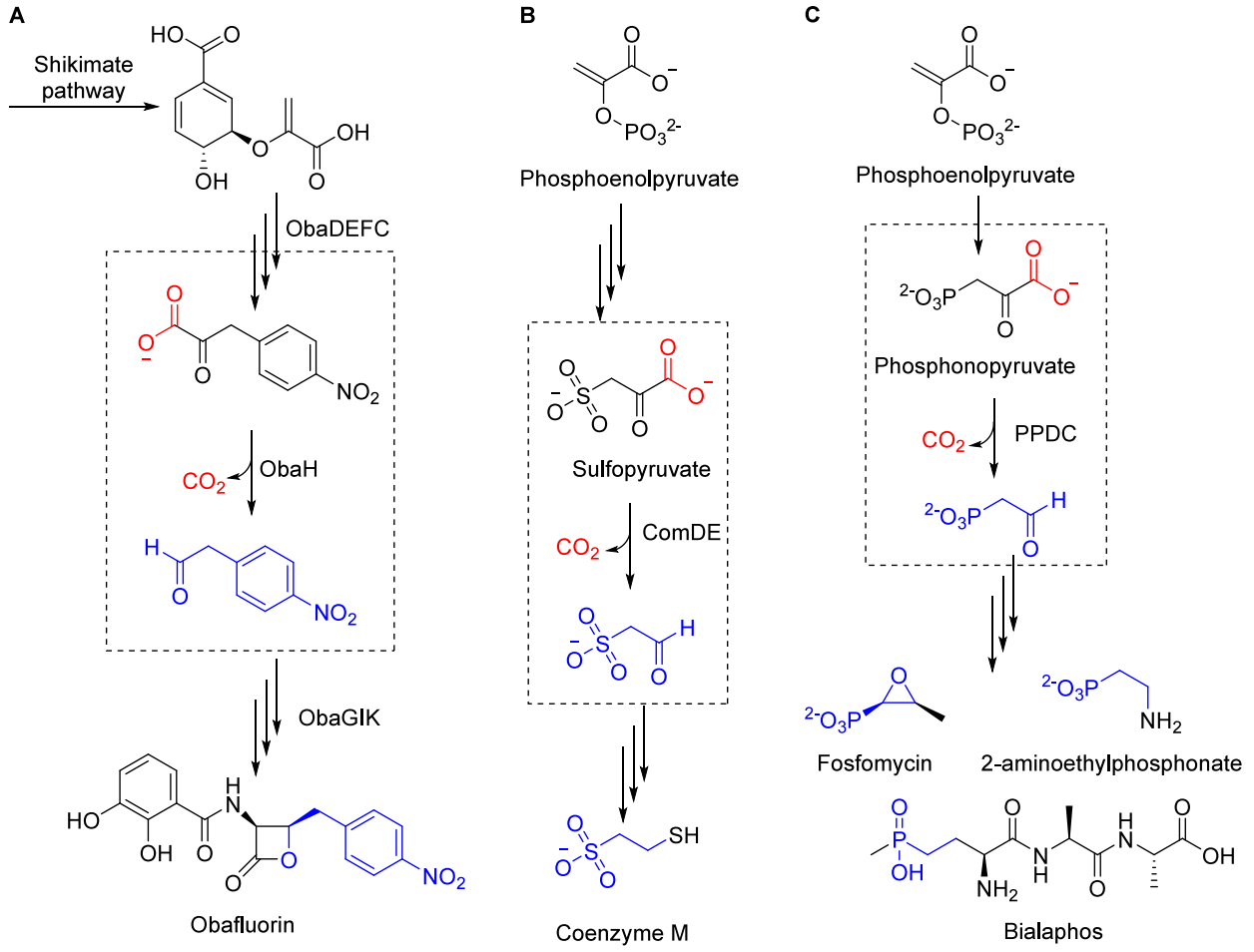

Figure 2. Biosynthetic pathway of (A) obafluorin, (B) coenzyme M, and (C) bialaphos with the decarboxylation step catalyzed by TPP-dependent enzymes highlighted.

2. TPP-DEPENDENT DECARBOXYLASES

TPP-dependent decarboxylases are enzymes within the broader group of TPP-dependent enzymes. These enzymes play a critical role in catalyzing a wide range of reactions, including the creation and breakdown of bonds adjacent to a carbonyl group. TPP-dependent decarboxylases are found in three specific superfamilies: pyruvate decarboxylase-like enzymes, sulfopyruvate decarboxylases, and phosphonopyruvate decarboxylases.[9] Despite the difference in domain organization in these decarboxylases, a shared mechanism is observed, beginning with the formation of a ylide or C2-carbanion-TPP intermediate. This process involves the proton abstraction of the imino tautomer form of TPP by a conserved glutamic acid residue located at the active site (Figure 1A).[8] The ylide acts as a nucleophile, adding to the α-carbonyl of an α-keto acid substrate. Decarboxylation occurs, yielding a carbanion intermediate, which undergoes a rearrangement to form an enamine intermediate with the negative charge delocalized into the thiazolium nitrogen of TPP. Finally, the enamine is protonated, leading to the release of the product as an aldehyde (Figure 1B).

2.1. Pyruvate Decarboxylase-like Enzymes in the Biosynthesis of Obafluorin

The pyruvate decarboxylase-like enzyme (EC 4.1.1.1) superfamily encompasses multiple subfamilies with diverse catalytic mechanisms, including decarboxylation, carboligation, and oxidation. Examples of decarboxylases within this superfamily include pyruvate, indolepyruvate, phenylpyruvate, branched chain 2-keto acid, and benzoylformate decarboxylases. These enzymes are involved in the decarboxylation of various α-keto acid substrates found in primary metabolic pathways such as yeast fermentation,[16] amino acid metabolism,[17] and the mandelate pathway.[18] TPP-dependent decarboxylases are also involved in the production of secondary metabolites; for example, the biosynthesis of the β-lactone antibiotic obafluorin in *Pseudomonas fluorescens* employs the TPP-dependent decarboxylase, ObaH, to generate the key intermediate 4-nitrophenyl acetaldehyde (Figure 2A).[19]

Extensive studies have been conducted on enzymes within the superfamily of pyruvate decarboxylase-like enzymes, particularly those involved in primary metabolism, to better understand and alter substrate specificity. However, attempts to modify substrate specificity through rational design approaches, such as residue swapping, have yielded limited success.[5,8] Further research is needed to uncover the mechanisms that determine how TPP-dependent decarboxylases recognize and interact with their substrates.

2.2. Sulfopyruvate Decarboxylase in Coenzyme M Biosynthesis

Sulfopyruvate decarboxylase (SPDC) (EC 4.1.1.79) is part of the biosynthetic pathway for mercaptoethane sulfonate (or coenzyme M), an essential coenzyme involved in methane formation in methanoarchaea[20,21] and the metabolism of

https://doi.org/10.1021/jacsau.4c00425
JACS Au 2024, 4, 2715−2745

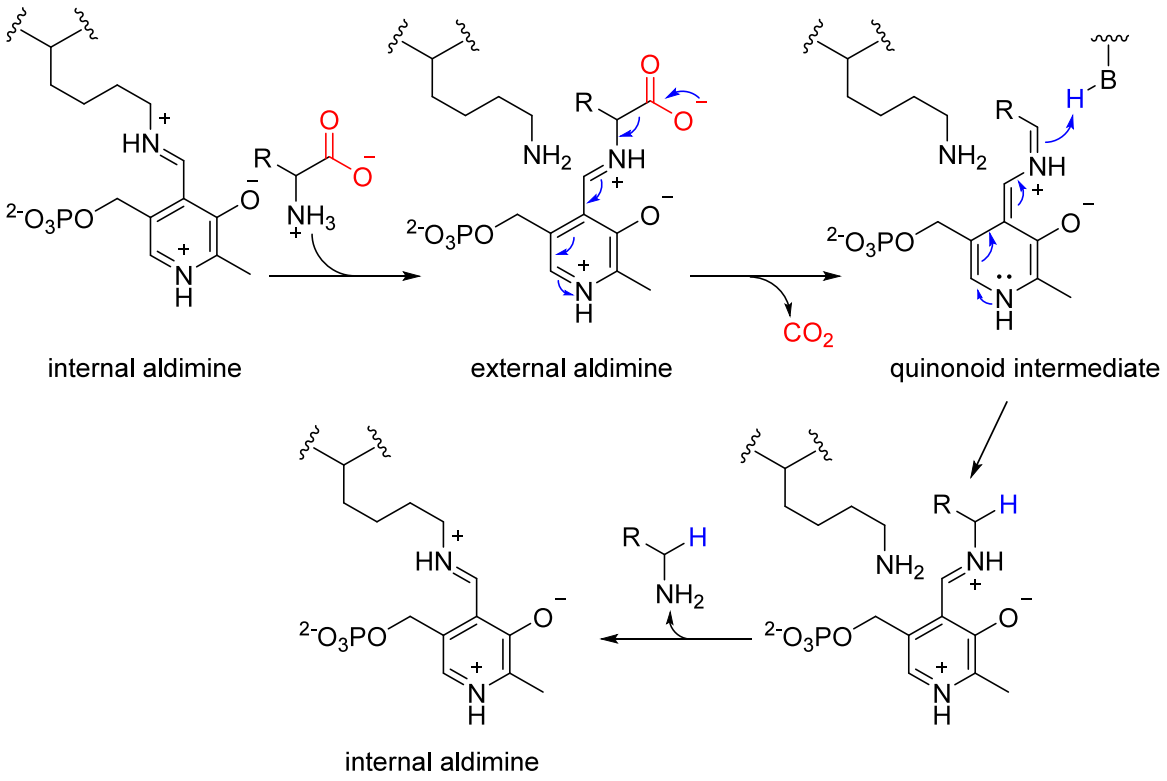

Figure 3. Mechanism of α-decarboxylation by PLP-dependent decarboxylases. Note that the specific active site residue involved in protonating the quinonoid intermediate may differ between enzymes and is therefore represented generically.[6,29]

Table 2. Classification of PLP-Dependent Decarboxylases (DC) (EC 4.1.1) Based on Structure, Sequence, and Function

	Structure			
	Fold Type I			Fold Type III
Sequence	DC Group I	DC Group II	DC Group III	DC Group IV
Enzymes	Glycine dehydrogenase/ decarboxylase	Glu, His, Tyr, aromatic DC	Bacterial Orn, Lys, Arg DC	Eukaryotic Orn, Lys, Arg diaminopimelate DC, RiPP DC, NRPS DC

aliphatic alkenes in *Syntrophoarchaeum* species.[22] SPDC, found in the methanogenic pathway, catalyzes the decarboxylation of 3-sulfopyruvate to produce 2-sulfoacetaldehyde. The pyrophosphate binding domain and the pyrimidine binding domain of most SPDC enzymes are encoded by separate genes, *comD* and *comE*. ComDE has a limited substrate scope and cannot utilize phosphonopyruvate or pyruvate as substrates (Figure 2B).[21]

2.3. Phosphonopyruvate Decarboxylase in the Biosynthesis of Phosphorus-Containing NPs

Phosphonopyruvate decarboxylase (PPDC) (EC 4.1.1.82) catalyzes the transformation of 3-phosphonopyruvate to 2-phosphonoacetaldehyde, a precursor for several phosphorus-containing natural products (Figure 2C).[23] The decarboxylation step is essential to the formation of carbon-phosphorus (C-P) bonds and acts as a driving force to shift the equilibrium between phosphoenolpyruvate and 3-phosphonopyruvate.[24] PPDC is involved in the biosynthesis of notable phosphorus-containing natural products, including the herbicide bialaphos,[25] the antibiotic fosfomycin (BGC0000938),[26] and the 2-aminoethylphosphonate unit of polysaccharide B, a component of the capsular polysaccharide complex of *Bacteroides fragilis*.[23] In contrast to SPDC, PPDC can accept both sulfopyruvate and pyruvate as substrates but exhibits a significantly higher turnover rate with phosphonopyruvate, suggesting the phosphono group of phosphonopyruvate serves as the binding site.[23]

3. PLP-DEPENDENT DECARBOXYLASES

PLP-dependent decarboxylases are part of the larger family of pyridoxal 5′-phosphate (PLP) dependent enzymes, which catalyze diverse reactions such as decarboxylation, racemization, transamination, and condensation of amine and amino acid substrates.[27] While most reactions involve α-decarboxylation, examples of β-decarboxylation have been documented, including the notable example of IdnL3 in the incednine biosynthetic pathway,[28] discussed below.

The chemical mechanism of α-decarboxylation catalyzed by PLP-dependent enzymes is well established (Figure 3).[10] Initially, PLP forms an internal aldimine by the formation of a Schiff-base with the α-amino group of a catalytic lysine residue within the protein. The lysine residue is subsequently replaced by the substrate amino group, forming an "external aldamine" Schiff-base intermediate, followed by decarboxylation. PLP functions as an electron sink, stabilizing the carbanions generated during decarboxylation by directing the negative charge into the π bonds system, resulting in the formation of a quinonoid intermediate. Protonation at the Cα position is facilitated by a general acid, leading to the formation of an imine product. Transaldimination with the catalytic lysine residue follows, releasing the corresponding amine product and regenerating the internal aldimine.

https://doi.org/10.1021/jacsau.4c00425
JACS Au 2024, 4, 2715−2745

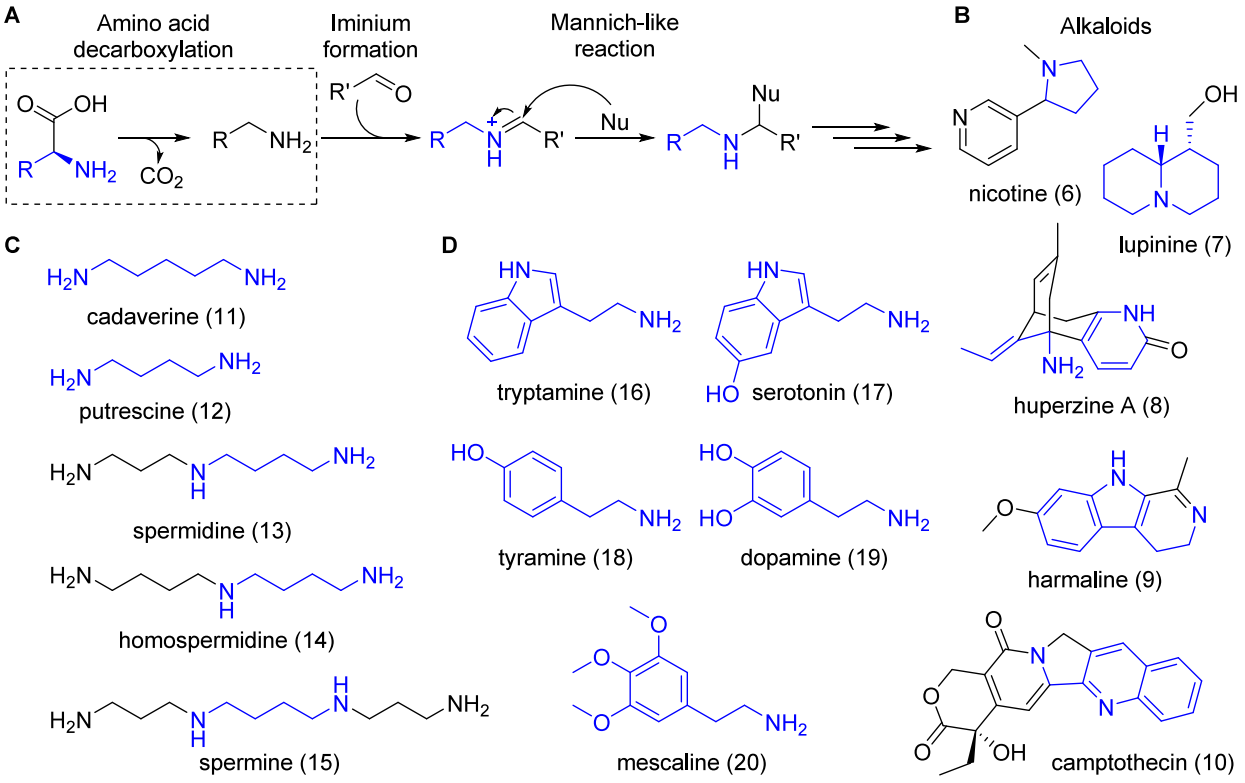

Figure 4. (A) Biosynthesis of alkaloids. (B) Structures of some alkaloids. Structures of (C) aliphatic amines and (D) aromatic amines.

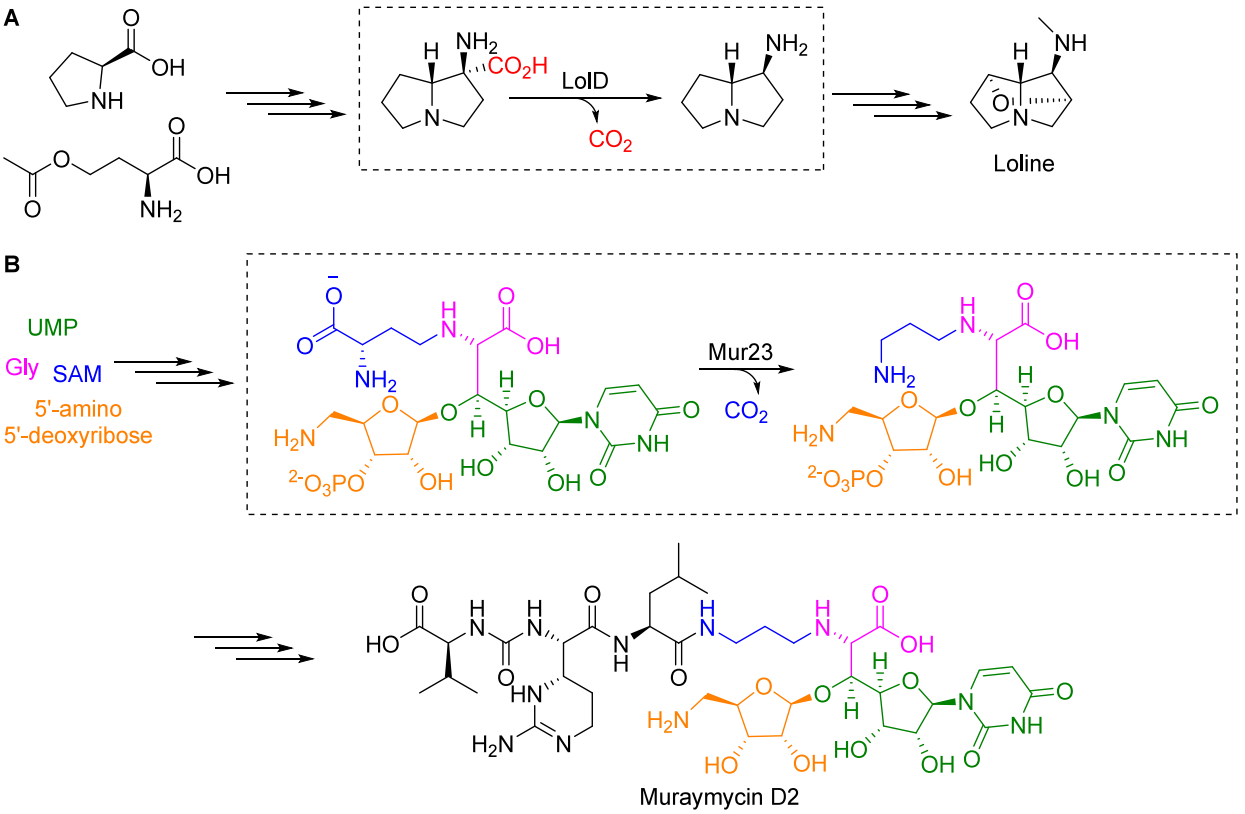

Figure 5. (A) Loline and (B) muraymycin D2 biosynthetic pathways.

Based on structural and sequence alignment, PLP-dependent enzymes are classified into 7-fold types.[10] Structurally, PLP-dependent decarboxylases are classified as either fold type I or III. These fold types differ in the organization of their protein domains, the catalytic lysine residue, the PLP-interacting glycine-rich loop, and their oligomer form. Based on sequence

https://doi.org/10.1021/jacsau.4c00425
JACS Au 2024, 4, 2715−2745

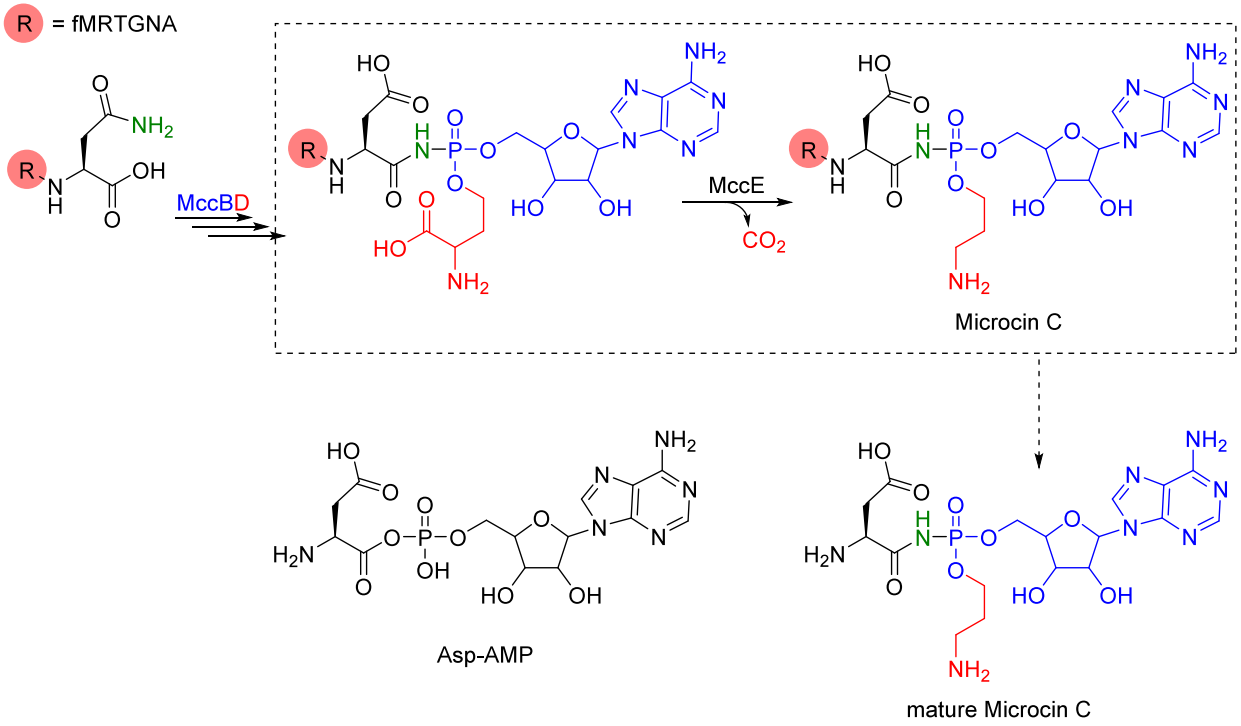

Figure 6. Microcin C maturation pathway and the formation of the bioactive processed Microcin C and the structure of Asp-AMP, the native substrate of the aspartyl-tRNA synthetase.

alignment, PLP-dependent decarboxylases are classified into four groups (Table 2).

PLP-dependent decarboxylases participate in the biosynthesis of secondary metabolites, including alkaloids and some simple amines, a ribosomally synthesized and post-translationally modified peptide (RiPP), and several nonribosomal peptides (NRPs), which we discuss in more detail in the following sections.

3.1. α-Decarboxylation by PLP-Dependent Enzymes

3.1.1. Alkaloids. Alkaloids are a diverse category of nitrogen-containing secondary metabolites for which decarboxylation is the initial biosynthetic step. PLP-dependent decarboxylases convert amino acids to amines that later condense with an aldehyde to form an iminium intermediate that undergoes a Mannich-like reaction to achieve diverse and complex alkaloid scaffolds (Figure 4A,B).[30] Major alkaloid subtypes, including nicotine, tropane, lycopodium, and quinolizidine, are distinguished based on their structural scaffolds. Despite the observed structural diversity, the alkaloid amines originate from two primary sources both involving decarboxylation: (1) aliphatic polyamines, such as cadaverine, putrescine, and putrescine derivatives, are derived from Orn/Arg/Lys metabolism (Figure 4C) and (2) aromatic amines, such as tryptamine, dopamine, and tyramine, originate from Trp/Tyr metabolism (Figure 4D).

In addition to their well-known involvement in the early stage of alkaloid biosynthesis for accumulating amine precursors, PLP decarboxylases also play a significant role in the later stages of biosynthetic pathways. This is exemplified by loline (Figure 5A), a broad-spectrum anti-insect alkaloid commonly found in endophytic fungi. The loline biosynthetic gene cluster (BGC0000815) comprises 11 genes, including LolD, a PLP-dependent decarboxylase.[31] Recent experimental verification by Gao et al. demonstrated that LolD can decarboxylate pyrrolizidine α-quaternary amino acid.[32] In a subsequent study, Liu et al. demonstrated the substrate versatility of LolD, enabling rapid generation of diverse enantiopure amino-izidine motifs.[33]

It is worth noting that LolD is not the only type III PLP-dependent decarboxylase that can process substrates other than common amino acids. For example, the enzyme Mur23, found in the muraymycin biosynthetic pathway, can decarboxylate nucleoside-containing substrates (Figure 5B).[34,35] Additionally, type III PLP-dependent decarboxylases can also process larger substrates such as peptides and amino acids tethered to carrier proteins in RiPP and NRP biosynthesis, respectively. These findings highlight the versatility and potential of type III PLP-dependent decarboxylases as promising biocatalysts in various biosynthetic pathways and suggests that much remains to be discovered in the substrate range of this enzyme class.

3.1.2. Ribosomally Synthesized and Post-translationally Modified Peptides. Among RiPPs, an example of PLP-dependent decarboxylation can be found in microcin C biosynthesis. Microcin C is an antibiotic found in *E. coli* and closely related bacteria. Inside the targeted bacterial cells, microcin C is enzymatically processed to form the mature microcin C that structurally resembles Asp-AMP (Figure 6). The mechanism by which mature microcin C exerts its action is through strong inhibition of aspartyl-tRNA synthetase, thereby interfering with translation.[36] Microcin C biosynthesis starts with the ribosomal synthesis of the N-formylated precursor heptapeptide (MccA) fMRTGNAN, followed by modification by the adenylyltransferase MccB, which catalyzes the ATP-dependent isomerization of the C-terminal asparagine to a succinimide followed by N-phosphorylation and ring-opening to afford a P-linked carboxamide.[37,38] Subsequently, the S-adenosyl methionine (SAM) dependent enzyme MccD transfers the 3-amino-3-carboxypropyl (ACP) group from the SAM to the phosphoamidate group of the adenylated MccA. Decarbox-

https://doi.org/10.1021/jacsau.4c00425
JACS Au 2024, 4, 2715−2745

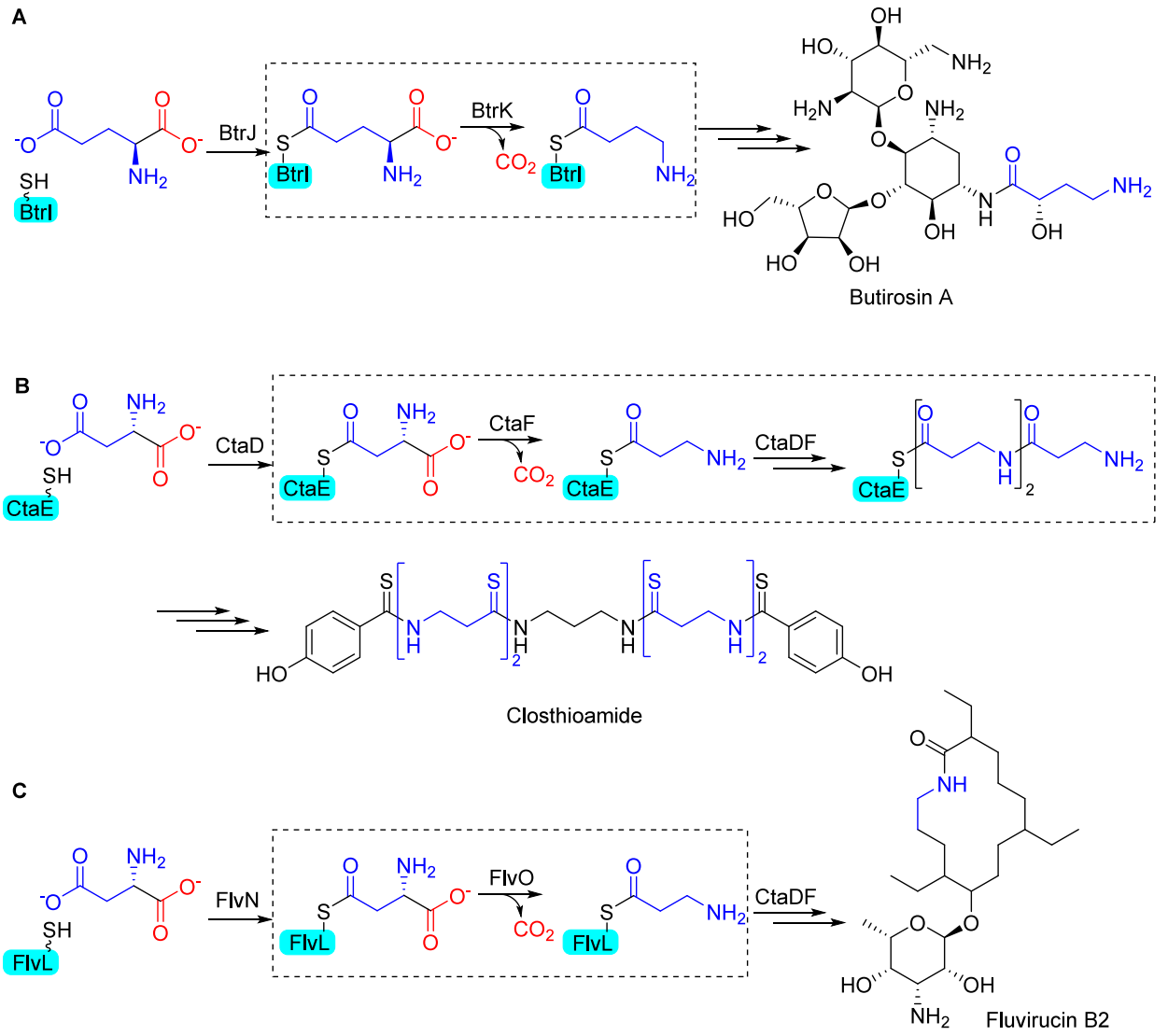

Figure 7. Biosynthetic pathway of (A) butirosin A, (B) closthioamide, and (C) fluvirucin B2.

ylation of the resulting 3-amino-3-carboxypropylated MccA is catalyzed by the N-terminal domain of the MccE enzyme ($MccE^{NTD}$), a PLP-dependent decarboxylase, leading to the generation of mature microcin C.[39]

MccE is a two-domain protein; the N-terminal domain ($MccE^{NTD}$) is homologous to PLP-dependent decarboxylases group IV, while the C-terminal domain ($MccE^{CTD}$) catalyzes the inactivation of microcin C via acetylation.[40,41] The 3-amino-propyl moiety introduced by ACP-transferase MccD and MccE has been found to increase the affinity of processed McC for AspRS.[42] Studies have demonstrated that MccE/MccD can modify a variety of adenylated peptides with different amino acid sequences and lengths, originating from *mcc* operons of various bacteria, including *E. coli*, *Lactobacillus johnsonii* (MccA peptide MHRIMKN), *Helicobacter pylori* (MccA peptide MKLSYRN), and a 20 amino acid C-terminal fragment of *Synechococcussp. CC9605* (MccA peptide LQPKRLDKVAKNQLWADMMN).[39,43]

3.1.3. Polyketides/Nonribosomal Peptides. PLP-dependent decarboxylases have a substrate scope that includes amino acids tethered to an acyl carrier protein (ACP), as they participate in the early biosynthetic step of several polyketides and nonribosomal peptides, including butirosins (BGC0000694), fluvirucins, and closthioamide (BGC0001891) (Figure 7).[44−46] Glutamate or aspartate, initially activated by adenylation (BtrJ, CtaD, FlvN), are ligated to an ACP via their side chain carboxyl group, forming aminoacyl-ACP (BtrI, CtaE, FlvL). The α-carboxyl group of the aminoacyl-ACP is then decarboxylated by a PLP-dependent decarboxylase (BtrK, CtaF, FlvO) to produce a γ-aminobutyrate or β-alanine.[47] In the case of butirosin, γ-aminobutyrate is further modified to the 4-amino-2-hydroxybutyryl moiety in the final aminoglycoside product. The introduction of the 4-amino-2-hydroxybutyryl moiety enhances several pharmacological properties and prevents modifications such as O-phosphorylation, O-nucleotidylylation, and N-acetylation that can deactivate the aminoglycoside antibiotic activities (Figure 7A).[48,49] In the biosynthesis of closthioamide, the decarboxylases CtaF not only decarboxylate Asp-S-CtaE but also act on the extending polypeptide-ACP substrate, where two additional Asp resides are loaded by CtaD and decarboxylated in the same manner (Figure 7B).[44−46,50−52] In polyketide-derived macrolactams like fluvirucin, β-alanine is part of the core macrolide structure (Figure 7C).[50]

https://doi.org/10.1021/jacsau.4c00425
JACS Au 2024, 4, 2715−2745

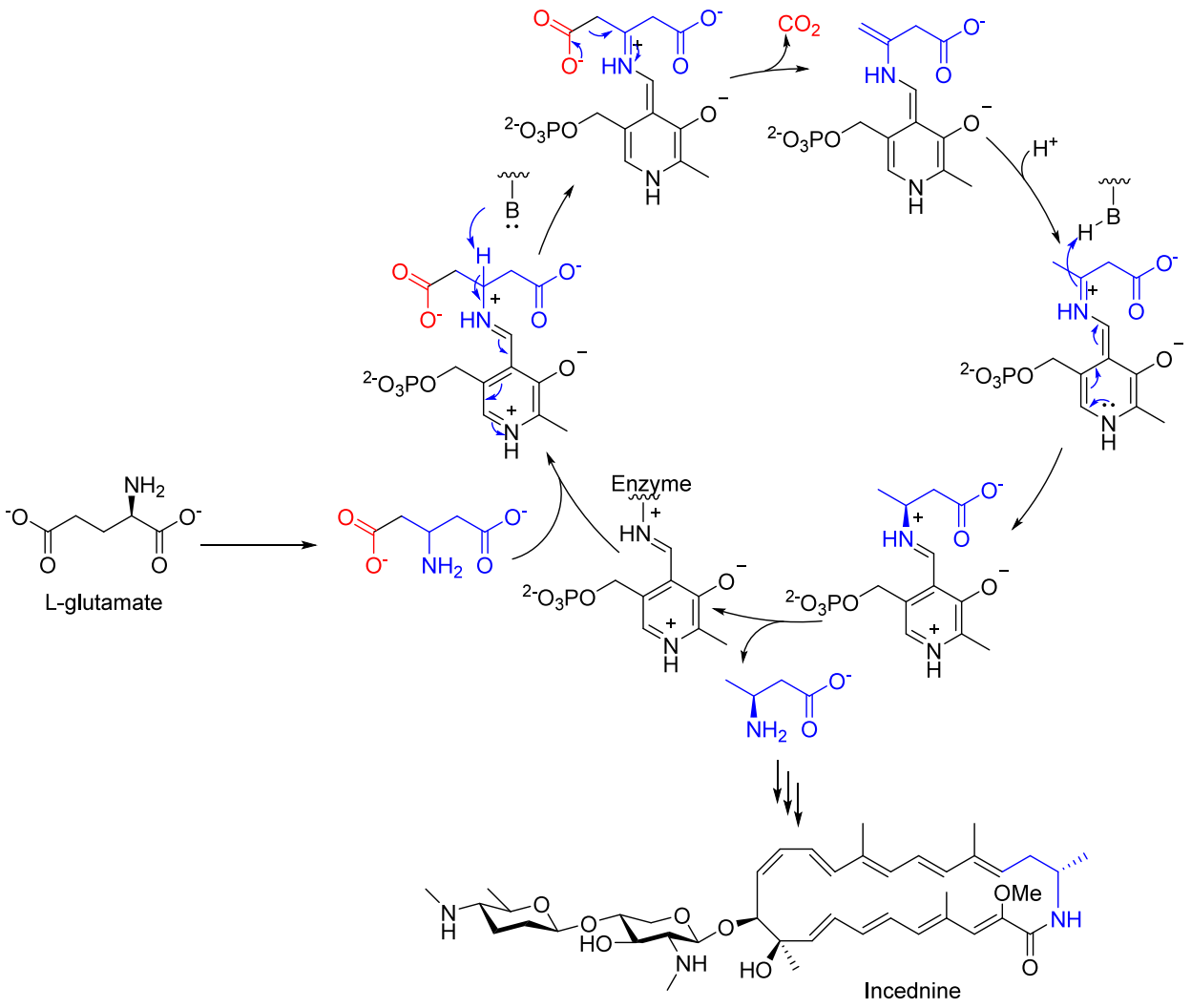

Figure 8. Mechanism of β-decarboxylation of β-glutamate by the PLP-dependent enzyme IdnL3.

3.2. β-Decarboxylation by a PLP-Dependent Enzyme in Incednine Biosynthesis

The biosynthesis of incednine (BGC0000078), a macrolactam antibiotic from *Streptomyces* sp., involves β-decarboxylation catalyzed by IndL3 (Figure 8). IdnL3 catalyzes the key conversion of β-glutamate (which is formed from L-glutamate by the 2,3-aminomutase IdnL4) to (S)-3-aminobutyrate, the starting unit of polyketide synthase (PKS) assembly in the incednine biosynthetic pathway. Homologues of IdnL3 have also been identified in the BGC of several 3-aminobutyric acid-containing macrolactam polyketides including sipanmycin, salinilactam, micromono-lactam, and lobosamide A.[53,54] The substrate specificity of IdnL3 has been thoroughly examined, revealing that it selectively recognizes β-glutamate as its substrate.[28] The substrate recognition mechanism for IdnL3 remains unclear due to the absence of a crystal structure.

4. PRENYLATED FMN-DEPENDENT (DE)CARBOXYLASES

Prenylated flavin (prFMN)-dependent decarboxylases (also known as UbiD homologues; EC 4.1.1.98) rely on a modified flavin cofactor (Figure 9A) that enables challenging decarboxylations and carboxylations of a wide-range of aromatic and unsaturated acids (Figure 9B, C). Biosynthesis of prFMN is catalyzed by UbiX-like enzymes (EC 2.5.1.129) that perform alkylation and cyclization of reduced $FMNH_2$ to yield a reduced prFMN, forming a fourth nonaromatic ring between the N-5 and C-6 positions of the tricyclic heterocyclic isoalloxazine ring (Figure 9A).[55] To enable catalytic turnover, the reduced prFMN requires oxidative maturation to form the active $prFMN^{iminium}$ species which is believed to occur within the UbiD active site. The sensitivity of certain UbiD enzymes to light and/or oxygen, such as Fdc (light sensitive), AroY (oxygen sensitive) and HmfF (both light and oxygen sensitive), has been assigned to the oxidative maturation and light-induced isomerization of the active $prFMN^{iminium}$ species, although the underlying mechanism is not fully understood. Bridging this knowledge gap would facilitate the engineering of prFMN-dependent decarboxylases for broader industrial applications. The $prFMN^{iminium}$ facilitates decarboxylation through either a 1,3-dipolar cycloaddition or an electrophilic aromatic substitution mechanism at the C4a-N5-C1' positions. While genes encoding for UbiD and UbiX enzymes are often found in the same BGC, there are instances where UbiD enzymes can be supported by another UbiX-like enzyme encoded elsewhere in the host genome, such as in the case of naphthalene carboxylase found in sulfate-reducing culture N47.[56]

The UbiD/UbiX system is widely present in microbe genomes, spanning archaea, bacteria, and fungi. It plays a crucial

https://doi.org/10.1021/jacsau.4c00425
JACS Au 2024, 4, 2715−2745

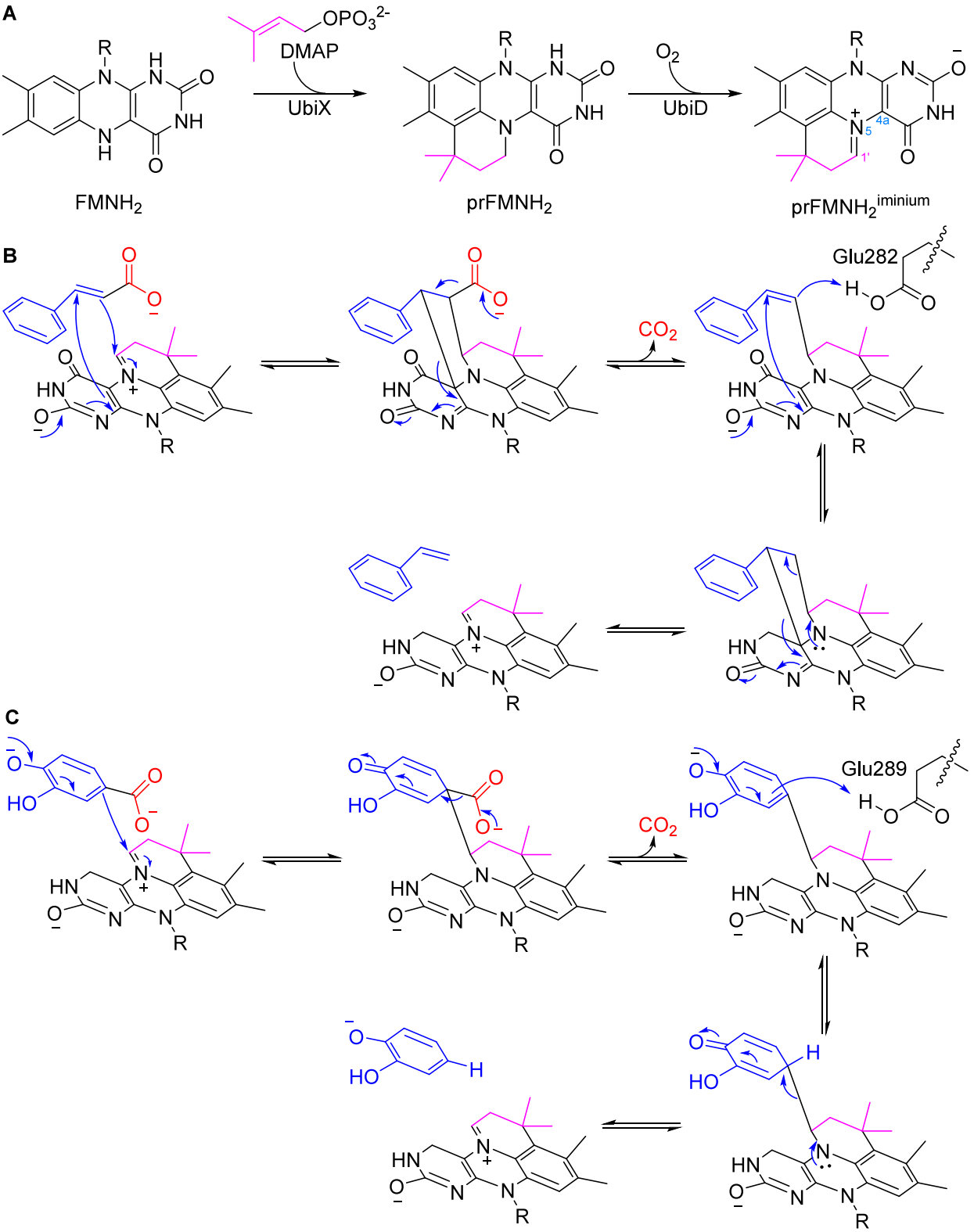

Figure 9. (A) Biosynthesis of prFMN. (B) Proposed 1,3-dipolar cycloaddition mechanism for the decarboxylation of cinnamic acid by *Aspergillus niger* Fdc (PDB ID: 4ZAB).[57] (C) Proposed electrophilic aromatic substitution mechanism for the decarboxylation of protocatechuic acid by *Enterobacter cloacae* P240 AroY(PDB ID: 5O3N).[58] In both Fdc and AroY, the catalytic Glu residue is part of an ionic network involving Glu-Arg-Glu. This network is critical for the activity of UbiD, and mutations at these residues result in the loss of activity. The current state of mechanistic studies of prFMN-dependent decarboxylases is recently reviewed.[59]

role in various metabolic pathways, contributing to the biosynthesis of primary metabolites like ubiquinone and secondary metabolites such as tautomycetin (BGC0000157) and 9-methylstreptimidone (BGC0000171).[60−62] These enzymes are also involved in the degradation of diverse (poly)aromatic hydrocarbons such as benzene, naphthalene,

https://doi.org/10.1021/jacsau.4c00425
JACS Au 2024, 4, 2715−2745

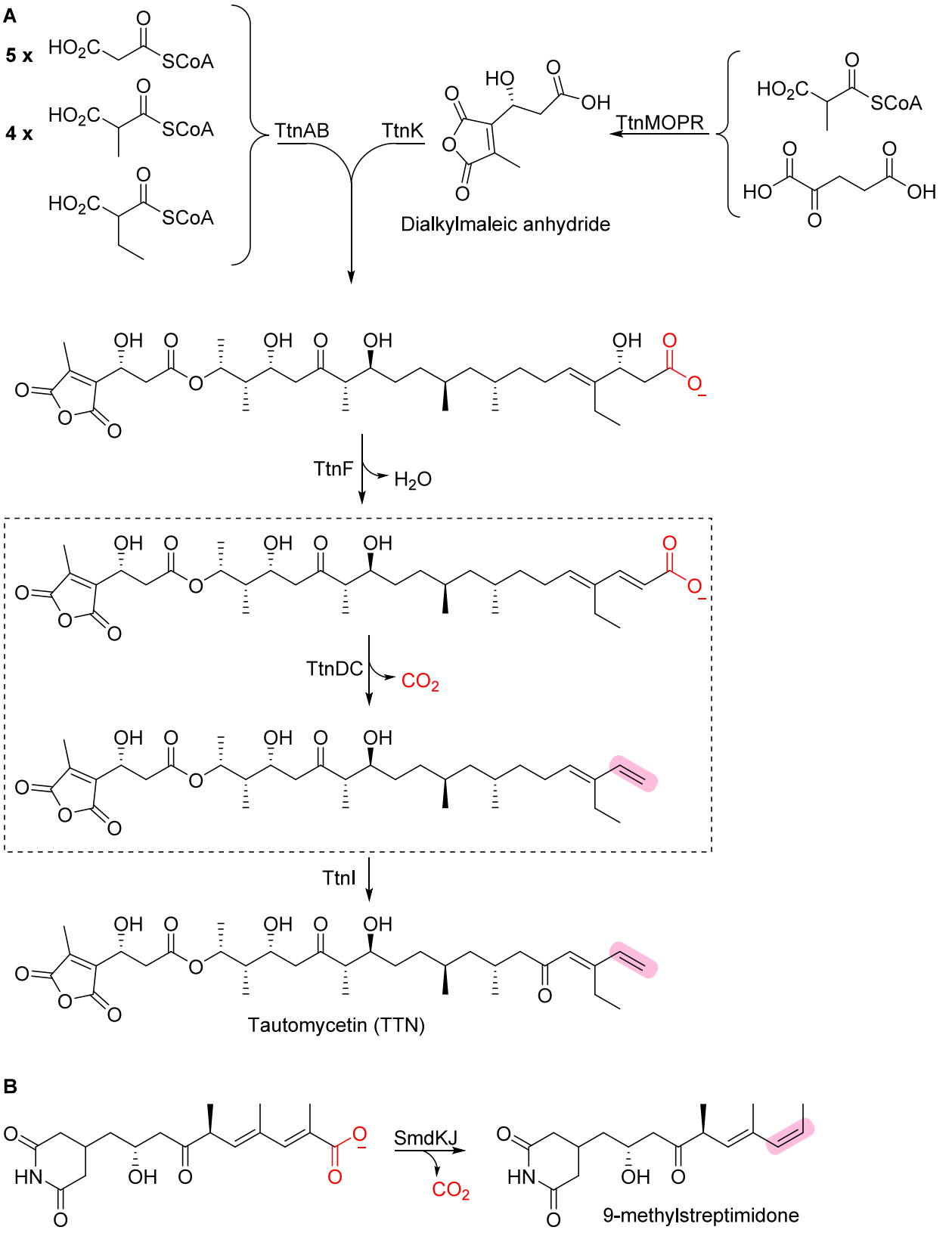

Figure 10. Biosynthetic pathway of (A) tautomycetin and (B) 9-methylstreptimidone.

and phthalate.[63] Recent phylogenetic research has classified UbiD-like enzymes into three subgroups based on their native substrate preference: aromatic acids (UbiD or AroY), phenylacrylic acid (Fdc1), and α,β-unsaturated aliphatic acids (TtnD, SmdK).[60] The proposed decarboxylation mechanism for acrylic acid substrates and other α,β-unsaturated acids is the 1,3-dipolar cycloaddition mechanism shown in Figure 9B. In contrast, the electrophilic aromatic substitution mechanism is suggested for the decarboxylation of aryl acids (Figure 9C).

https://doi.org/10.1021/jacsau.4c00425
JACS Au 2024, 4, 2715−2745

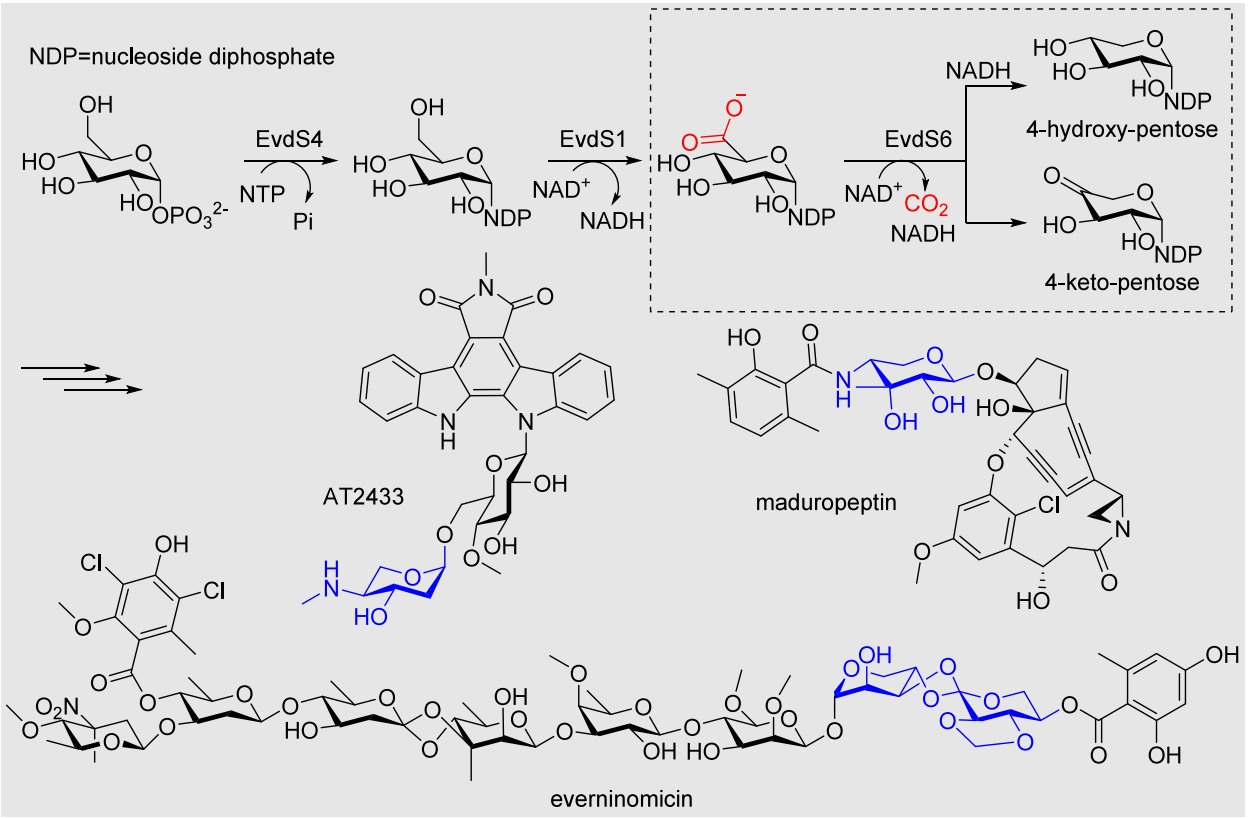

Figure 11. Proposed biosynthetic pathway for pyranose deoxypentose precursors of deoxygenated carbohydrate natural products: everninomicin and AT2433.

4.1. prFMN Decarboxylase in the Biosynthesis of Tautomycetin

Tautomycetin (TTN), derived from *Streptomyces griseochromogenes*, is a polyketide compound with a terminal alkene that exhibits antifungal activity by selectively inhibiting PP1, one of seven families of protein serine/threonine phosphatases.[64] TTN's high selectivity for PP1 inhibition makes it particularly intriguing for studying the function and substrates of PP1 without interfering with other essential cellular phosphorylation processes.[65] Structural analysis of the PP1:TTN complex has revealed that the diene/alkene moiety of TTN plays a crucial role in accessing and interacting with the hydrophobic groove of the PP1 active site. The diene facilitates the formation of a covalent bond with the Cys127 of PP1, as demonstrated through crystallography, mass spectrometry, and mutation studies.[65] In the biosynthetic pathway of TTN, the UbiD/UbiX class TtnDC system catalyzes a key decarboxylation in the penultimate step, leading to the formation of the critical terminal alkene moiety (Figure 10A).[60,66]

The polyketide backbone of TTN is constructed from five molecules of malonyl-CoA, four molecules of methylmalonyl-CoA, and one molecule of ethylmalonyl-CoA through the action of the type I polyketide synthases TtnAB. Subsequently, a dialkylmaleic anhydride moiety synthesized from α-ketoglutarate and propionate by TtnMOPR is incorporated into the polyketide backbone with the assistance of TtnK, resulting in a TTN F-1 intermediate. TtnF facilitates the dehydration of TTN F-1, leading to the generation of an α,β-unsaturated acid. This acid then undergoes decarboxylation, catalyzed by the TtnDC system.[60] The final oxidation step, which completes the biosynthesis of mature TTN, is catalyzed by TtnI. TtnD encodes a prFMN-dependent decarboxylase, while TtnC encodes for the prenyltransferase. The activity of TtnD has been thoroughly characterized biochemically and structurally.[60] TtnD exhibits substrate promiscuity, accepting a broad range of biosynthetic intermediates from TTN pathways, with the notable exception of TTN F-1, which lacks the double bond at the C$\alpha\beta$-position of the acid substrate.[60]

4.2. prFMN Decarboxylase in the Biosynthesis of 9-Methylstreptimidone

Another polyketide that has been characterized with a terminal alkene is 9-methylstreptimidone with a UbiD/UbiX pair encoded by the *smdKJ* genes (Figure 10B).[61,67] The activity of SmdK, a UbiD decarboxylase, was characterized by knockout experiments leading to the accumulation of the carboxylated congener of 9-methylstreptimidone, suggesting that decarboxylation to afford the terminal alkene is the final step in biosynthesis.[61] 9-methylstreptimidone has demonstrated antifungal,[68] antiviral activity,[67] and induces apoptosis selectively in adult T-cell leukemia cells.[69] SAR studies have attributed its activity against leukemia T-cells to the hydrophobic terminal alkene moiety, underlining the importance of decarboxylation in the bioactivity of this natural product.[69]

5. OXIDATION DECARBOXYLATION

The decarboxylation of otherwise unreactive molecules can be achieved by introducing electron sinks β to the carboxylate, such as ketone, thial, or *p*-quinone methide, which stabilize the carbanion-formed upon decarboxylation by conjugation.[70,71] In Nature, enzymes frequently couple oxidation and decarboxylation reactions to decarboxylate β-hydroxy, thiol, or phenol acid substrates, and it is often unclear whether the decarbox-

https://doi.org/10.1021/jacsau.4c00425
JACS Au 2024, 4, 2715−2745

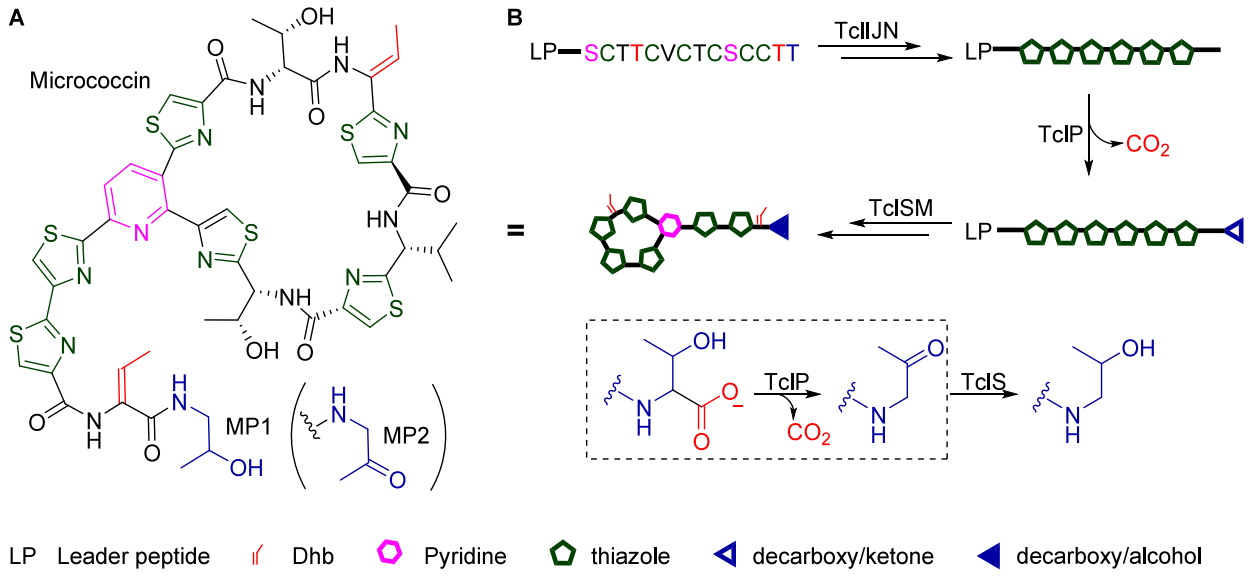

Figure 12. (A) Structure of micrococcin. (B) Biosynthetic pathway of micrococcin and the modification of the C-terminal threonine by TclP and TclS.

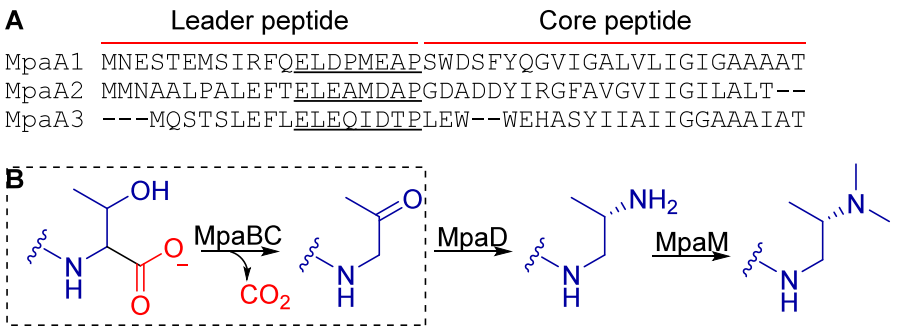

Figure 13. (A) Sequence alignment of different daptide substrate peptides. The region in the leader peptide that serves as a recognition sequence is underlined. (B) Biosynthetic pathway of the (*S*)-N_2,N_2-dimethyl-1,2-propanediamine moiety.

ylation step itself is spontaneous or enzyme accelerated. The oxidation step in this process can occur through different mechanisms, utilizing a wide range of cofactors. NAD^+ is used as a cofactor by short-chain dehydrogenase/reductases (SDR), such as the glucuronic acid decarboxylases or the micrococcin decarboxylase.[72−76] A RiPP DC, recently described as belonging to the alcohol dehydrogenase family, is proposed to use $NADP^+$.[77] Flavins, including flavin adenine dinucleotide (FAD) and flavin mononucleotide (FMN), are also used in the homo-oligomeric flavin-containing Cys decarboxylases (HFCD) family in RiPP and NRP natural products.[78,79]

5.1. NAD(P)$^+$-Dependent Decarboxylases

5.1.1. Glucuronic Acid Decarboxylases in the Biosynthesis of Pyranose Deoxypentose-Containing NPs. Deoxygenated carbohydrate moieties, prevalent in antibiotics, antimicrobials, and therapeutic agents, play a crucial role in imparting biological functionality and enhancing receptor affinity.[80,81] Pyranose deoxypentoses, deoxy sugars found in various natural products (Figure 11), are predominantly synthesized through glucuronic acid decarboxylases, members of the short-chain dehydrogenase/reductase (SDR) enzyme family.[72−74] As shown in Figure 11, an example deoxypentose biosynthesis involves (1) activation of α-D-glucose-1-phosphate by α-D-glucose-1-phosphate nucleotidyltransferase (EvdS4) to give NDP-α-D-glucose, (2) oxidation of NDP-α-D-glucose by NDP-α-D-glucosedehydrogenase (EvdS1) to give NDP-α- D-glucuronic acid, (3) C-4 oxidation of NDP-α-D-glucuronic acid using NAD^+ by glucuronic acid decarboxylase (EvdS6), facilitating C-6 decarboxylation. The intermediate formed after the decarboxylation can be either 4-keto-pentose or 4-hydroxy-pentose. Further discussion will primarily focus on the differences in product formation. It is worth noting that the decarboxylation mechanism carried out by the SDR superfamily has been extensively examined elsewhere and, thus, will not be discussed further here.[82−84]

To explain the observation of 4-keto versus 4-hydroxypentose products, crystal structures of glucuronic acid decarboxylases, including ArnA (PDB ID: 2BLL),[85] hUxs1 (PDB ID: 2B69),[86] and EvdS6 (PDB ID: 8SK0),[73] were solved. These enzymes produce 4-keto-pentose, 4-hydroxy-pentose, and both intermediates, respectively. Despite the differences in product profile between these three enzymes, the positioning of the side chains in the SDR superfamily catalytic triad Tx_nYxxxK exhibits no significant variation. The differences in product profile can instead be attributed to the relative kinetics of the oxidative decarboxylation and reduction reactions: in enzymes that favor 4-ketopentose production the release of 4-keto-pentose and NADH occurs faster than the reduction reaction. Interestingly, the product profile can be altered by extending incubation time as the formation of 4-hydroxy-pentose is observed in the case of

https://doi.org/10.1021/jacsau.4c00425
JACS Au 2024, 4, 2715−2745

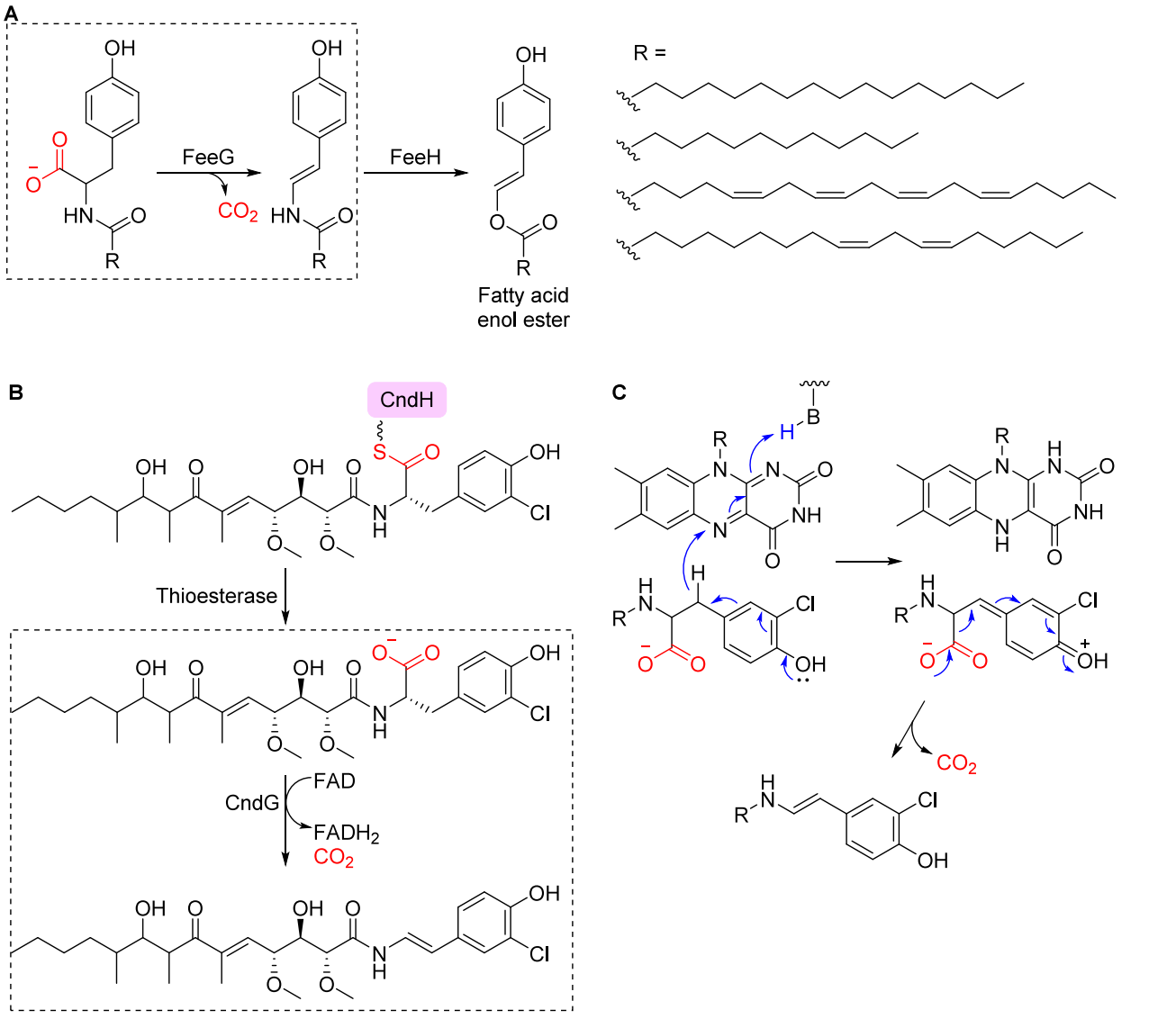

Figure 14. Oxidative decarboxylation steps are proposed for the biosynthesis of (A) fatty acid enol ester and (B) chondrochloren. (C) Proposed mechanism of the oxidative decarboxylation catalyzed by vanillyl alcohol phenyl oxidase/*p*-cresol methyl hydroxylases.

ArnA, which was initially thought to only produce the keto product.[87] The kinetics of these reactions are believed to be controlled by a flexible loop containing Arg279 and Arg278 residues. Mutating these residues to Ala enhances loop flexibility, improving the rate of ketone product release and resulting in a significantly lower yield of the 4-hydroxy-pentose product.[73] Additionally, mutations in key residues involved in the hydride transfer of the reduction, such as Thr126, which coordinates the activated ketone, can cause a near-complete loss in 4-hydroxy-pentose production. To further understand the role of conformation and proposed active site interactions in catalysis, future studies using bound UDP-glucuronic acid may be necessary.

5.1.2. Short-Chain Dehydrogenase/Reductase in Micrococcin Biosynthesis. the RiPP compound micrococcin, a potent thiopeptide targeting *Mycobacterium tuberculosis*, features another SDR enzyme, TclP, that facilitates oxidative decarboxylation (Figure 12).[75,76,88] TclP catalyzes the conversion of the terminal Thr residue of the substrate peptide to a ketone, that is subsequently reduced to an alcohol by another SDR enzyme, TclS, resulting in the final product, micrococcin P1. Micrococcin biosynthesis entails two stages: (1) thiazole formation through cyclodehydration and dehydration of Cys residues and (2) Ser/Thr processing involving dehydration and macrocyclization, forming the characteristic pyridine ring of a thiopeptide RiPP natural product (Figure 12B).[75,76]

5.1.3. Iron-Type Alcohol Dehydrogenase-like Enzymes in Daptide Biosynthesis. The newly identified RiPP class, daptides, reported in 2023, features a distinctive (*S*)-N,N-dimethyl-1,2-propanediamine (Dmp)-modified C-terminus, achieved through the coordinated action of four enzymes, MpaBCDM, in a three-step pathway (Figure 13).[77] MpaBC, comprising the oxidative decarboxylase MpaC and the RRE-containing adapter MpaB, catalyzes the oxidative decarboxylation of the C-terminal Thr residue to yield a C-terminal ketone. Subsequently, the C-terminal ketone undergoes conversion to an amine via the PLP-dependent transaminase MpaD and then alkylation by the SAM-dependent methyltransferase MpaM. MpaC, classified as an iron-type alcohol dehydrogenase-like enzyme, is predicted to require $NADP^+$ as a

https://doi.org/10.1021/jacsau.4c00425
JACS Au 2024, 4, 2715−2745

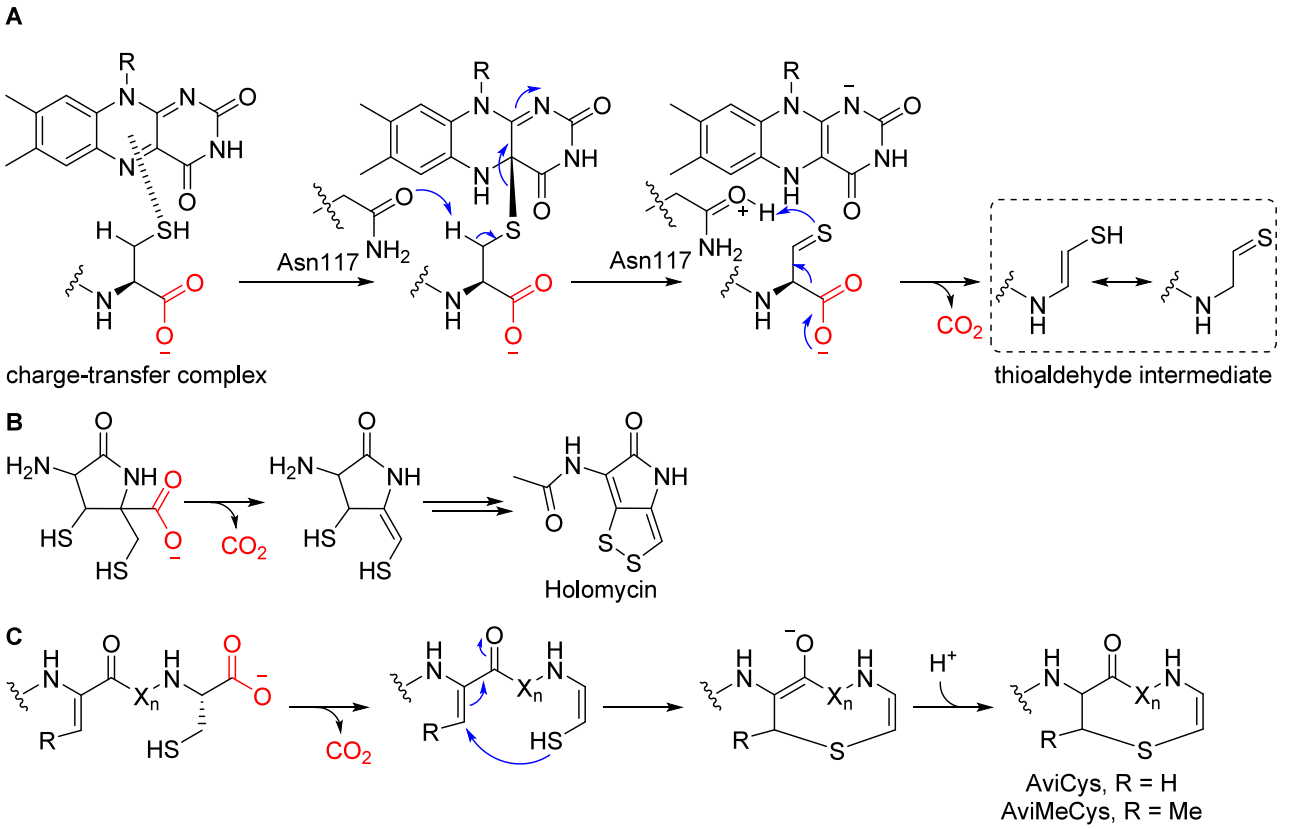

Figure 15. (A) Mechanism of homo-oligomeric flavin-containing cysteine decarboxylases is illustrated using EpiD as an example (PDB ID: 1G63). Roles of HFCDs in the biosynthesis of (B) holomycin and (C) AviCys-containing RiPPs.

cofactor based on sequence similarity and to exhibit a broad substrate scope based on three canonical substrate peptides in the BGC. Mutation of the core peptide confirms that MpaC can modify a wide range of substrate peptides with a C-terminal Thr. The structural characteristics of daptides, including a hydrophobic α-helical conformation and amidated C-terminus, resemble melittin, a membrane-disrupting component of honeybee venom. Notably, daptides demonstrate hemolytic activity against bovine erythrocytes, suggesting the potential use of the Dmp-modified C-terminus as a strategy for drug design to enhance interactions with cell membranes. The MpaBC-like systems and downstream tailoring enzymes exhibit promise for enzymatic C-terminal modification of peptides.

5.2. Flavin-Dependent Decarboxylase

In addition to the prFMN-dependent decarboxylases mentioned above, Nature employs unmodified flavin cofactors FMN and FAD as electron acceptors in oxidative decarboxylation reactions. Two flavoenzyme families with distinct mechanisms catalyze decarboxylation in secondary metabolism: (1) vanillyl alcohol phenyl oxidase/p-cresol methyl hydroxylase (VAO/PCMH) in long-chain fatty acid enol esters and PKS/NRPS biosynthesis and (2) homo-oligomeric flavin-containing Cys decarboxylase (HFCD) in RiPP and NRPS biosynthesis.[14,89,90] Additionally, there are flavin-dependent halogenases, such as Bmp2[91] and Bmp5[92] that induce decarboxylation of substrates during halogenation processes.

5.2.1. Vanillyl Alcohol Phenyl Oxidase (VAO)/p-Cresol Methyl Hydroxylase (PCMH) Family Enzymes in Fatty Acid Enol Ester and PKS/NRPS Biosynthesis. Two exemplary flavin-dependent decarboxylation reactions can be found in the biosynthesis of the polyketide-peptide antibiotic chondrochloren as well as the long-chain fatty acid enol esters, both involving decarboxylation of an N-substituted tyrosine intermediate (Figure 14AB). The key decarboxylation step is catalyzed by flavoenzymes FeeG (long-chain fatty acid enol esters) and CndG (chondrochloren).[93−95] Both enzymes belong to the 4-phenyl oxidizing subgroup of the VAO/PCMH flavoprotein family.[14] The proposed mechanism, derived from a mechanistic study of vanillyl-alcohol oxidase by Fraaije et al.,[90] involves hydride transfer from the Cα atom of the substrate to the N5 of the isoalloxazine ring, forming a quinoid species as the first intermediate. The *p*-quinone methide moiety serves as an electron sink, facilitating Cβ-decarboxylation, resulting in the formation of the hydroxyl-styryl-containing product. The catalytic cycle concludes with O_2-assisted oxidation of the reduced $FADH_2$, regenerating the oxidized FAD (Figure 14C). A crystal structure is currently unavailable for this class of enzymes.

5.2.2. Homo-oligomeric Flavin-Containing Cys Decarboxylases (HFCDs). Another class of flavoproteins catalyzing decarboxylation is the HFCDs. Enzymes of this class are found in the BGCs of holomycin (BGC0000373, a dithiopyrroles NRPS antibiotic) and in several classes of AviCys-containing RiPP, including epidermin (BGC0000508, a lanthipeptide),[96] thioviridamide (a thioamitide),[97] microbisporicin (a lanthipeptide),[98] and cypemycin (BGC0000582, a type A linaridine) (Figure 15).[99,100] The proposed reaction mechanism of HFCDs begins with the formation of a charge-transfer complex between the thiol group of Cys residue and the oxidized flavin (Figure 15A),[101] followed by nucleophilic addition of the Cys thiol group to C4a of the oxidized flavin. Deprotonation at Cβ of Cys

https://doi.org/10.1021/jacsau.4c00425
JACS Au 2024, 4, 2715−2745

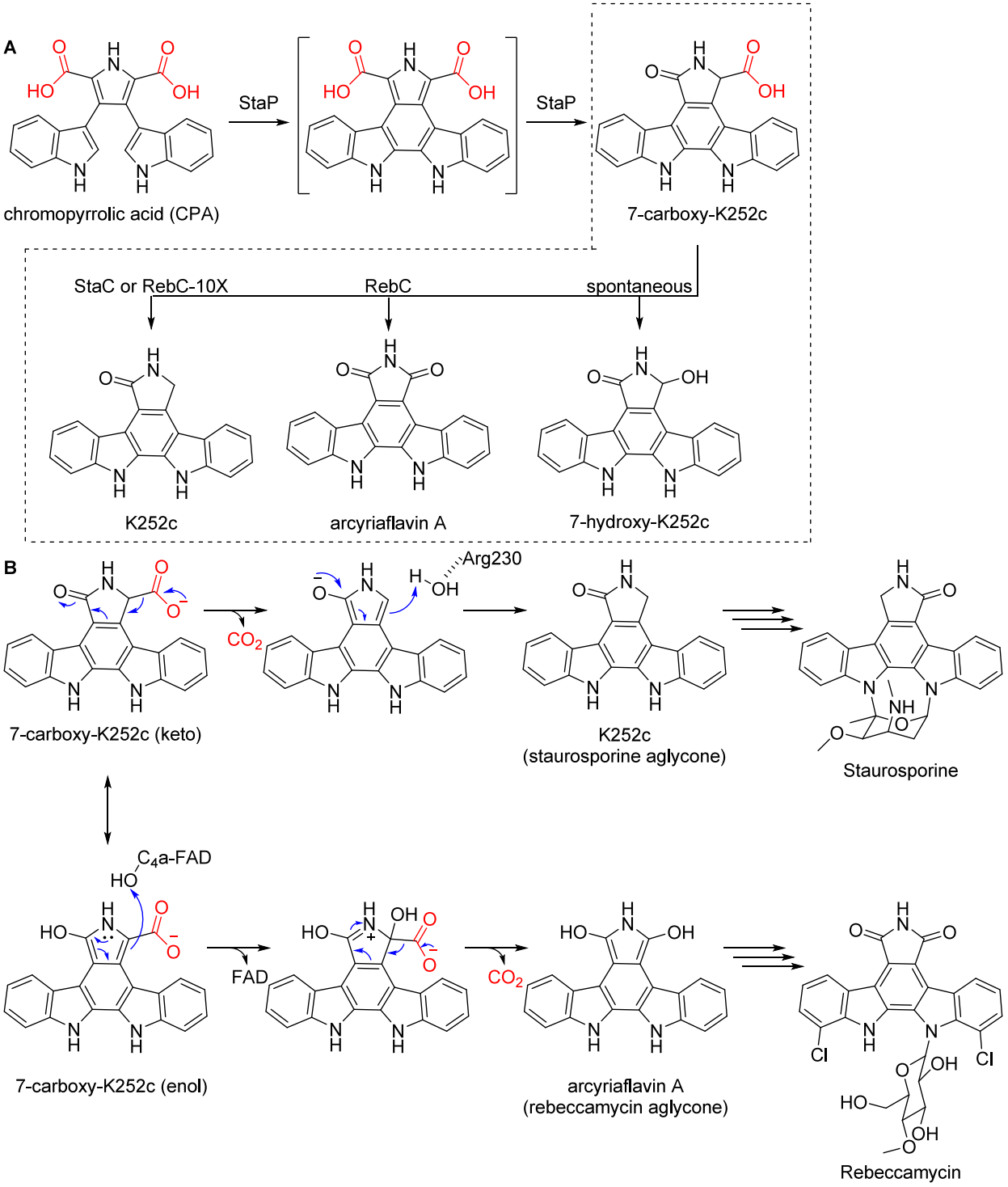

Figure 16. (A) Formation of the crucial intermediate 7-carboxy-K252c from chromopyrrolic acid (CPA) through aryl−aryl coupling, catalyzed by the P450 enzyme StaP/RebP. The subsequent step involves the decarboxylation of 7-carboxy-K252c, yielding different products mediated by the FAD-dependent enzymes StaC and RebC. (B) Mechanism of decarboxylation catalyzed by StaC/RebC-10X and RebC yielding different products. Arg residue is numbered based on crystal structure of RebC-10X (PDB IB: 4EIQ).

residue facilitates the heterolytic cleavage of the C4a−S bond to yield reduced flavin and thioaldehyde intermediate. The thioaldehyde serves as an electron sink to stabilize the decarboxylation and yield a thioenol. This thioenol later serves to facilitate the formation of the dithiopyrrole moiety in holomycins (Figure 15B) and C-terminal *S*-[(*Z*)-2-aminovinyl]-d-cysteine (AviCys) in RiPPs (Figure 15C).

AviCys-modified peptides, which display potent antimicrobial or anticancer activity, possess an intricate C-terminal ring that is critical for desirable drug-like properties such as heat and pH stability, high target specificity, and resistance toward proteases and that locks the peptide in an active conformation for target binding. Recently, there has been a detailed review on the participation of HFCDs in the biosynthesis of AviCys-

https://doi.org/10.1021/jacsau.4c00425
JACS Au 2024, 4, 2715−2745

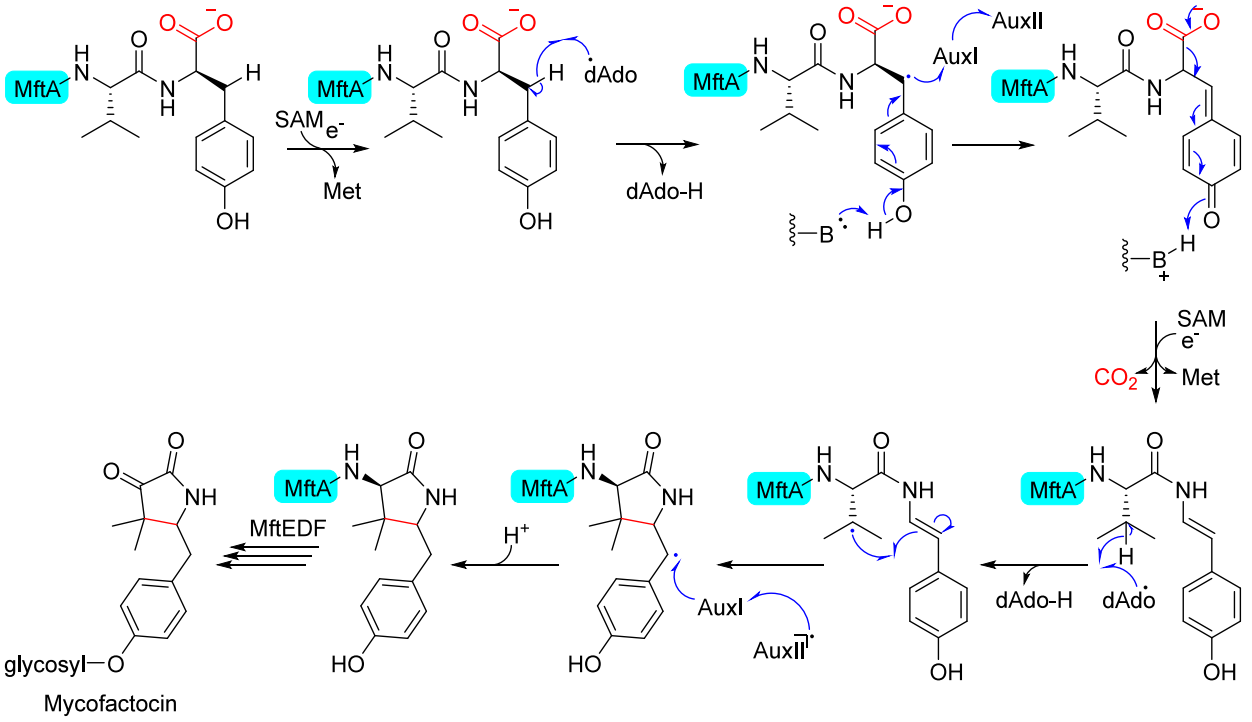

Figure 17. Proposed mechanism of the decarboxylation and ligation catalyzed by MftC consuming two equivalents of SAM to modify one equivalent of substrate peptide.

containing peptides.[100] The enzymes responsible for catalyzing the initial decarboxylation step in AviCys formation have been extensively studied, and successful reconstitution of several biosynthetic pathways has been achieved.[98,100,102] However, the subsequent step of thioether cyclization, which completes the AviCys formation, is not fully understood. It is currently proposed to be either an enzyme-catalyzed or a spontaneous process.[100] Notably, the AviCys decarboxylase CypD exhibits a broad substrate scope, suggesting its potential utility as a biocatalyst for AviCys synthesis in modified peptides.[100] The role of HFCDs in AviCys-containing peptide biosynthesis has recently been reviewed in detail.[100]

5.2.3. FAD-Dependent Decarboxylase in Indolocarbazole Biosynthesis. Indolocarbazoles[103] comprise a diverse array of alkaloid natural products that exhibit multifaceted pharmaceutical activities, including the inhibition of protein kinase,[104] DNA replication,[103] and anticancer effects.[105,106] The diversity of indolocarbazoles partially stems from variations in the oxidation states of the pyrroline ring moiety, products of oxidative decarboxylation catalyzed by FAD-dependent enzymes. In the biosynthesis of rebeccamycin (BGC0000821) and staurosporine (BGC0000825), this key step is catalyzed by RebC and StaC, respectively. The biosynthesis of indolocarbazoles involves the formation of the chromopyrrolic acid (CPA) intermediate from two tryptophan molecules. As shown in Figure 16A, CPA undergoes aryl-aryl coupling, followed by decarboxylation catalyzed by P450 enzymes, StaP or RebP, to yield 7-carboxy-K252c. This intermediate is then decarboxylated by StaC to yield K252c or is decarboxylated and oxidized by RebC to yield arcyriaflavin A. In the absence of StaC and RebC, the product of the StaP/RebP-catalyzed transformation of CPA yields multiple products, including K252c, 7-hydroxy-K252c, and arcyriaflavin A, with 7-hydroxy-K252c being the primary product, highlighting the importance of StaC and RebC in controlling the formation of the correct indolocarbazole cores while preventing site reactions.

While StaC and RebC share a 65% sequence similarity, they are distinct in FAD-binding affinity and product profile. Interestingly, introducing two mutations to RebC (F216V and R239N) allows the reaction mechanism to switch to that of StaC.[107,108] The cocrystal structures of the 7-carboxy-K252c substrate with RebC and RebC-10X (a mutated RebC with StaC-like activity) reveal that RebC-10X selectively binds the nonplanar keto tautomer, while RebC binds the planar enol tautomer of the substrate (Figure 16B).[109] In the keto tautomer, spontaneous decarboxylation is facilitated due to conjugation with Cβ, serving as an electron sink. In contrast, in the enol form, C-7 is at sp^2 hybridization and does not facilitate spontaneous decarboxylation. FAD-assisted hydroxylation at C-7 is proposed to change the hybridization of C-7 from sp^2 to sp^3, facilitating decarboxylation.

6. HOMOLYTIC DECARBOXYLATION

In contrast to the above examples of heterolytic (2-electron) decarboxylation, here we detail examples of homolytic decarboxylation, which leverages various natural oxidants to induce decarboxylation. Most often β-oxidation is invoked in proposed mechanisms, though in at least one case, the mechanism is proposed to proceed through a carboxyl radical.

6.1. Radical SAM-Dependent Decarboxylase in the Biosynthesis of Mycofactocin

MftC is an enzyme that belongs to the radical SAM (rSAM) enzyme superfamily, which is the largest known protein superfamily utilizing a [4Fe-4S] cluster for the reductive cleavage of SAM to form L-methionine and a strongly oxidizing 5-deoxyadenosine radical (dAdo$^\bullet$).[110] Once formed, the dAdo$^\bullet$ radical can participate in various transformations, including cyclization, methylation, and dehydration. Among the members

https://doi.org/10.1021/jacsau.4c00425
JACS Au 2024, 4, 2715−2745

of this large protein family, MftC belongs to a specific rSAM subfamily that is characterized by a 100-amino acid C-terminal domain called SPASM shared by rSAM enzymes involved in the biosynthesis of subtilosin A, pyrroloquinoline quinone, anaerobic sulfatase, and mycofactocin.[111] While rSAM-SPASM proteins typically catalyze oxidative bond-forming reactions, MftC is an exception. Its catalytic activity involves a decarboxylation reaction and the formation of a C−C bond.[112] MftC uses two equivalents of SAM: one for decarboxylation and the second to forge a C-C bond between Cα of a Tyr residue and Cβ of a Val residue, both found in the C-terminus of the substrate peptide MftA.[113] MftC features three [4Fe-4S] clusters: the rSAM cluster, where dAdo$^{\bullet}$ formation happens, and the two auxiliary clusters found within the SPASM domain. All these clusters are crucial for MftC activity.[113] The first auxiliary cluster, AuxI, is proposed to play a role in substrate binding and electron shuttling between the active site, and the second auxiliary cluster AuxII, which serves as electron storage.[114] It is noteworthy that the MftC reaction exclusively takes place in the presence of the peptide chaperone MftB.[115]

The proposed mechanism for the decarboxylation and ligation processes catalyzed by MftC unfolds as follows (Figure 17): MftC initiates the process by reductively cleaving SAM, generating a 5-deoxyadenosine radical (dAdo$^{\bullet}$). In the first phase of decarboxylation, the dAdo$^{\bullet}$ extracts a hydrogen from the substrate peptide, producing an alkyl radical at Cβ-Tyr30. Subsequently, 1-electron oxidation occurs at the alkyl radical, coupled with the deprotonation of the phenolic proton, to form a quinone methide intermediate. This quinone methide serves as an electron sink, facilitating the decarboxylation process and forming a vinyl phenol-containing intermediate, which serves as the substrate for the second stage of ligation. In this stage, a second dAdo$^{\bullet}$ extracts a hydrogen from the Cβ-of the penultimate Val29. The newly formed alkyl radical then attacks the neighboring C-C unsaturated bond at the C position, resulting in the formation of a 5-membered ring. The remaining electron from the double bond has the potential to form a radical on Cβ or the phenol ring of Tyr30. This radical is subsequently quenched to yield the final product. It is important to note that the identity of the electron, hydrogen acceptor, and donor in the proposed mechanism are unknown.

The activity of MftC relies on the presence of a hydrogen-donating group in the phenol, demonstrated by the lack of activity observed in the mutated substrate Y30F. The MftC-catalyzed decarboxylation resembles the mechanism observed in the 4-phenyl oxidizing subgroup of vanillyl alcohol phenyl oxidase/p-cresol methyl hydroxylase in N-substituted tyrosine decarboxylase (refer to Section 5.2.1). Both mechanisms require the formation of a p-quinone intermediate, emphasizing a shared step in these enzymatic processes.

6.2. Fe-Dependent Decarboxylases

Decarboxylation reactions catalyzed by iron-dependent enzymes have been observed in both heme (P450) and nonheme iron enzymes. While most iron-dependent enzymes catalyze a two-electron oxidative decarboxylation, a few enzymes, such as the recently discovered multinuclear nonheme iron-dependent (MNIO) enzyme ApyH or Fe(II) and α-ketoglutarate (Fe(II)/α-KG)-dependent ScoE, can perform four-electron oxidative decarboxylation.[116−118]

The mechanisms of iron-dependent decarboxylases involve several shared steps. First, the iron cofactor activates dioxygen or hydrogen peroxide to form reactive species such as the high

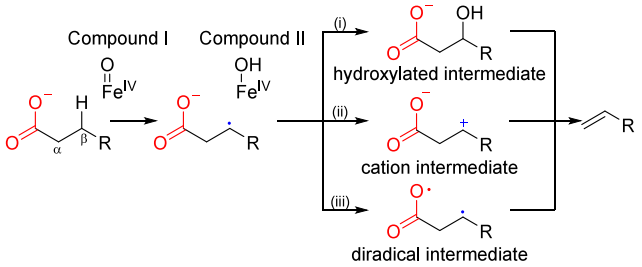

Figure 18. General mechanisms of homolytic decarboxylation catalyzed by iron-dependent enzymes.

valent iron-oxo intermediate Fe^{IV}=O (Figure 18). The reactive species abstracts a hydrogen at the Cβ of the carboxylic acid, yielding an alkyl radical. In two-electron oxidative decarboxylation, three possible pathways are proposed for the decarboxylation of alkyl radical (Figure 18). The first pathway is an OH-rebound pathway involving radical hydroxylation followed by dehydration and decarboxylation. The second pathway is a single-electron transfer pathway in which the unpaired electron is transferred from the radical to the Fe^{III}−OH species to produce a substrate cation that subsequently undergoes decarboxylation. The third pathway involves diradical intermediate formation to support homolytic decarboxylation. While all three pathways have been proposed, studies on two different enzymes suggest that the OH-rebound pathway (i) is less favored. Rapid kinetic studies of the P450 peroxygenase OleT$_{Je}$ (Section 6.2.1.2) have shown an unusually stable compound II, whose lifetime exceeds that of the radical species.[119] Additionally, investigations on the Fe(II)/α-KG decarboxylase IsnB (Section 6.2.2.1) incubated with β-hydroxy acid did not observe a decarboxylated product.[120] Further research is needed to gain a deeper understanding of the mechanism of two-electron oxidative decarboxylation. The four-electron oxidative decarboxylation catalyzed by ApyH and ScoE has some features similar to the above, which will be discussed separately below.

6.2.1. Heme-Dependent Decarboxylases. Cytochrome P450 enzymes (P450s or CYPs) are a diverse group of heme-thiolate proteins capable of catalyzing numerous reactions, including hydroxylation, epoxidation, dehalogenation, and decarboxylation. These reactions are mediated by the reactive intermediate called Compound I, which is generated through two different pathways. Enzymes such as P450 monooxygenases utilize O_2 and NAD(P)H as the source of oxygen and electron sources, while enzymes like P450 peroxygenases directly employ hydrogen peroxide via the peroxide shunt pathway to produce Compound I (Figure 19A). P450 decarboxylases, which can utilize either of these pathways, will be discussed further in the following section.

6.2.1.1. P450 Enzyme in Bottromycin A2 Biosynthesis. In the penultimate biosynthetic step en route to the potent antibiotic bottromycin A2 (BGC0000468),[121] BotJ (also known as Bot^{CYP}), a cytochrome P450 decarboxylase enzyme,[122] catalyzes the oxidative decarboxylation of the C-terminal thiazoline to a des-carboxy thiazole (Figure 19B). A similar modification, catalyzed by another P450 enzyme, is observed in the biosynthesis of the plant alkaloid camalexin (Figure 19C). The activity of Bot^{CYP} has been successfully reconstituted *in vitro* using the ferredoxin-ferredoxin reductase system.[122] *In vitro* reconstitution also shows that Bot^{CYP} selectively acts on a D-Asp-containing intermediate.[123] The origin of this selectivity

https://doi.org/10.1021/jacsau.4c00425
JACS Au 2024, 4, 2715−2745

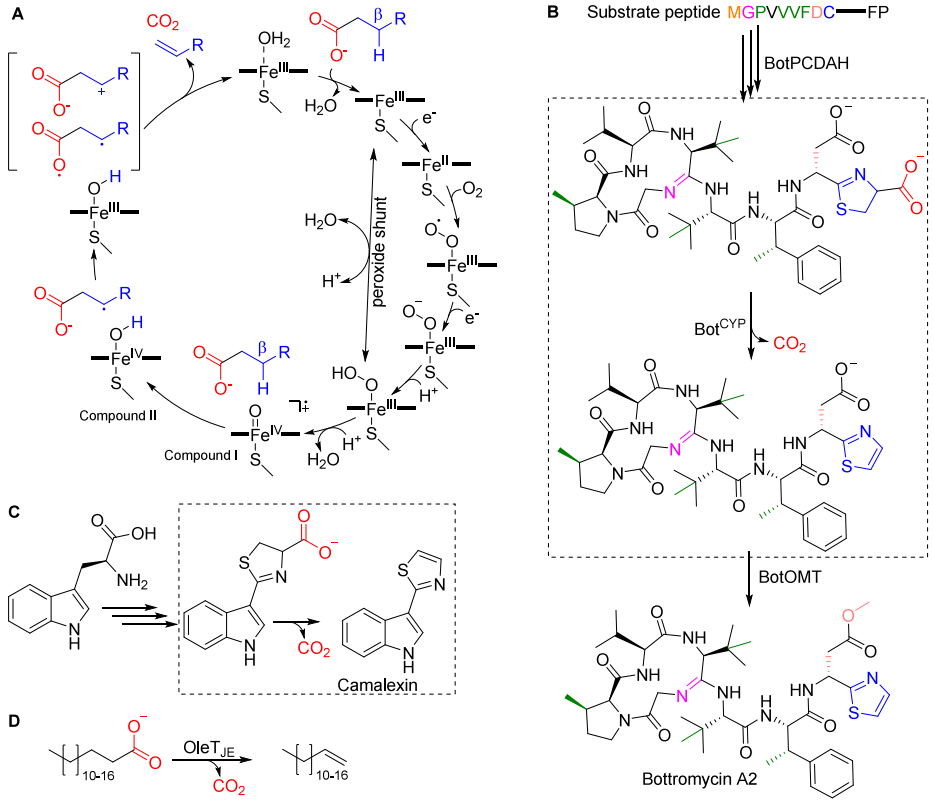

Figure 19. (A) Catalytic cycle of cytochrome P450 monooxygenases and peroxygenases: P450 peroxygenases utilize the peroxide shunt pathway to directly convert the substrate-bound P450 to the ferric-hydroperoxo species using H_2O_2. Biosynthetic pathways of (B) bottromycin A2, (C) camalexin, and (D) terminal olefins.

remains to be determined since the crystal structure of a close homologue of Bot^{CYP} (Sal^{CYP} from *Salinispora tropica* PDB: 7ABB) did not provide an adequate explanation.[122]

6.2.1.2. P450 Peroxygenase in Olefin Biosynthesis. OleT$_{JE}$ (Figure 19D) is a member of the peroxygenase family, a subfamily of P450-containing proteins.[124] This enzyme is responsible for catalyzing the oxidative decarboxylation of fatty acids, resulting in the production of corresponding terminal olefins. Initially discovered in the genome of the bacteria *Jeotgalicoccus* spp., OleT$_{JE}$ has been found to generate terminal olefins such as 18-methyl-1-nonadecene and 17-methyl-1-nonadecene.[124] Noncanonical substrates, such as short-chain aliphatic or phenyl-substituted fatty acids, yield Cα and Cβ hydroxyl products.[125−127] The regio- and chemoselectivity of the reaction depend on multiple factors, including the structure of the substrate, the positioning of the substrate within the active site, and the accessibility of the oxidizing species Fe^{IV}=O to the substrate.

Recently, OleTP$_{RN}$, a homologue of OleT$_{JE}$, was discovered in the *Rothia* genus. OleTP$_{RN}$ generates alkenes from a broad range of saturated and unsaturated fatty acids, including oleic and linoleic acids, the most naturally abundant fatty acids.[128] Two structural features differentiate the chemo-selectivity between OleT$_{JE}$ and OleTP$_{RN}$ (PDB ID: 5M0N and 8D8P, respectively). First, OleTP$_{RN}$ lacks a long F-G loop, which anchors the fatty acids through residue Leu176 in OleT$_{JE}$. Second, OleTP$_{RN}$ possesses a hydrophobic cradle in the distal region of the substrate-binding pocket. This cradle plays a crucial role in the activity of OleTP$_{RN}$ on long-chain fatty acids and facilitates the release of products derived from short-chain fatty acids.

6.2.2. Mononuclear Nonheme Iron Decarboxylases.

6.2.2.1. Fe(II)/α-KG Decarboxylases in the Biosynthesis of Isonitrile-Containing Natural Products. Many natural products contain isonitrile moieties. Two biosynthetic pathways to isonitriles have been characterized, both involve oxidative decarboxylations catalyzed by Fe(II)/α-KG oxygenases. These enzymes utilize iron, oxygen, and α-ketoglutarate as cosubstrates to generate a reactive Fe^{IV}=O species (Figure 20A). This species then oxidizes the substrates through a radical mechanism, allowing for a wide range of transformations such as hydroxylation, epimerization, halogenation, ring closure and expansion, in addition to decarboxylation. The first pathway proceeds through isonitrile synthases and Fe(II)/α-KG decarboxylases to produce vinyl isonitriles, including hapalindoles, rhabduscins, and byelyankacins (Figure 20B).[129−131] In the second pathway, a dual-function thioesterase and a Fe(II)/α-KG decarboxylase are responsible for the production of isonitrile lipopeptides such as SF2768, aerocyanidin, and amycomicin (Figure 20C).[118]

In the vinyl isonitrile biosynthetic pathway, the isonitrile synthase converts a Trp or a Tyr and a ribulose-5-phosphate to form isocyanopropanic acids. The isocyanopropanic acid subsequently undergoes an oxidative decarboxylation catalyzed by a Fe(II)/α-KG decarboxylase to yield indole/phenol vinyl isonitriles, which undergo further transformations to the final natural products (Figure 20A).[132,133] Extensive research has been conducted on the Fe(II)/α-KG decarboxylases involved in the biosynthesis pathway of vinyl isonitrile, specifically the enzymes AmbI3 and IsnB.[134,135] AmbI3, involved in ambiguine biosynthesis, exclusively synthesizes the Z isomer. Its homologue IsnB, strictly produces E isomer vinyl isonitriles.[136] The

https://doi.org/10.1021/jacsau.4c00425
JACS Au 2024, 4, 2715−2745

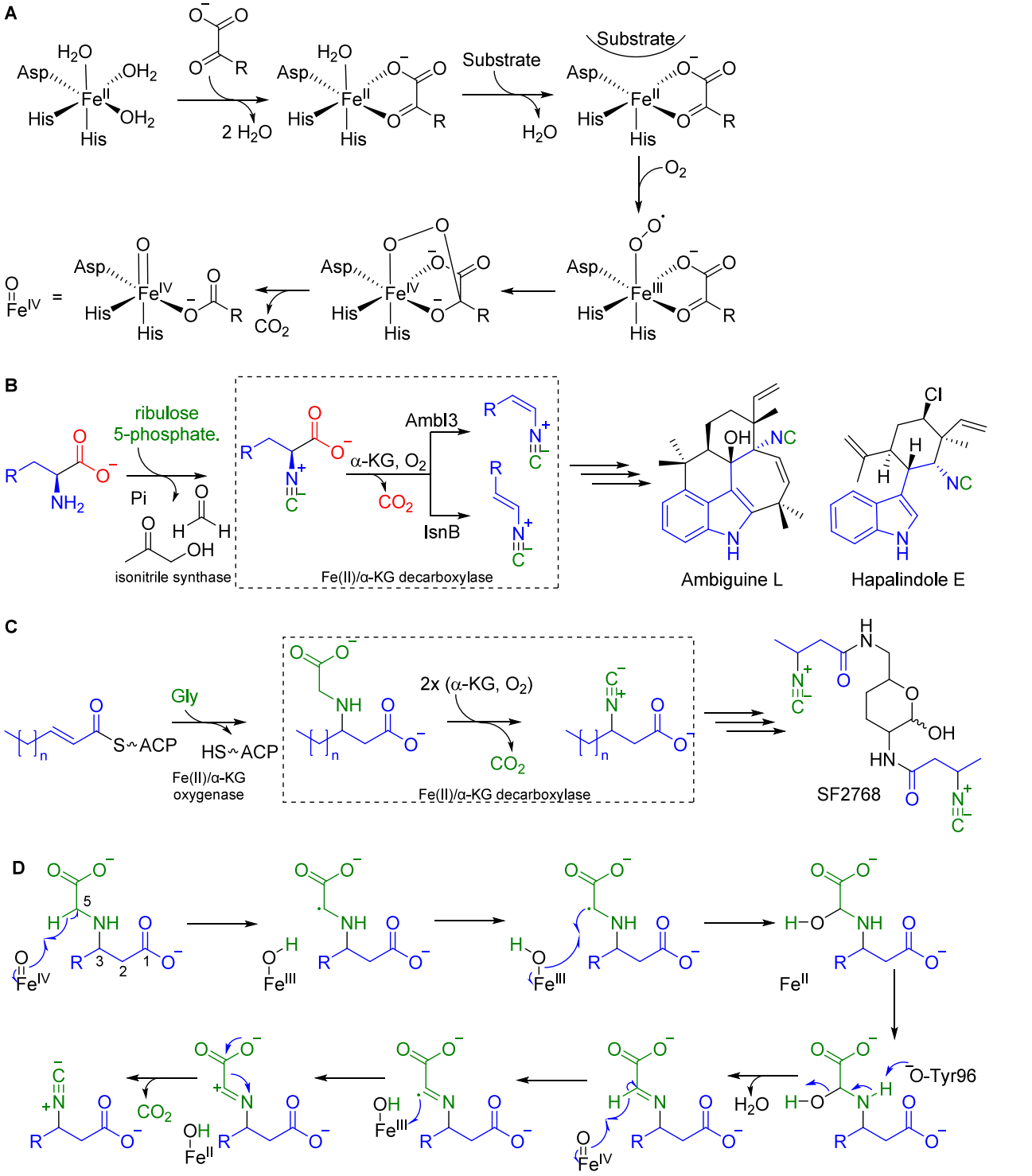

Figure 20. Fe(II)/α-KG decarboxylases in the biosynthesis of isonitrile-containing natural products and their mechanisms. (A) Biosynthetic pathway of vinyl isonitrile-containing natural products involving isonitrile synthase followed by mononuclear iron Fe(II)/α-KG decarboxylase IsnB or AmbI3. (B) Biosynthetic pathway of the isonitrile lipopeptide SF2768 with the four-electron oxidative decarboxylation catalyzed by ScoE. (C) Mechanism of forming the ferryl species in Fe(II)/α-KG enzymes. (D) Mechanism of Fe(II)/α-KG dioxygenases catalyze the oxidative decarboxylation of *N*-alkyl glycine.

enzyme demonstrates versatility with different indolic substrates. A substrate scope study has revealed that the size of the substitution groups on the indole ring has a more significant impact on the biosynthesis of ambiguine derivatives than their position.[137]

In the biosynthesis of isonitrile lipopeptides, the dual-function thioesterase facilitates the Michael addition of glycine to an α,β-unsaturated thioester, forming an N-alkyl glycine moiety. This is followed by a four-electron oxidative decarboxylation catalyzed by a Fe(II)/α-KG decarboxylase to generate the key isonitrile moiety. This pathway has been extensively investigated in the

https://doi.org/10.1021/jacsau.4c00425
JACS Au 2024, 4, 2715−2745

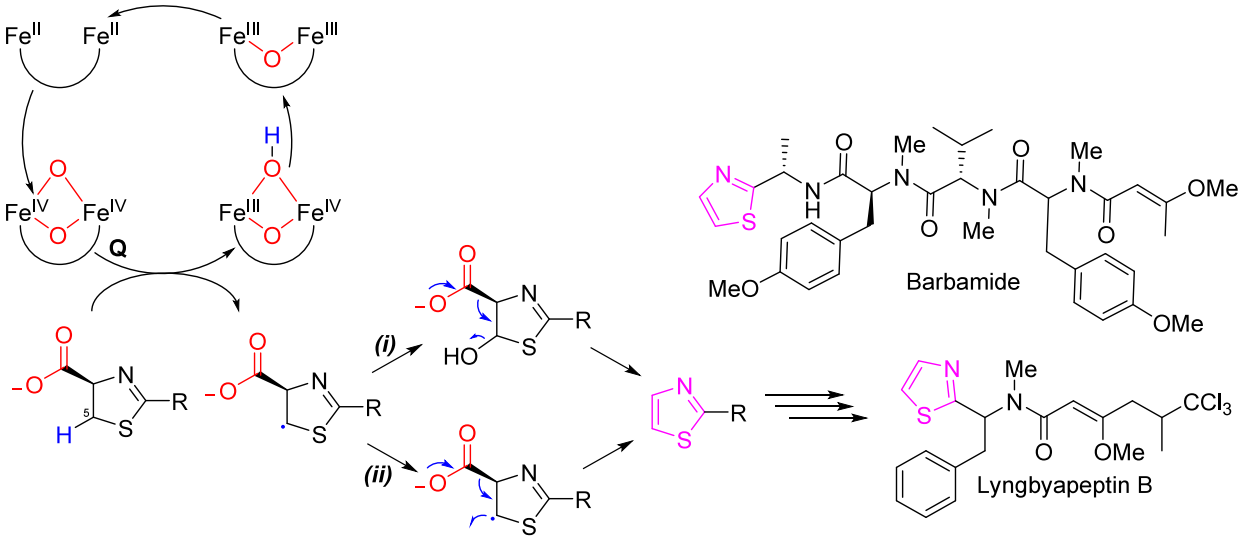

Figure 21. Structure of lyngbyapeptin and barbamide and the proposed mechanism of the decarboxylation catalyzed by diiron decarboxylase LynB7.

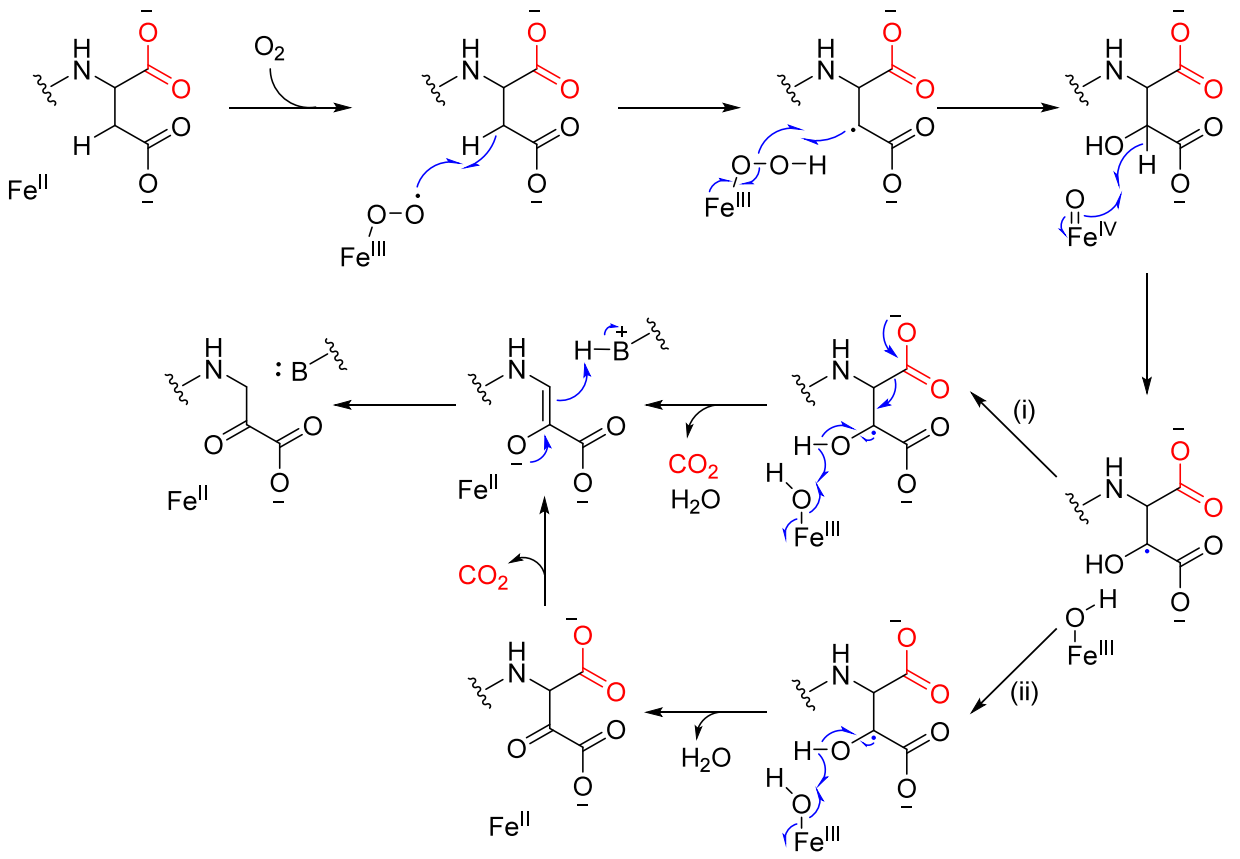

Figure 22. Mechanism of the four-electron oxidative decarboxylation of *N*-alkyl glycine by multinuclear nonheme iron-dependent enzyme ApyH.

production of antibiotic isonitrile lipopeptides SF2369 and SF2768, derived from *Actinomycetes* and *Streptomyces* sp., respectively.[138] In SF2369 biosynthesis, Fe(II)/α-KG decarboxylase ScoE converts (R)-3-((carboxymethyl)amino)-butanoic acid into (R)-3-isocyanobutanoic acid. The crystal structures of ScoE and its homologue SfaA have been reported, including the cocrystal of an N-alkyl glycine substrate and ScoE.[138,139] The structure revealed that one of the hydrogen atoms attached to C5 of the N-alkyl glycine substrate points toward the iron center at a distance shorter than 4.9 Å, suggesting its potential site of oxidation. It is important to note that ScoE utilizes two equivalents of α-KG in the decarboxylation process to produce two equivalents of the ferryl species, which ultimately leads to the formation of one equivalent of the isonitrile compound. The proposed mechanism for isonitrile formation by ScoE-type enzymes is illustrated in Figure 20D. In this mechanism, the ferryl species initiates dehydration by abstracting a hydrogen atom, followed by hydroxylation at the C5 position. This hydroxylated intermediate then undergoes dehydration, facilitated by Tyr96 (ScoE numbering) acting as a

https://doi.org/10.1021/jacsau.4c00425
JACS Au 2024, 4, 2715−2745

base, resulting in the formation of an imine intermediate. In the second oxidation step, the regenerated Fe^{IV}=O species abstracts a hydrogen atom at the C5 position within the imine intermediate, leading to the formation of a radical. This radical undergoes single electron transfer to the Fe^{III}-OH species, followed by decarboxylation, ultimately leading to the production of the desired isonitrile product.

6.2.3. Multinuclear Nonheme Iron Decarboxylases. *6.2.3.1. Nonheme Diiron Oxygenase/Decarboxylases in the Biosynthesis of Lyngbyapeptins and Barbamide.* Another mode of carboxythiazoline decarboxylation to yield thiazoles is showcased in the biosynthesis of lyngbyapeptins and barbamide. By contrast with P450 catalyzed decarboxylation for bottromycin described above (section 6.2.1.1), thiazoles in lyngbyapeptidns and barbamide are formed via nonheme diiron decarboxylase-catalyzed decarboxylation of carboxy thiazolines (Figure 21).[140,141] In a recent investigation led by Kudo et al., decarboxylase LynB7 was found to decarboxylate non-native truncated substrates (Figure 21, R = H, Ph), highlighting its synthetic versatility.[140] A proposed mechanism for LynB7-catalyzed decarboxylation, based on a kinetic isotope effect study at C5 of the thiazoline ring, suggests that the bis(μ-oxo)diiron^{IV} species (intermediate Q) abstracts a hydrogen atom at C5, yielding a radical intermediate.[140,142] This radical species then undergoes hydroxylation followed by decarboxylation (pathway i) or may undergo a further 1e- oxidation to induce decarboxylation to yield the thiazole product (pathway ii).

6.2.3.2. Multinuclear Nonheme Iron-Dependent Oxidative (MNIO) Enzymes in RiPP Biosynthesis. According to crystal structure analysis, MNIO enzymes, a recently discovered enzyme class, contain two or three iron ions in their active sites.[143−145] Despite being a relatively new enzyme class, MNIO enzymes have displayed remarkable capabilities in catalyzing intricate transformations of peptide substrates, including rearrangement, deformylation, and N-Cα bond cleavage.[143,146,147] In a recent study, the reactivity of MNIO enzymes has been expanded to include the first reported example of oxidative decarboxylation within this enzyme family.[116] This reaction is catalyzed by the oxidase ApyH, which works in conjunction with its partner protein ApyI (Figure 22). ApyH catalyzes the decarboxylation of the C-terminal Asp residue of the substrate peptide to yield a C-terminal aminopyruvic acid. In the proposed mechanism, the Fe^{II} ion initiates the reaction by abstracting hydrogen and hydroxylating the C-terminal Asp at Cβ. Subsequently, the enzyme abstracts another hydrogen at Cβ. The resulting radical intermediate can then undergo proton-coupled electron transfer, forming a β-keto acid that undergoes decarboxylation. Alternatively, the radical may stimulate decarboxylation, leading to the formation of an enol that tautomerizes into a ketone at Cβ.

6.2.3.3. Binuclear Nonheme Iron(II) Enzyme in Olefin Biosynthesis. It is not uncommon to observe different enzyme classes catalyzing similar reactions, particularly among those capable of catalyzing a broad range of transformations, as exemplified by carboxythiazoline decarboxylation (Section 6.2.1.1 and Section 6.2.3.1). Similarly, fatty acid decarboxylation to form olefins can be achieved through the action of enzymes such as the P450 peroxygenase $OleT_{JE}$ (described in section 6.2.1.2), or the binuclear nonheme iron(II) enzyme UndA. UndA is responsible for the oxidative decarboxylation of lauric acid to afford 1-undecene, a prevalent hydrocarbon semivolatile metabolite in *Pseudomonas* (Figure 23).[148−150] The crystal

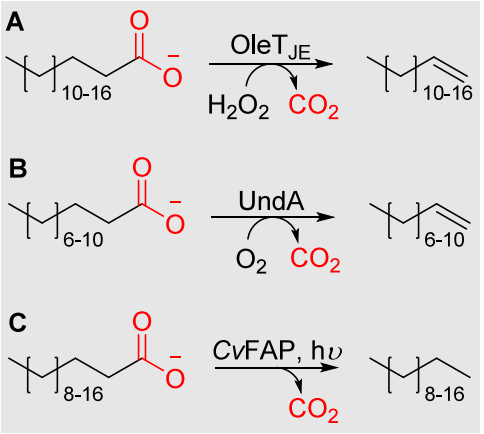

Figure 23. Fatty acid decarboxylation catalyzed by (A) P450 peroxygenase $OleT_{JE}$ (Section 6.2.1.2), (B) binuclear nonheme iron(II) enzyme UndA (Section 6.2.3.3), and (C) photodecarboxylase *Cv*FAP (Section 6.3).

structure of UndA (PDB ID: 4WWZ) reveals a substrate-binding site comprising a profound hydrophobic tunnel extending from the surface to the active site. This tunnel's length governs UndA's substrate scope, encompassing medium-chain fatty acids within the range of C10 to C14.[148] Examining the crystal structure further reveals the presence of two iron binding clusters in UndA of 4.9 Å between the two iron atoms. This distance significantly exceeds the average of 3.3 Å observed in soluble methane monooxygenases (sMMO). Moreover, the critical intermediate Q (Figure 21), essential for the sMMO-like mechanism, remains elusive in the case of UndA based on the Mössbauer spectroscopic characterization. This observation, coupled with chemical models derived from X-ray crystal structures and density functional calculations, leads to a proposed mechanism of forming the active iron radical species that diverge from the traditional sMMO mechanism. This uncommon mechanism of UndA has been described in detail in the work of Wang et al.[151]

6.3. Photodecarboxylase in the Biosynthesis of Alkanes

Fatty acid decarboxylation can be achieved through yet another mechanism by the fatty acid photodecarboxylase *Cv*FAP, leading to the production of alkanes rather than alkenes as described above (Figure 23). *Cv*FAP, discovered in the microalgae *Chlorella variabilis* NC64A,[152] represents a unique algal-specific branch within the glucose methanol choline oxidoreductase family. Activated by blue light (λ = 400−520 nm), *Cv*FAP efficiently catalyzes the decarboxylation of fatty acids, yielding CO_2 and the corresponding alkanes (Figure 23C).

The crystal structure of *Cv*FAP (PDB: 6YRU) reveals a narrow hydrophobic tunnel serving as the substrate binding site. Within this tunnel, the hydrophobic tail of the fatty acid substrate interacts with Tyr466, while the carboxylate part interacts with the side chains of Arg451, Cys432, and Gln486. The FAD cofactor is positioned at the closed end of the tunnel, with its tricyclic ring oriented toward the carboxylic group of the substrate.[152] This organization suggests that FAD, a light-absorbing chromophore, can serve as a medium to transfer energy from blue light to the carboxylic group of the substrate. This observation allows Sorigué et al. to lay the foundation for the mechanistic study of *Cv*FAP, further explored by Scrutton et al., who described a red-shifted flavin intermediate (Figure

https://doi.org/10.1021/jacsau.4c00425
JACS Au 2024, 4, 2715−2745

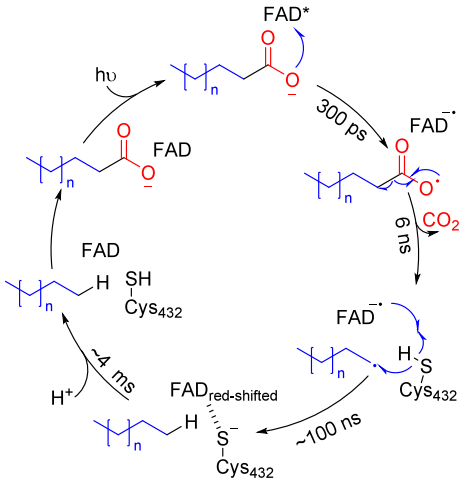

Figure 24. Proposed mechanism of the decarboxylation catalyzed by *Cv*FAP.

24).[152−155] In the proposed mechanism, blue light triggers the excitation of the FAD cofactor; the photoexcited cofactor (FAD*) seizes one electron from the anionic acid RCOO−, resulting in the formation of an anionic semiquinone $FAD^{\bullet-}$ and a carbonyloxy radical $RCOO^{\bullet}$. The homolytic decarboxylation of the carbonyloxy radical RCOO·, giving rise to an alkyl radical R· and a CO_2 molecule, outpaces the slow back electron transfer, establishing decarboxylation as the predominant pathway. Subsequently, the alkyl radical undergoes a transformation into the alkane product RH through the return of electrons from $FAD^{\bullet-}$ and proton transfer from an unidentified donor.

The unique properties of *Cv*FAP have positioned it as a potential biocatalyst for the conversion of low-cost microbial biomass into economically viable biofuels.[152] Under blue light illumination, *Cv*FAP has demonstrated near-quantitative yields of alkanes, with turnover numbers reaching up to 8000.[156] Significant efforts have been directed toward expanding substrate selectivity,[157−159] and improving catalytic efficiency.[160,161] Proof-of-concept studies have demonstrated integration of *Cv*FAP into catalytic cascades,[162−164] these and other applications have been recently reviewed.[165]

7. COFACTOR-INDEPENDENT DECARBOXYLASES UTILIZING ACID−BASE CATALYSIS

Previously mentioned decarboxylases employ cofactors like thiamine pyrophosphate, pyridoxal phosphate, flavin, nicotinamide, and metals to facilitate the process. Nature has also evolved cofactor-independent decarboxylases, which predominantly operate through acid−base mechanisms, heavily relying on active site microenvironments and substrate electronics. In secondary metabolite biosynthesis, these cofactor-independent decarboxylases participate in synthesizing *β*-branching polyketides (Figure 25). The biosynthetic process encompasses three steps, with two involving decarboxylation. The initial step forms acetyl- or propionyl-S-ACP_{donor} through two distinct pathways, either ketosynthase (KS)-like domain catalyzed or

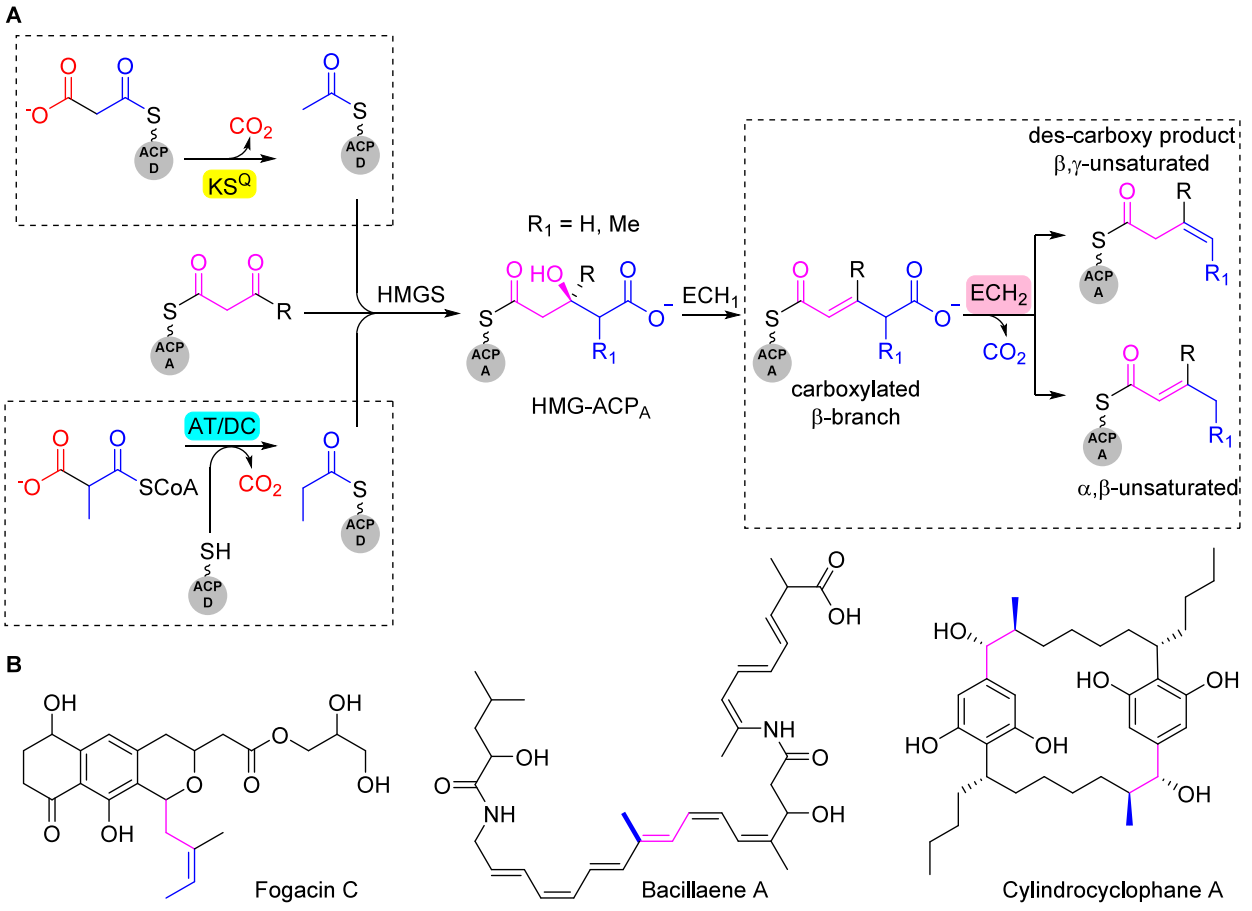

Figure 25. (A) Biosynthetic pathway and (B) structure of *β*-branching polyketides.

https://doi.org/10.1021/jacsau.4c00425
JACS Au 2024, 4, 2715−2745

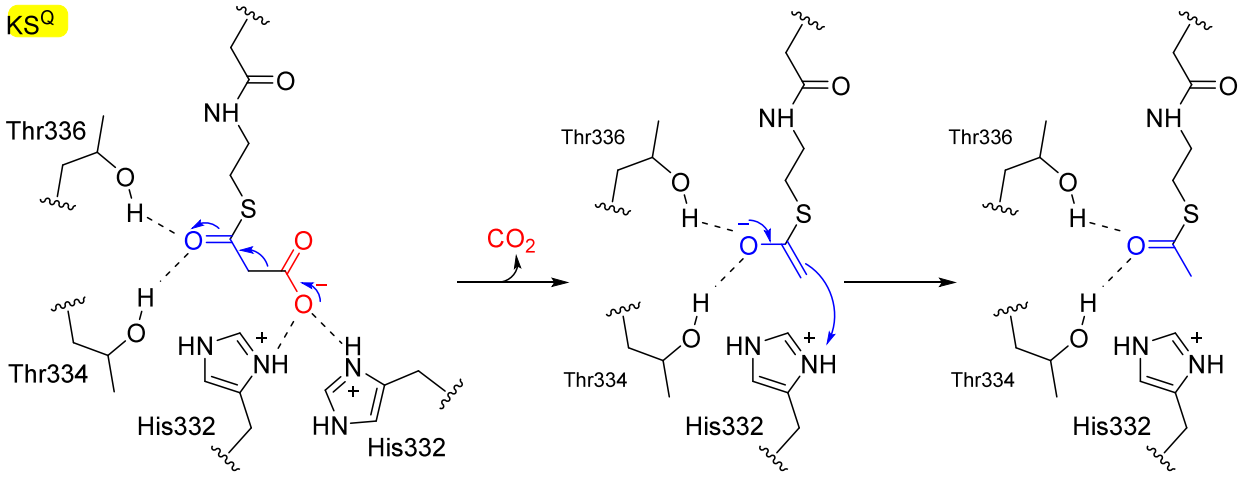

Figure 26. Acid−base catalysis in the mechanism of the decarboxylation catalyzed by KS^Q.

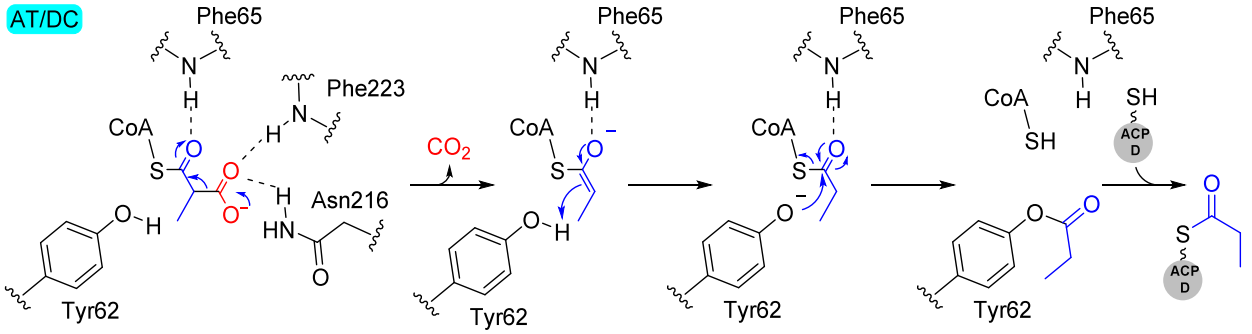

Figure 27. Mechanism of the decarboxylation catalyzed by the bifunctional AT/DC LnmK.

acyltransferase/decarboxylase (AT/DC) catalyzed, both of which involve decarboxylation. The second step in β-branching, catalyzed by a multiprotein 3-hydroxy-3-methylglutaryl synthase (HMGS) cassette, entails an aldol addition resulting in a 3-hydroxy-3-methylglutaryl intermediate. The third step in β-branching comprises a hydration and an optional decarboxylation, catalyzed by an enoyl-CoA hydratase domain (ECH1 and ECH2, respectively) leading to carboxy or des-carboxy β-branching products, the latter of which may be β,γ or α,β-unsaturated.

7.1. Ketosynthase-like Domain (KS^Q) Pathway to Acetyl-S-ACP_{donor}

In the initial step of β-branching polyketide biosynthesis, distinct pathways produce acetyl-S-ACP_{donor} and propionyl-S-ACP_{donor}. Acetyl-S- ACP_{donor} biosynthesis involves a tridomain loading module, widely distributed in various polyketides, including β-branching polyketides. The module comprises ketosynthase-like (KS^Q), acyltransferase (AT), and acyl carrier protein (ACP) domain. The AT domain loads malonyl moiety from malonyl-CoA to the ACP domain, followed by malonyl-ACP decarboxylation catalyzed by the KS^Q domain to yield acetyl starter unit.[166,167] Structural insights into the decarboxylation process are detailed in the work by Chisuga, et al.,[168] for the KS^Q domains GfsA KS^Q and CmiP4 KS^Q, found in the biosynthesis of macrolide antibiotics FD-891 and cremimycin, respectively.[169,170] Analyzing the crystal structure of GfsA-KS^Q with a malonyl thioester substrate analog enables the identification of essential residues involved in the decarboxylation mechanism. This mechanism resembles the decarboxylation process observed in β-keto acids (Figure 26). GfsA-KS^Q initiates decarboxylation by precisely positioning the substrate, facilitating the stabilization of the enolate intermediate through two conserved threonine residues in the active site of GsfA-KS^Q.

7.2. Bifunctional Acyltransferase/Decarboxylase Pathway to Propionyl-S-ACP_{donor}

The second pathway that yields propionyl-S-ACP_{donor} involves a decarboxylation followed by condensation of methylmalonyl-CoA catalyzed by a bifunctional AT/DC.[171] This pathway is observed in the biosynthesis of leinamycin,[172] myxovirescin,[173] largimycin,[171] and fogacin C.[174] Lohman et al. reported the cocrystal structure of the bifunctional AT/DC LnmK from leinamycin biosynthesis with methylmalonyl-CoA, revealing a shared active site for decarboxylase and acyltransferase activities.[175] Importantly, the sequence of events dictates that DC activity precedes AT activity. The proposed mechanism for the bifunctional enzyme LnmK unfolds as follows: (2R)-methylmalonyl-CoA undergoes decarboxylation, forming an enolate intermediate stabilized by Phe65 (Figure 27). The enolate then deprotonates the hydroxy group of Tyr62, giving rise to a phenolate. This phenolate, acting as a nucleophile, facilitates acyl transfer from propionyl-CoA to the enzyme, forming the pivotal intermediate propionyl-O-LnmK. Subsequently, the propionyl moiety is transferred to LnmL (ACP_{donor}), ultimately yielding propionyl-S-ACP_{donor}.[176]

https://doi.org/10.1021/jacsau.4c00425
JACS Au 2024, 4, 2715−2745

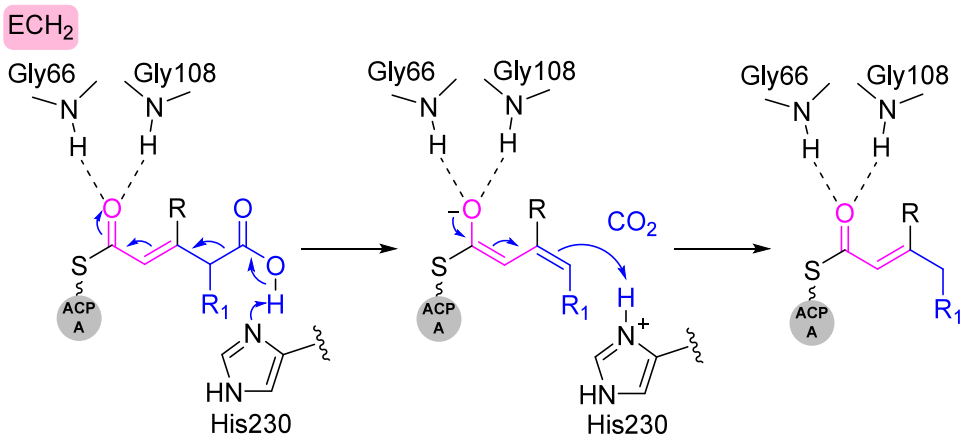

Figure 28. Mechanism of decarboxylation catalyzed by the enoyl-CoA hydratase domain ECH2 PksI.

7.3. ECH2 Domain-Catalyzed Decarboxylation to Yield β,γ- or α,β-Unsaturated Polyketides

The final step in some β-branched natural products is a decarboxylation step, catalyzed by the ECH2 domain, and is pivotal to shaping the diversity of β-branching polyketides. This step results in the formation of β,γ- or α,β-unsaturated products, which can undergo further modifications at the unsaturated moiety to yield even more diverse polyketide products (Figure 28). However, the factors that determine the formation of β,γ- or α,β-unsaturated products in this step are still unknown. Understanding these factors is essential for engineering the ECH2 domain to enable the biosynthesis of β-branched polyketides. The crystal structure of the ECH2 domain has been reported for CurF (PDB ID: 2Q2X) in curacins biosynthesis[177] and PksI (PDB ID: 4Q1G) in bacillaene biosynthesis (BGC0001089).[178] The mechanism closely resembles that of other cofactor-independent decarboxylases, commencing with the deprotonation of the carboxylic acid by an active site histidine (Figure 28). Following decarboxylation, the enolate is stabilized within an oxyanion hole formed by the backbone NHs of alanine and glycine residues at the active site. Finally, either another lysine (CurF) or the catalytic histidine (PksI) is proposed to protonate the intermediate. The ACP-bound substrate is found to be preferred over the CoA-bound substrate.[177,178]

8. CONCLUSION

Living organisms extract energy from a variety of carbon substrates through multistep oxidation cascades and frequently utilize decarboxylation reactions to extract additional reducing equivalents from oxidizable substrates. The stepwise oxidation reactions that Nature relies on for energy lead to the biosynthesis of numerous metabolites that bear carboxylic acid functional groups. Natural products are often synthesized by utilizing these primary metabolites as building blocks and frequently repurpose primary metabolic enzymes for their biosynthesis. In order to build complex, bioactive structures it is often necessary to remove the carboxylic acid groups inherited from these primary metabolic building blocks. For instance, in alkaloid and carbohydrate biosynthesis, decarboxylation takes place at the monomer stage prior to subsequent elaboration into more complex structures and has repurposed enzymes already present in primary metabolic pathways such as PLP- and TPP-dependent decarboxylases. In other instances, decarboxylation tailors natural products to achieve bioactive, drug-like structures, for example, in the C-terminal modification found in daptides, AviCys-containing peptides, and carboxythiazoline decarboxylation.

Given the importance of decarboxylation to natural product biosynthesis and the broad array of substrates that undergo decarboxylation, it is unsurprising that nature has evolved a diverse range of enzymatic decarboxylative mechanisms tailored to match the electronic requirements of the substrate. Decarboxylation can occur via two-electron mechanisms, utilizing cofactors such as TPP and PLP to stabilize the carbanion formed during carbon-carboxylate bond cleavage. These cofactors establish a covalent bond with the substrate via carbonyl or amine and serve as electron sinks during decarboxylation. Substrates with substituent groups (such as -OH, -SH, or hydroxyphenyl) at the Cβ position can undergo oxidation to create an electronic sink within the substrate itself. In contrast, those lacking substituent groups at both the Cα and Cβ may require a radical species to activate the Cβ-H bond necessary for decarboxylation.

Due to the widespread availability of carboxylic acid substrates for commercial synthesis, there is significant interest in pursuing synthetic methods which proceed via decarboxylation. Decarboxylases show significant potential as biocatalysts for use in the synthesis of such chemicals. TPP- and PLP-dependent dependent enzymes have been successfully engineered to produce numerous commodity chemicals. TPP-dependent decarboxylases are widely used in constructing artificial biosynthetic pathways for the production of alcohols such as isobutanol, n-pentanol, and 1,2,4-butanetriol,[179−181] while PLP-dependent decarboxylases have been exploited to produce commodity chemicals and important precursors such as γ-aminobutyric acid, cadaverine (a biopolymer precursor), and dopamine.[182−184] Additionally, given that numerous decarboxylases are involved in the production of alkene and alkanes from abundant fatty acids, there is significant potential for their use in biofuel production.

Given the microscopic reversibility of enzymatic reactions, decarboxylases can also catalyze carboxylation despite the uphill thermodynamics.[185] Indeed, carboxylation reactions have been demonstrated with both TPP and prFMN-dependent enzymes. Recently, TPP-dependent enzymes have been employed in amino acid production from aldehydes by coupling the decarboxylase with a transaminase or amino acid dehydrogenase.[186] On the other hand, prFMN enzymes display carboxylation activity toward various substrates, including diverse

https://doi.org/10.1021/jacsau.4c00425
JACS Au 2024, 4, 2715−2745

aromatic compounds, and have been the subject of investigation for potential applications, although further research is necessary.[187−191]

The rational engineering of novel metabolites or therapeutics combining enzymes from different biosynthetic pathways is a major goal of synthetic biology. Decarboxylases play a crucial role in this endeavor. For example, Fe(II)/α-KG enzymes can introduce clickable moieties in isonitrile-containing natural products, facilitating simplified synthesis of derivative molecules with increasing structural complexity or modification of their pharmacokinetic properties. In peptide-based natural products, decarboxylation of the C-terminal carboxylic acid group has been observed in various pathways. While further structure−activity studies are necessary to fully define the significance of C-terminal decarboxylation in terms of stability and activity, there are obvious benefits to this reaction for peptides. For instance, removing the C-terminal carboxylic acid group can reduce degradation by carboxypeptidases due to the crucial role of the carboxylic acid functionality in carboxypeptidase substrate binding.[192] Decarboxylation improves the membrane permeability of peptides,[193] and facilitates cyclization processes, as evidenced by mycofactocin and Avi(Me)Cys-containing natural products.[100,115] With an eye toward applications, decarboxylases present in RiPP BGCs may also find utility in surface display methods that allow free C-termini as in certain subtypes of phage and yeast display.[194,195]

With the rapid progress in genome sequencing and genome mining techniques, an increasing number of biosynthetic pathways are being elucidated, shedding light on the catalytic role of decarboxylation by novel classes of enzymes. Recent developments have unveiled fascinating examples, such as the iron-type alcohol dehydrogenase-like enzyme MpaBC involved in daptides biosynthesis,[77] as well as multinuclear nonheme iron-dependent oxidative enzymes capable of catalyzing a four-electron oxidative decarboxylation.[116] These discoveries highlight the potential for the future discovery of novel decarboxylases and their diverse substrates. Since decarboxylation is by its very nature a 'traceless' reaction, we anticipate that numerous new natural product decarboxylases remain to be uncovered. This exploration will invariably lead to the discovery of novel enzyme classes, expanding our current understanding and offering possibilities for harnessing decarboxylases to produce valuable compounds, including biofuels, fine chemicals, and medicines.

AUTHOR INFORMATION

Corresponding Author

John A. McIntosh − *Merck & Co., Inc., Boston, Massachusetts 02115, United States;* orcid.org/0000-0002-9487-490X; Email: john.mcintosh1@merck.com

Authors

Nguyet A. Nguyen − *Merck & Co., Inc., Boston, Massachusetts 02115, United States*

Jacob H. Forstater − *Merck & Co., Inc., Rahway, New Jersey 07065, United States;* orcid.org/0000-0003-0268-1009

Complete contact information is available at: https://pubs.acs.org/10.1021/jacsau.4c00425

Author Contributions

The manuscript was written through contributions of all authors. All authors have given approval to the final version of the manuscript. CRediT: N.A.N.: writing-original draft, writing-review & editing; J.H.F.: writing-review & editing; J.A.M.: conceptualization, writing-review & editing. CRediT: **J.H.F.**: writing-review & editing; **J.A.M.**: conceptualization, writing-review & editing.

Notes

The authors declare no competing financial interest.

ACKNOWLEDGMENTS

The authors would like to thank Stephanie Galanie and Richard Ayikpoe for their insightful discussions.

REFERENCES

(1) Layer, G. Heme Biosynthesis in Prokaryotes. *Biochim. Biophys. Acta* **2021**, *1868* (1), 118861.

(2) Wei, Z.; Wilkinson, R. C.; Rashid, G. M. M.; Brown, D.; Fulop, V.; Bugg, T. D. H. Characterization of Thiamine Diphosphate-Dependent 4-Hydroxybenzoylformate Decarboxylase Enzymes from *Rhodococcus jostii* RHA1 and *Pseudomonas fluorescens* Pf-5 Involved in Degradation of Aryl C(2) Lignin Degradation Fragments. *Biochemistry* **2019**, *58* (52), 5281−5293.

(3) Cerqueira, N. M. F. S. A.; Oliveira, E. F.; Gesto, D. S.; Santos-Martins, D.; Moreira, C.; Moorthy, H. N.; Ramos, M. J.; Fernandes, P. A. Cholesterol Biosynthesis: A Mechanistic Overview. *Biochemistry* **2016**, *55* (39), 5483−5506.

(4) Walsh, C. T. Biologically Generated Carbon Dioxide: Nature's Versatile Chemical Strategies for Carboxy Lyases. *Nat. Prod. Rep.* **2020**, *37* (1), 100−135.

(5) Buchholz, P. C. F.; Ferrario, V.; Pohl, M.; Gardossi, L.; Pleiss, J. Navigating Within Thiamine Diphosphate-dependent Decarboxylases: Sequences, Structures, Functional Positions, and Binding Sites. *Proteins* **2019**, *87* (9), 774−785.

(6) Liang, J.; Han, Q.; Tan, Y.; Ding, H.; Li, J. Current Advances on Structure-Function Relationships of Pyridoxal 5′-Phosphate-Dependent Enzymes. *Front Mol. Biosci.* **2019**, *6*, 4.

(7) Li, T.; Huo, L.; Pulley, C.; Liu, A. Decarboxylation Mechanisms in Biological System. *Bioorg. Chem.* **2012**, *43*, 2−14.

(8) Andrews, F. H.; McLeish, M. J. Substrate Specificity in Thiamin Diphosphate-dependent Decarboxylases. *Bioorg. Chem.* **2012**, *43*, 26−36.

(9) Shiraishi, T.; Kuzuyama, T. Biosynthetic Pathways and Enzymes Involved in the Production of Phosphonic Acid Natural Products. *Biosci. Biotechnol. Biochem.* **2021**, *85* (1), 42−52.

(10) Liang, J.; Han, Q.; Tan, Y.; Ding, H.; Li, J. Current Advances on Structure-Function Relationships of Pyridoxal 5′-Phosphate-Dependent Enzymes. *Front. Mol. Biosci.* **2019**, *6*, 4.

(11) Du, Y. L.; Ryan, K. S. Pyridoxal Phosphate-dependent Reactions in the Biosynthesis of Natural Products. *Nat. Prod. Rep.* **2019**, *36* (3), 430−457.

(12) Jiang, Y.; Li, S., Chapter Twelve - P450 Fatty Acid Decarboxylase. In *Methods in Enzymology*; Renata, H., Ed.; Academic Press: 2023; Vol. *693*, pp 339−374.

(13) Saaret, A.; Balaikaite, A.; Leys, D. Biochemistry of Prenylated-FMN Enzymes. *Enzymes* **2020**, *47*, 517−549.

(14) Guengerich, F. P.; Yoshimoto, F. K. Formation and Cleavage of C-C Bonds by Enzymatic Oxidation-Reduction Reactions. *Chem. Rev.* **2018**, *118* (14), 6573−6655.

(15) Payer, S. E.; Faber, K.; Glueck, S. M. Non-Oxidative Enzymatic (De)Carboxylation of (Hetero)Aromatics and Acrylic Acid Derivatives. *Adv. Synth. Catal.* **2019**, *361* (11), 2402−2420.

(16) Ishchuk, O. P.; Voronovsky, A. Y.; Stasyk, O. V.; Gayda, G. Z.; Gonchar, M. V.; Abbas, C. A.; Sibirny, A. A. Overexpression of Pyruvate Decarboxylase in the Yeast *Hansenula polymorpha* Results in Increased Ethanol Yield in High-Temperature Fermentation of Xylose. *FEMS Yeast Res.* **2008**, *8* (7), 1164−1174.

(17) Harris, D. M. M.; Berrué, F.; Kerr, R.; Patten, C. L. Metabolomic Analysis of Indolepyruvate Decarboxylase Pathway Derivatives in the Rhizobacterium *Enterobacter cloacae*. *Rhizosphere* **2018**, *6*, 98−111.
(18) Hegeman, G. D. Benzoylformate Decarboxylase (*Pseudomonas putida*). *Meth. Enzymol.* **1970**, *17*, 674−678.
(19) Scott, T. A.; Heine, D.; Qin, Z.; Wilkinson, B. An L-threonine Transaldolase is Required for L-threo-β-hydroxy-α-amino Acid Assembly during Obafluorin Biosynthesis. *Nat. Commun.* **2017**, *8* (1), 15935.
(20) DiMarco, A. A.; Bobik, T. A.; Wolfe, R. S. Unusual Coenzymes of Methanogenesis. *Annu. Rev. Biochem.* **1990**, *59*, 355−94.
(21) Graupner, M.; Xu, H.; White, R. H. Identification of the Gene Encoding Sulfopyruvate Decarboxylase, an Enzyme Involved in Biosynthesis of Coenzyme M. *J. Bacteriol.* **2000**, *182* (17), 4862−4867.
(22) Allen, J. R.; Clark, D. D.; Krum, J. G.; Ensign, S. A. A Role for Coenzyme M (2-mercaptoethanesulfonic Acid) in a Bacterial Pathway of Aliphatic Epoxide Carboxylation. *Proc. Natl. Acad. Sci. U. S. A.* **1999**, *96* (15), 8432−7.
(23) Zhang, G.; Dai, J.; Lu, Z.; Dunaway-Mariano, D. The Phosphonopyruvate Decarboxylase from Bacteroides fragilis. *J. Biol. Chem.* **2003**, *278* (42), 41302−41308.
(24) Walsh, C. T.; Tang, Y. *Natural Product Biosynthesis: Chemical Logic and Enzymatic Machinery*; The Royal Society of Chemistry: 2017.
(25) Nakashita, H.; Watanabe, K.; Hara, O.; Hidaka, T.; Seto, H. Studies on the Biosynthesis of Bialaphos. Biochemical Mechanism of C-P Bond Formation: Discovery of Phosphonopyruvate Decarboxylase which Catalyzes the Formation of Phosphonoacetaldehyde From Phosphonopyruvate. *J. Antibiot.* **1997**, *50* (3), 212−9.
(26) Woodyer, R. D.; Shao, Z.; Thomas, P. M.; Kelleher, N. L.; Blodgett, J. A. V.; Metcalf, W. W.; van der Donk, W. A.; Zhao, H. Heterologous Production of Fosfomycin and Identification of the Minimal Biosynthetic Gene Cluster. *Chem. Biol.* **2006**, *13* (11), 1171−1182.
(27) Alexander, F. W.; Sandmeier, E.; Mehta, P. K.; Christen, P. Evolutionary Relationships Among Pyridoxal-5′-phosphate-dependent Enzymes. Regio-specific Alpha, Beta and Gamma Families. *Eur. J. Biochem.* **1994**, *219* (3), 953−60.
(28) Takaishi, M.; Kudo, F.; Eguchi, T. Identification of The Incednine Biosynthetic Gene Cluster: Characterization of Novel β-Glutamate-β-Decarboxylase IdnL3. *J. Antibiot.* **2013**, *66* (12), 691−699.
(29) Liang, J.; Han, Q.; Ding, H.; Li, J. Biochemical identification of residues that discriminate between 3,4-dihydroxyphenylalanine decarboxylase and 3,4-dihydroxyphenylacetaldehyde synthase-mediated reactions. *Insect Biochem. Mol. Biol.* **2017**, *91*, 34−43.
(30) Lichman, B. R. The Scaffold-forming Steps of Plant Alkaloid Biosynthesis. *Nat. Prod. Rep.* **2021**, *38* (1), 103−129.
(31) Spiering, M. J.; Moon, C. D.; Wilkinson, H. H.; Schardl, C. L. Gene Clusters for Insecticidal Loline Alkaloids in the Grass-Endophytic Fungus *Neotyphodium uncinatum*. *Genetics* **2005**, *169* (3), 1403−1414.
(32) Gao, J.; Liu, S.; Zhou, C.; Lara, D.; Zou, Y.; Hai, Y. A Pyridoxal 5′-phosphate-dependent Mannich Cyclase. *Nat. Catal.* **2023**, *6* (6), 476−486.
(33) Liu, S.; Hai, Y. Chemoenzymatic Approaches to Izidine Alkaloids: An Efficient Total Synthesis of (+)-Absouline and Laburnamine. *ACS Catal.* **2023**, *13* (24), 15725−15729.
(34) Cui, Z.; Overbay, J.; Wang, X.; Liu, X.; Zhang, Y.; Bhardwaj, M.; Lemke, A.; Wiegmann, D.; Niro, G.; Thorson, J. S.; Ducho, C.; Van Lanen, S. G. Pyridoxal-5′-phosphate-dependent Alkyl Transfer in Nucleoside Antibiotic Biosynthesis. *Nat. Chem. Biol.* **2020**, *16* (8), 904−911.
(35) Zadeh, S. M.; Chen, M.-H.; Wang, Z.-C.; Astani, E. K.; Lo, I. W.; Lin, K.-H.; Hsu, N.-S.; Adhikari, K.; Lyu, S.-Y.; Tsai, H.-Y.; Terasawa, Y.; Yabe, M.; Yamamoto, K.; Ichikawa, S.; Li, T.-L. β-Hydroxylation of α-amino-β-hydroxylbutanoyl-glycyluridine Catalyzed by a Nonheme Hydroxylase Ensures the Maturation of Caprazamycin. *Commun. Chem.* **2022**, *5* (1), 87.
(36) Metlitskaya, A.; Kazakov, T.; Kommer, A.; Pavlova, O.; Praetorius-Ibba, M.; Ibba, M.; Krasheninnikov, I.; Kolb, V.; Khmel, I.; Severinov, K. Aspartyl-tRNA Synthetase Is the Target of Peptide Nucleotide Antibiotic Microcin C. *J. Biol. Chem.* **2006**, *281* (26), 18033−18042.
(37) Roush, R. F.; Nolan, E. M.; Löhr, F.; Walsh, C. T. Maturation of an *Escherichia coli* ribosomal peptide antibiotic by ATP-consuming N-P bond formation in microcin C7. *J. Am. Chem. Soc.* **2008**, *130* (11), 3603−9.
(38) Dong, S. H.; Kulikovsky, A.; Zukher, I.; Estrada, P.; Dubiley, S.; Severinov, K.; Nair, S. K. Biosynthesis of the RiPP trojan horse nucleotide antibiotic microcin C is directed by the N-formyl of the peptide precursor. *Chem. Sci.* **2019**, *10* (8), 2391−2395.
(39) Kulikovsky, A.; Serebryakova, M.; Bantysh, O.; Metlitskaya, A.; Borukhov, S.; Severinov, K.; Dubiley, S. The Molecular Mechanism of Aminopropylation of Peptide-Nucleotide Antibiotic Microcin C. *J. Am. Chem. Soc.* **2014**, *136* (31), 11168−75.
(40) Novikova, M.; Kazakov, T.; Vondenhoff, G. H.; Semenova, E.; Rozenski, J.; Metlytskaya, A.; Zukher, I.; Tikhonov, A.; Van Aerschot, A.; Severinov, K. MccE Provides Resistance to Protein Synthesis Inhibitor Microcin C by Acetylating the Processed Form of the Antibiotic. *J. Biol. Chem.* **2010**, *285* (17), 12662−12669.
(41) Agarwal, V.; Metlitskaya, A.; Severinov, K.; Nair, S. K. Structural Basis for Microcin C7 Inactivation by the MccE Acetyltransferase. *J. Biol. Chem.* **2011**, *286* (24), 21295−303.
(42) Metlitskaya, A.; Kazakov, T.; Vondenhoff, G. H.; Novikova, M.; Shashkov, A.; Zatsepin, T.; Semenova, E.; Zaitseva, N.; Ramensky, V.; Aerschot, A. V.; Severinov, K. Maturation of the Translation Inhibitor Microcin C. *J. Bacteriol.* **2009**, *191* (7), 2380−2387.
(43) Bantysh, O.; Serebryakova, M.; Makarova, K. S.; Dubiley, S.; Datsenko, K. A.; Severinov, K. Enzymatic Synthesis of Bioinformatically Predicted Microcin C-like Compounds Encoded by Diverse Bacteria. *mBio* **2014**, *5* (3), No. e01059-14.
(44) Llewellyn, N. M.; Li, Y.; Spencer, J. B. Biosynthesis of Butirosin: Transfer and Deprotection of the Unique Amino Acid Side Chain. *Chem. Biol.* **2007**, *14* (4), 379−86.
(45) Barajas, J. F.; Zargar, A.; Pang, B.; Benites, V. T.; Gin, J.; Baidoo, E. E. K.; Petzold, C. J.; Hillson, N. J.; Keasling, J. D. Biochemical Characterization of β-Amino Acid Incorporation in Fluvirucin B(2) Biosynthesis. *Chembiochem* **2018**, *19* (13), 1391−1395.
(46) Dunbar, K. L.; Dell, M.; Gude, F.; Hertweck, C. Reconstitution of Polythioamide Antibiotic Backbone Formation Reveals Unusual Thiotemplated Assembly Strategy. *Proc. Natl. Acad. Sci. U. S. A.* **2020**, *117* (16), 8850−8858.
(47) Rivas Arenas, L. A.; de Paiva, F. C. R.; de O. Rossini, N.; Li, Y.; Spencer, J.; Leadlay, P.; Dias, M. V. B. Crystal Structure of BtrK, a Decarboxylase Involved in the (S)-4-amino-2-hydroxybutyrate (AHBA) Formation During Butirosin Biosynthesis. *J. Mol. Struct.* **2022**, *1267*, 133576.
(48) Cox, G.; Ejim, L.; Stogios, P. J.; Koteva, K.; Bordeleau, E.; Evdokimova, E.; Sieron, A. O.; Savchenko, A.; Serio, A. W.; Krause, K. M.; Wright, G. D. Plazomicin Retains Antibiotic Activity against Most Aminoglycoside Modifying Enzymes. *ACS Infect. Dis.* **2018**, *4* (6), 980−987.
(49) Li, Y.; Llewellyn, N. M.; Giri, R.; Huang, F.; Spencer, J. B. Biosynthesis of the Unique Amino Acid Side Chain of Butirosin: Possible Protective-Group Chemistry in an Acyl Carrier Protein-Mediated Pathway. *Chem. Biol.* **2005**, *12* (6), 665−675.
(50) Kudo, F.; Miyanaga, A.; Eguchi, T. Biosynthesis of Natural Products Containing Beta-amino Acids. *Nat. Prod. Rep.* **2014**, *31* (8), 1056−73.
(51) Li, Y.; Llewellyn, N. M.; Giri, R.; Huang, F.; Spencer, J. B. Biosynthesis of the unique amino acid side chain of butirosin: possible protective-group chemistry in an acyl carrier protein-mediated pathway. *Chem Biol* **2005**, *12* (6), 665−75.
(52) Sonousi, A.; Sarpe, V. A.; Brilkova, M.; Schacht, J.; Vasella, A.; Bottger, E. C.; Crich, D. Effects of the 1- N-(4-Amino-2 S-hydroxybutyryl) and 6'- N-(2-Hydroxyethyl) Substituents on Ribosomal Selectivity, Cochleotoxicity, and Antibacterial Activity in the Sisomicin Class of Aminoglycoside Antibiotics. *ACS Infect. Dis.* **2018**, *4* (7), 1114−1120.

https://doi.org/10.1021/jacsau.4c00425
JACS Au 2024, 4, 2715−2745

(53) Miyanaga, A. Biosynthesis of β-Amino Acid-Containing Macrolactam Polyketides. *New Tide of Natural Product Chemistry* **2023**, 147−176.
(54) Zhao, W.; Jiang, H.; Liu, X. W.; Zhou, J.; Wu, B. Polyene Macrolactams from Marine and Terrestrial Sources: Structure, Production Strategies, Biosynthesis and Bioactivities. *Mar Drugs* **2022**, *20* (6), 360.
(55) White, M. D.; Payne, K. A. P.; Fisher, K.; Marshall, S. A.; Parker, D.; Rattray, N. J. W.; Trivedi, D. K.; Goodacre, R.; Rigby, S. E. J.; Scrutton, N. S.; Hay, S.; Leys, D. UbiX is a Flavin Prenyltransferase Required for Bacterial Ubiquinone Biosynthesis. *Nature* **2015**, *522* (7557), 502−506.
(56) Koelschbach, J. S.; Mouttaki, H.; Merl-Pham, J.; Arnold, M. E.; Meckenstock, R. U. Identification of Naphthalene Carboxylase Subunits of the Sulfate-reducing Culture N47. *Biodegradation* **2019**, *30* (2−3), 147−160.
(57) Payne, K. A. P.; White, M. D.; Fisher, K.; Khara, B.; Bailey, S. S.; Parker, D.; Rattray, N. J. W.; Trivedi, D. K.; Goodacre, R.; Beveridge, R.; Barran, P.; Rigby, S. E. J.; Scrutton, N. S.; Hay, S.; Leys, D. New cofactor supports α,β-unsaturated acid decarboxylation via 1,3-dipolar cycloaddition. *Nature* **2015**, *522* (7557), 497−501.
(58) Payer, S. E.; Marshall, S. A.; Bärland, N.; Sheng, X.; Reiter, T.; Dordic, A.; Steinkellner, G.; Wuensch, C.; Kaltwasser, S.; Fisher, K.; Rigby, S. E. J.; Macheroux, P.; Vonck, J.; Gruber, K.; Faber, K.; Himo, F.; Leys, D.; Pavkov-Keller, T.; Glueck, S. M. Regioselective para-Carboxylation of Catechols with a Prenylated Flavin Dependent Decarboxylase. *Angew. Chem., Int. Ed. Engl.* **2017**, *56* (44), 13893−13897.
(59) Roberts, G. W.; Leys, D. Structural insights into UbiD reversible decarboxylation. *Curr. Opin. Struct. Biol.* **2022**, *75*, 102432.
(60) Annaval, T.; Han, L.; Rudolf, J. D.; Xie, G.; Yang, D.; Chang, C. Y.; Ma, M.; Crnovcic, I.; Miller, M. D.; Soman, J.; Xu, W.; Phillips, G. N., Jr; Shen, B. Biochemical and Structural Characterization of TtnD, a Prenylated FMN-Dependent Decarboxylase from the Tautomycetin Biosynthetic Pathway. *ACS Chem. Biol.* **2018**, *13* (9), 2728−2738.
(61) Wang, B.; Song, Y.; Luo, M.; Chen, Q.; Ma, J.; Huang, H.; Ju, J. Biosynthesis of 9-Methylstreptimidone Involves a New Decarboxylative Step for Polyketide Terminal Diene Formation. *Org. Lett.* **2013**, *15* (6), 1278−1281.
(62) Bar-Tana, J.; Howlett, B. J.; Hertz, R. Ubiquinone Synthetic Pathway in Flagellation of *Salmonella typhimurium*. *J. Bacteriol.* **1980**, *143* (2), 637−43.
(63) Bloor, S.; Michurin, I.; Titchiner, G. R.; Leys, D. Prenylated Flavins: Structures and Mechanisms. *FEBS J.* **2023**, *290* (9), 2232−2245.
(64) Kobayashi, Y.; Ko, K.; Yamaguchi, I.; Snen, Y.-C.; Isono, K. A New Antibiotic, Tautomycetin. *J. Antibiot.* **1989**, *42* (1), 141−144.
(65) Choy, M. S.; Swingle, M.; D'Arcy, B.; Abney, K.; Rusin, S. F.; Kettenbach, A. N.; Page, R.; Honkanen, R. E.; Peti, W. PP1:Tautomycetin Complex Reveals a Path toward the Development of PP1-Specific Inhibitors. *J. Am. Chem. Soc.* **2017**, *139* (49), 17703−17706.
(66) Li, W.; Luo, Y.; Ju, J.; Rajski, S. R.; Osada, H.; Shen, B. Characterization of The Tautomycetin Biosynthetic Gene Cluster from *Streptomyces griseochromogenes* Provides New Insight Into Dialkylmaleic Anhydride Biosynthesis. *J. Nat. Prod.* **2009**, *72* (3), 450−9.
(67) Saito, N.; Kitame, F.; Kikuchi, M.; Ishida, N. Studies on a New Antiviral Antibiotic, 9-methylstreptimidone. *J. Antibiot.* **1974**, *27* (3), 206−14.
(68) Urakawa, A.; Otani, T.; Yoshida, K.; Nakayama, M.; Suzukake-Tsuchiya, K.; Hori, M. Isolation, Structure Determination and Biological Activities of a Novel Antifungal Antibiotic, S-632-C, Closely Related To Glutarimide Antibiotics. *J. Antibiot.* **1993**, *46* (12), 1827−33.
(69) Takeiri, M.; Ota, E.; Nishiyama, S.; Kiyota, H.; Umezawa, K. Structure-activity Relationship of 9-methylstreptimidone, a Compound that Induces Apoptosis Selectively in Adult T-Cell Leukemia Cells. *Oncol. Res.* **2012**, *20* (1), 7−14.
(70) Lindberg, M.; Gautschi, F.; Bloch, K. Ketonic Intermediates in the Demethylation of Lanosterol. *J. Biol. Chem.* **1963**, *238* (5), 1661−1664.
(71) Pollack, R. M. Decarboxylations of β-Keto Acids and Related Compounds. In *Transition States of Biochemical Processes*; Gandour, R. D., Schowen, R. L., Eds.; Springer US: Boston, MA, 1978; pp 467−492.
(72) Peltier-Pain, P.; Singh, S.; Thorson, J. S. Characterization of Early Enzymes Involved in TDP-Aminodideoxypentose Biosynthesis en Route to Indolocarbazole AT2433. *Chembiochem* **2015**, *16* (15), 2141−6.
(73) Dulin, C. C.; Sharma, P.; Frigo, L.; Voehler, M. W.; Iverson, T. M.; Bachmann, B. O. EvdS6 is a Bifunctional Decarboxylase from the Everninomicin Gene Cluster. *J. Biol. Chem.* **2023**, *299* (7), 104893.
(74) Yang, C. L.; Zhang, B.; Xue, W. W.; Li, W.; Xu, Z. F.; Shi, J.; Shen, Y.; Jiao, R. H.; Tan, R. X.; Ge, H. M. Discovery, Biosynthesis, and Heterologous Production of Loonamycin, a Potent Anticancer Indolocarbazole Alkaloid. *Org. Lett.* **2020**, *22* (12), 4665−4669.
(75) Bennallack, P. R.; Burt, S. R.; Heder, M. J.; Robison, R. A.; Griffitts, J. S. Characterization of a Novel Plasmid-borne Thiopeptide Gene Cluster in *Staphylococcus epidermidis* Strain 115. *J. Bacteriol.* **2014**, *196* (24), 4344−50.
(76) Bewley, K. D.; Bennallack, P. R.; Burlingame, M. A.; Robison, R. A.; Griffitts, J. S.; Miller, S. M. Capture of Micrococcin Biosynthetic Intermediates Reveals C-terminal Processing as an Obligatory Step For *in vivo* Maturation. *Proc. Natl. Acad. Sci. U. S. A.* **2016**, *113* (44), 12450−12455.
(77) Ren, H.; Dommaraju, S. R.; Huang, C.; Cui, H.; Pan, Y.; Nesic, M.; Zhu, L.; Sarlah, D.; Mitchell, D. A.; Zhao, H. Genome Mining Unveils a Class of Ribosomal Peptides with Two Amino Termini. *Nat. Commun.* **2023**, *14* (1), 1624.
(78) Ma, S.; Zhang, Q. Linaridin Natural Products. *Nat. Prod. Rep.* **2020**, *37* (9), 1152−1163.
(79) Li, B.; Walsh, C. T. Identification of the Gene Cluster for the Dithiolopyrrolone Antibiotic Holomycin in *Streptomyces clavuligerus*. *Proc. Natl. Acad. Sci. U. S. A.* **2010**, *107* (46), 19731−19735.
(80) Rupprath, C.; Schumacher, T.; Elling, L. Nucleotide Deoxysugars: Essential Tools for the Glycosylation Engineering of Novel Bioactive Compounds. *Curr. Med. Chem.* **2005**, *12* (14), 1637−75.
(81) Marino, C.; Bordoni, A. V. Deoxy Sugars. General Methods for Carbohydrate Deoxygenation and Glycosidation. *Org. Biomol. Chem.* **2022**, *20* (5), 934−962.
(82) Filling, C.; Berndt, K. D.; Benach, J.; Knapp, S.; Prozorovski, T.; Nordling, E.; Ladenstein, R.; Jörnvall, H.; Oppermann, U. Critical Residues for Structure and Catalysis in Short-chain Dehydrogenases/Reductases *. *J. Biol. Chem.* **2002**, *277* (28), 25677−25684.
(83) Kavanagh, K. L.; Jörnvall, H.; Persson, B.; Oppermann, U. Medium- and short-chain dehydrogenase/reductase gene and protein families. *Cell. Mol. Life Sci.* **2008**, *65* (24), 3895.
(84) Borg, A. J. E.; Beerens, K.; Pfeiffer, M.; Desmet, T.; Nidetzky, B. Stereo-electronic control of reaction selectivity in short-chain dehydrogenases: Decarboxylation, epimerization, and dehydration. *Curr. Opin. Chem. Biol.* **2021**, *61*, 43−52.
(85) Gatzeva-Topalova, P. Z.; May, A. P.; Sousa, M. C. Structure and Mechanism of ArnA: Conformational Change Implies Ordered Dehydrogenase Mechanism in Key Enzyme for Polymyxin Resistance. *Structure* **2005**, *13* (6), 929−42.
(86) Eixelsberger, T.; Sykora, S.; Egger, S.; Brunsteiner, M.; Kavanagh, K. L.; Oppermann, U.; Brecker, L.; Nidetzky, B. Structure and Mechanism of Human UDP-xylose Synthase: Evidence for a Promoting Role of Sugar Ring Distortion in a Three-Step Catalytic Conversion of Udp-Glucuronic Acid. *J. Biol. Chem.* **2012**, *287* (37), 31349−31358.
(87) Polizzi, S. J.; Walsh, R. M., Jr; Peeples, W. B.; Lim, J.-M.; Wells, L.; Wood, Z. A. Human UDP-α-d-xylose Synthase and Escherichia coli ArnA Conserve a Conformational Shunt That Controls Whether Xylose or 4-Keto-Xylose Is Produced. *Biochemistry* **2012**, *51* (44), 8844−8855.
(88) Degiacomi, G.; Personne, Y.; Mondésert, G.; Ge, X.; Mandava, C. S.; Hartkoorn, R. C.; Boldrin, F.; Goel, P.; Peisker, K.; Benjak, A.; Barrio, M. B.; Ventura, M.; Brown, A. C.; Leblanc, V.; Bauer, A.; Sanyal,

https://doi.org/10.1021/jacsau.4c00425
JACS Au 2024, 4, 2715−2745

S.; Cole, S. T.; Lagrange, S.; Parish, T.; Manganelli, R. Micrococcin P1 - A Bactericidal Thiopeptide Active Against *Mycobacterium tuberculosis*. *Tuberculosis* **2016**, *100*, 95−101.
(89) Strauss, E.; Zhai, H.; Brand, L. A.; McLafferty, F. W.; Begley, T. P. Mechanistic Studies on Phosphopantothenoylcysteine Decarboxylase: Trapping of an Enethiolate Intermediate with a Mechanism-Based Inactivating Agent. *Biochemistry* **2004**, *43* (49), 15520−15533.
(90) Fraaije, M. W.; van den Heuvel, R. H. H.; Roelofs, J. C. A. A.; van Berkel, W. J. H. Kinetic Mechanism of Vanillyl-alcohol Oxidase with Short-chain 4-alkylphenols. *Eur. J. Biochem.* **1998**, *253* (3), 712−719.
(91) El Gamal, A.; Agarwal, V.; Diethelm, S.; Rahman, I.; Schorn, M. A.; Sneed, J. M.; Louie, G. V.; Whalen, K. E.; Mincer, T. J.; Noel, J. P.; Paul, V. J.; Moore, B. S. Biosynthesis of coral settlement cue tetrabromopyrrole in marine bacteria by a uniquely adapted brominase-thioesterase enzyme pair. *Proc. Natl. Acad. Sci. U.S.A* **2016**, *113* (14), 3797−3802.
(92) Agarwal, V.; El Gamal, A. A.; Yamanaka, K.; Poth, D.; Kersten, R. D.; Schorn, M.; Allen, E. E.; Moore, B. S. Biosynthesis of polybrominated aromatic organic compounds by marine bacteria. *Nat. Chem. Biol.* **2014**, *10* (8), 640−647.
(93) Ewing, T. A.; Fraaije, M. W.; Mattevi, A.; van Berkel, W. J. H. The VAO/PCMH Flavoprotein Family. *Arch. Biochem. Biophys.* **2017**, *632*, 104−117.
(94) Rachid, S.; Revermann, O.; Dauth, C.; Kazmaier, U.; Müller, R. Characterization of a Novel Type of Oxidative Decarboxylase Involved in the Biosynthesis of the Styryl Moiety of Chondrochloren from an Acylated Tyrosine. *J. Biol. Chem.* **2010**, *285* (17), 12482−12489.
(95) Brady, S. F.; Clardy, J. Synthesis of Long-Chain Fatty Acid Enol Esters Isolated from an Environmental DNA Clone. *Org. Lett.* **2003**, *5* (2), 121−124.
(96) Kupke, T.; Kempter, C.; Gnau, V.; Jung, G.; Götz, F. Mass Spectroscopic Analysis of a Novel Enzymatic Reaction. Oxidative Decarboxylation of the Lantibiotic Precursor Peptide EpiA Catalyzed by the Flavoprotein EpiD. *J. Biol. Chem.* **1994**, *269* (8), 5653−5659.
(97) Lu, J.; Li, J.; Wu, Y.; Fang, X.; Zhu, J.; Wang, H. Characterization of the FMN-Dependent Cysteine Decarboxylase from Thioviridamide Biosynthesis. *Org. Lett.* **2019**, *21* (12), 4676−4679.
(98) Ortega, M. A.; Cogan, D. P.; Mukherjee, S.; Garg, N.; Li, B.; Thibodeaux, G. N.; Maffioli, S. I.; Donadio, S.; Sosio, M.; Escano, J.; Smith, L.; Nair, S. K.; van der Donk, W. A. Two Flavoenzymes Catalyze the Post-Translational Generation of 5-Chlorotryptophan and 2-Aminovinyl-Cysteine during NAI-107 Biosynthesis. *ACS Chem. Biol.* **2017**, *12* (2), 548−557.
(99) Mo, T.; Liu, W.-Q.; Ji, W.; Zhao, J.; Chen, T.; Ding, W.; Yu, S.; Zhang, Q. Biosynthetic Insights into Linaridin Natural Products from Genome Mining and Precursor Peptide Mutagenesis. *ACS Chem. Biol.* **2017**, *12* (6), 1484−1488.
(100) Grant-Mackie, E. S.; Williams, E. T.; Harris, P. W. R.; Brimble, M. A. Aminovinyl Cysteine Containing Peptides: A Unique Motif That Imparts Key Biological Activity. *J. Am. Chem. Soc. Au* **2021**, *1* (10), 1527−1540.
(101) Strauss, E.; Begley, T. P. Mechanistic Studies on Phosphopantothenoylcysteine Decarboxylase. *J. Am. Chem. Soc.* **2001**, *123* (26), 6449−6450.
(102) Lu, J.; Li, J.; Wu, Y.; Fang, X.; Zhu, J.; Wang, H. Characterization of the FMN-Dependent Cysteine Decarboxylase from Thioviridamide Biosynthesis. *Org. Lett.* **2019**, *21* (12), 4676−4679.
(103) Bailly, C.; Riou, J. F.; Colson, P.; Houssier, C.; Rodrigues-Pereira, E.; Prudhomme, M. DNA Cleavage by Topoisomerase I in the Presence of Indolocarbazole Derivatives of Rebeccamycin. *Biochemistry* **1997**, *36* (13), 3917−29.
(104) Rüegg, U. T.; Burgess, G. M. Staurosporine, K-252 and UCN-01: Potent but Nonspecific Inhibitors of Protein Kinases. *Trends Pharmacol. Sci.* **1989**, *10* (6), 218−20.
(105) Jimeno, A.; Rudek, M. A.; Purcell, T.; Laheru, D. A.; Messersmith, W. A.; Dancey, J.; Carducci, M. A.; Baker, S. D.; Hidalgo, M.; Donehower, R. C. Phase I and Pharmacokinetic Study of UCN-01 in Combination with Irinotecan in Patients with Solid Tumors. *Cancer Chemother. Pharmacol.* **2008**, *61* (3), 423−33.
(106) Nock, C. J.; Brell, J. M.; Bokar, J. A.; Cooney, M. M.; Cooper, B.; Gibbons, J.; Krishnamurthi, S.; Manda, S.; Savvides, P.; Remick, S. C.; Ivy, P.; Dowlati, A. A Phase I Study of Rebeccamycin Analog in Combination with Oxaliplatin in Patients with Refractory Solid Tumors. *Invest. New Drugs* **2011**, *29* (1), 126−30.
(107) ASAMIZU, S.; SHIRO, Y.; IGARASHI, Y.; NAGANO, S.; ONAKA, H. Characterization and Functional Modification of StaC and RebC, Which Are Involved in the Pyrrole Oxidation of Indolocarbazole Biosynthesis. *Biosci. Biotechnol. Biochem.* **2011**, *75* (11), 2184−2193.
(108) Groom, K.; Bhattacharya, A.; Zechel, D. L. Rebeccamycin and Staurosporine Biosynthesis: Insight into the Mechanisms of the Flavin-Dependent Monooxygenases RebC and StaC. *ChemBioChem* **2011**, *12* (3), 396−400.
(109) Goldman, P. J.; Ryan, K. S.; Hamill, M. J.; Howard-Jones, A. R.; Walsh, C. T.; Elliott, S. J.; Drennan, C. L. An Unusual Role for A Mobile Flavin in Stac-like Indolocarbazole Biosynthetic Enzymes. *Chem. Biol.* **2012**, *19* (7), 855−65.
(110) Broderick, J. B.; Duffus, B. R.; Duschene, K. S.; Shepard, E. M. Radical S-Adenosylmethionine Enzymes. *Chem. Rev.* **2014**, *114* (8), 4229−4317.
(111) Haft, D. H.; Basu, M. K. Biological Systems Discovery in Silico: Radical S-Adenosylmethionine Protein Families and Their Target Peptides for Posttranslational Modification. *J. Bacteriol.* **2011**, *193* (11), 2745−55.
(112) Mendauletova, A.; Kostenko, A.; Lien, Y.; Latham, J. How a Subfamily of Radical S-Adenosylmethionine Enzymes Became a Mainstay of Ribosomally Synthesized and Post-translationally Modified Peptide Discovery. *ACS Bio. Med. Chem. Au* **2022**, *2* (1), 53−59.
(113) Khaliullin, B.; Ayikpoe, R.; Tuttle, M.; Latham, J. A. Mechanistic Elucidation of the Mycofactocin-biosynthetic Radical S-adenosylmethionine Protein, MftC. *J. Biol. Chem.* **2017**, *292* (31), 13022−13033.
(114) Ayikpoe, R.; Ngendahimana, T.; Langton, M.; Bonitatibus, S.; Walker, L. M.; Eaton, S. S.; Eaton, G. R.; Pandelia, M.-E.; Elliott, S. J.; Latham, J. A. Spectroscopic and Electrochemical Characterization of the Mycofactocin Biosynthetic Protein, MftC, Provides Insight into Its Redox Flipping Mechanism. *Biochemistry* **2019**, *58* (7), 940−950.
(115) Khaliullin, B.; Aggarwal, P.; Bubas, M.; Eaton, G. R.; Eaton, S. S.; Latham, J. A. Mycofactocin Biosynthesis: Modification of the Peptide MftA by the Radical S-adenosylmethionine Protein MftC. *FEBS Lett.* **2016**, *590* (16), 2538−2548.
(116) Nguyen, D. T.; Zhu, L.; Gray, D. L.; Woods, T. J.; Padhi, C.; Flatt, K. M.; Mitchell, D. A.; van der Donk, W. A. Biosynthesis of Macrocyclic Peptides with C-Terminal β-Amino-α-keto Acid Groups by Three Different Metalloenzymes. *ACS Cent. Sci.* **2024**, *10* (5), 1022−1032.
(117) Ali, H. S.; Ghafoor, S.; de Visser, S. P. Density Functional Theory Study into the Reaction Mechanism of Isonitrile Biosynthesis by the Nonheme Iron Enzyme ScoE. *Top. Catal.* **2022**, *65* (1−4), 528−543.
(118) Li, H.; Liu, Y. Mechanistic Investigation of Isonitrile Formation Catalyzed by the Nonheme Iron/α-KG-Dependent Decarboxylase (ScoE). *ACS Catal.* **2020**, *10* (5), 2942−2957.
(119) Grant, J. L.; Mitchell, M. E.; Makris, T. M. Catalytic strategy for carbon-carbon bond scission by the cytochrome P450 OleT. *Proc. Natl. Acad. Sci. U.S.A* **2016**, *113* (36), 10049−10054.
(120) Yu, C.-P.; Tang, Y.; Cha, L.; Milikisiyants, S.; Smirnova, T. I.; Smirnov, A. I.; Guo, Y.; Chang, W.-c. Elucidating the Reaction Pathway of Decarboxylation-Assisted Olefination Catalyzed by a Mononuclear Non-Heme Iron Enzyme. *J. Am. Chem. Soc.* **2018**, *140* (45), 15190−15193.
(121) Shimamura, H.; Gouda, H.; Nagai, K.; Hirose, T.; Ichioka, M.; Furuya, Y.; Kobayashi, Y.; Hirono, S.; Sunazuka, T.; Ōmura, S. Structure Determination and Total Synthesis of Bottromycin A2: A Potent Antibiotic against MRSA and VRE. *Angew. Chem., Int. Ed.* **2009**, *48* (5), 914−917.
(122) Adam, S.; Franz, L.; Milhim, M.; Bernhardt, R.; Kalinina, O. V.; Koehnke, J. Characterization of the Stereoselective P450 Enzyme

https://doi.org/10.1021/jacsau.4c00425
JACS Au 2024, 4, 2715−2745

BotCYP Enables the In Vitro Biosynthesis of the Bottromycin Core Scaffold. *J. Am. Chem. Soc.* **2020**, *142* (49), 20560−20565.
(123) Franz, L.; Kazmaier, U.; Truman, A. W.; Koehnke, J. Bottromycins - biosynthesis, synthesis and activity. *Nat. Prod. Rep.* **2021**, *38* (9), 1659−1683.
(124) Rude, M. A.; Baron, T. S.; Brubaker, S.; Alibhai, M.; Cardayre, S. B. D.; Schirmer, A. Terminal Olefin (1-Alkene) Biosynthesis by a Novel P450 Fatty Acid Decarboxylase from *Jeotgalicoccus* Species. *Appl. Environ. Microbiol.* **2011**, *77* (5), 1718−1727.
(125) Pickl, M.; Kurakin, S.; CantúReinhard, F. G.; Schmid, P.; Pöcheim, A.; Winkler, C. K.; Kroutil, W.; de Visser, S. P.; Faber, K. Mechanistic Studies of Fatty Acid Activation by CYP152 Peroxygenases Reveal Unexpected Desaturase Activity. *ACS Catal.* **2019**, *9* (1), 565−577.
(126) Lin, Y.-T.; de Visser, S. P. Product Distributions of Cytochrome P450 OleTJE with Phenyl-Substituted Fatty Acids: A Computational Study. *Int. J. Mol. Sci.* **2021**, *22* (13), 7172.
(127) Matthews, S.; Belcher, J. D.; Tee, K. L.; Girvan, H. M.; McLean, K. J.; Rigby, S. E.; Levy, C. W.; Leys, D.; Parker, D. A.; Blankley, R. T.; Munro, A. W. Catalytic Determinants of Alkene Production by the Cytochrome P450 Peroxygenase OleT(JE). *J. Biol. Chem.* **2017**, *292* (12), 5128−5143.
(128) Rade, L. L.; Generoso, W. C.; Das, S.; Souza, A. S.; Silveira, R. L.; Avila, M. C.; Vieira, P. S.; Miyamoto, R. Y.; Lima, A. B. B.; Aricetti, J. A.; de Melo, R. R.; Milan, N.; Persinoti, G. F.; Bonomi, A.; Murakami, M. T.; Makris, T. M.; Zanphorlin, L. M. Dimer-assisted Mechanism of (Un)Saturated Fatty Acid Decarboxylation for Alkene Production. *Proc. Natl. Acad. Sci. U. S. A.* **2023**, *120* (22), No. e2221483120.
(129) Ittiamornkul, K.; Zhu, Q.; Gkotsi, D. S.; Smith, D. R. M.; Hillwig, M. L.; Nightingale, N.; Goss, R. J. M.; Liu, X. Promiscuous Indolyl Vinyl Isonitrile Synthases in the Biogenesis and Diversification of Hapalindole-type Alkaloids. *Chem. Sci.* **2015**, *6* (12), 6836−6840.
(130) Bhat, V.; Dave, A.; MacKay, J. A.; Rawal, V. H. The Chemistry of Hapalindoles, Fischerindoles, Ambiguines, and Welwitindolinones. *Alkaloids Chem Biol* **2014**, *73*, 65−160.
(131) Hillwig, M. L.; Zhu, Q.; Liu, X. Biosynthesis of Ambiguine Indole Alkaloids in Cyanobacterium Fischerella ambigua. *ACS Chemical Biology* **2014**, *9* (2), 372−377.
(132) Bhat, V.; Dave, A.; MacKay, J. A.; Rawal, V. H. The Chemistry of Hapalindoles, Fischerindoles, Ambiguines, and Welwitindolinones. *Alkaloids Chem. Biol.* **2014**, *73*, 65−160.
(133) Hillwig, M. L.; Zhu, Q.; Liu, X. Biosynthesis of Ambiguine Indole Alkaloids in Cyanobacterium *Fischerella ambigua*. *ACS Chem. Biol.* **2014**, *9* (2), 372−377.
(134) Brady, S. F.; Clardy, J. Cloning And Heterologous Expression of Isocyanide Biosynthetic Genes from Environmental DNA. *Angew. Chem., Int. Ed. Engl.* **2005**, *44* (43), 7063−5.
(135) Huang, J.-L.; Tang, Y.; Yu, C.-P.; Sanyal, D.; Jia, X.; Liu, X.; Guo, Y.; Chang, W.-c. Mechanistic Investigation of Oxidative Decarboxylation Catalyzed by Two Iron(II)- and 2-Oxoglutarate-Dependent Enzymes. *Biochemistry* **2018**, *57* (12), 1838−1841.
(136) Chang, W.-c.; Sanyal, D.; Huang, J.-L.; Ittiamornkul, K.; Zhu, Q.; Liu, X. In Vitro Stepwise Reconstitution of Amino Acid Derived Vinyl Isocyanide Biosynthesis: Detection of an Elusive Intermediate. *Org. Lett.* **2017**, *19* (5), 1208−1211.
(137) Ittiamornkul, K.; Zhu, Q.; Gkotsi, D. S.; Smith, D. R. M.; Hillwig, M. L.; Nightingale, N.; Goss, R. J. M.; Liu, X. Promiscuous indolyl vinyl isonitrile synthases in the biogenesis and diversification of hapalindole-type alkaloids. *Chemical Science* **2015**, *6* (12), 6836−6840.
(138) Harris, N. C.; Born, D. A.; Cai, W.; Huang, Y.; Martin, J.; Khalaf, R.; Drennan, C. L.; Zhang, W. Isonitrile Formation by a Non-Heme Iron(II)-Dependent Oxidase/Decarboxylase. *Angew. Chem., Int. Ed.* **2018**, *57* (31), 9707−9710.
(139) Chen, T.-Y.; Chen, J.; Tang, Y.; Zhou, J.; Guo, Y.; Chang, W.-c. Pathway from N-Alkylglycine to Alkylisonitrile Catalyzed by Iron(II) and 2-Oxoglutarate-Dependent Oxygenases. *Angew. Chem., Int. Ed.* **2020**, *59* (19), 7367−7371.
(140) Kudo, F.; Chikuma, T.; Nambu, M.; Chisuga, T.; Sumimoto, S.; Iwasaki, A.; Suenaga, K.; Miyanaga, A.; Eguchi, T. Unique Initiation and Termination Mechanisms Involved in the Biosynthesis of a Hybrid Polyketide-Nonribosomal Peptide Lyngbyapeptin B Produced by the Marine Cyanobacterium *Moorena bouillonii*. *ACS Chem. Biol.* **2023**, *18* (4), 875−883.
(141) Chang, Z.; Flatt, P.; Gerwick, W. H.; Nguyen, V.-A.; Willis, C. L.; Sherman, D. H. The Barbamide Biosynthetic Gene Cluster: a Novel Marine Cyanobacterial System of Mixed Polyketide Synthase (PKS)-Non-Ribosomal Peptide Synthetase (NRPS) Origin Involving an Unusual Trichloroleucyl Starter Unit. *Gene* **2002**, *296* (1), 235−247.
(142) Jasniewski, A. J.; Que, L. Jr., Dioxygen Activation by Nonheme Diiron Enzymes: Diverse Dioxygen Adducts, High-Valent Intermediates, and Related Model Complexes. *Chem. Rev.* **2018**, *118* (5), 2554−2592.
(143) Kenney, G. E.; Dassama, L. M. K.; Pandelia, M.-E.; Gizzi, A. S.; Martinie, R. J.; Gao, P.; DeHart, C. J.; Schachner, L. F.; Skinner, O. S.; Ro, S. Y.; Zhu, X.; Sadek, M.; Thomas, P. M.; Almo, S. C.; Bollinger, J. M.; Krebs, C.; Kelleher, N. L.; Rosenzweig, A. C. The Biosynthesis of Methanobactin. *Science* **2018**, *359* (6382), 1411−1416.
(144) Dou, C.; Long, Z.; Li, S.; Zhou, D.; Jin, Y.; Zhang, L.; Zhang, X.; Zheng, Y.; Li, L.; Zhu, X.; Liu, Z.; He, S.; Yan, W.; Yang, L.; Xiong, J.; Fu, X.; Qi, S.; Ren, H.; Chen, S.; Dai, L.; Wang, B.; Cheng, W. Crystal structure and catalytic mechanism of the MbnBC holoenzyme required for methanobactin biosynthesis. *Cell Res.* **2022**, *32* (3), 302−314.
(145) Park, Y. J.; Jodts, R. J.; Slater, J. W.; Reyes, R. M.; Winton, V. J.; Montaser, R. A.; Thomas, P. M.; Dowdle, W. B.; Ruiz, A.; Kelleher, N. L.; Bollinger, J. M., Jr; Krebs, C.; Hoffman, B. M.; Rosenzweig, A. C. A mixed-valent Fe(II)Fe(III) species converts cysteine to an oxazolone/thioamide pair in methanobactin biosynthesis. *Proc. Natl. Acad. Sci. U. S. A.* **2022**, *119* (13), No. e2123566119.
(146) McLaughlin, M. I.; Yu, Y.; van der Donk, W. A. Substrate Recognition by the Peptidyl-(S)-2-mercaptoglycine Synthase TglHI during 3-Thiaglutamate Biosynthesis. *ACS Chem. Biol.* **2022**, *17* (4), 930−940.
(147) Ayikpoe, R. S.; Zhu, L.; Chen, J. Y.; Ting, C. P.; van der Donk, W. A. Macrocyclization and Backbone Rearrangement During RiPP Biosynthesis by a SAM-Dependent Domain-of-Unknown-Function 692. *ACS Cent. Sci.* **2023**, *9* (5), 1008−1018.
(148) Rui, Z.; Li, X.; Zhu, X.; Liu, J.; Domigan, B.; Barr, I.; Cate, J. H. D.; Zhang, W. Microbial Biosynthesis of Medium-chain 1-alkenes by a Nonheme Iron Oxidase. *Proc. Natl. Acad. Sci. U. S. A.* **2014**, *111* (51), 18237−18242.
(149) Manley, O. M.; Fan, R.; Guo, Y.; Makris, T. M. Oxidative Decarboxylase UndA Utilizes a Dinuclear Iron Cofactor. *J. Am. Chem. Soc.* **2019**, *141* (22), 8684−8688.
(150) Zhang, B.; Rajakovich, L. J.; Van Cura, D.; Blaesi, E. J.; Mitchell, A. J.; Tysoe, C. R.; Zhu, X.; Streit, B. R.; Rui, Z.; Zhang, W.; Boal, A. K.; Krebs, C.; Bollinger, J. M. Jr., Substrate-Triggered Formation of a Peroxo-Fe2(III/III) Intermediate during Fatty Acid Decarboxylation by UndA. *J. Am. Chem. Soc.* **2019**, *141* (37), 14510−14514.
(151) Wang, Y.; Chen, S.-L. Mechanism for the Synthesis of Medium-chain 1-alkenes from Fatty Acids Catalyzed by Binuclear Iron UndA Decarboxylase. *J. Catal.* **2023**, *420*, 123−133.
(152) Sorigué, D.; Légeret, B.; Cuiné, S.; Blangy, S.; Moulin, S.; Billon, E.; Richaud, P.; Brugière, S.; Couté, Y.; Nurizzo, D.; Müller, P.; Brettel, K.; Pignol, D.; Arnoux, P.; Li-Beisson, Y.; Peltier, G.; Beisson, F. An Algal Photoenzyme Converts Fatty Acids to Hydrocarbons. *Science* **2017**, *357* (6354), 903−907.
(153) Hadjidemetriou, K.; Coquelle, N.; Barends, T. R. M.; De Zitter, E.; Schlichting, I.; Colletier, J.-P.; Weik, M. Time-Resolved Serial Femtosecond Crystallography on Fatty-Acid Photodecarboxylase: Lessons Learned. *Acta Crystallogr. D* **2022**, *78* (9), 1131−1142.
(154) Sorigué, D.; Hadjidemetriou, K.; Blangy, S.; Gotthard, G.; Bonvalet, A.; Coquelle, N.; Samire, P.; Aleksandrov, A.; Antonucci, L.; Benachir, A.; Boutet, S.; Byrdin, M.; Cammarata, M.; Carbajo, S.; Cuiné, S.; Doak, R. B.; Foucar, L.; Gorel, A.; Grünbein, M.; Hartmann, E.; Hienerwadel, R.; Hilpert, M.; Kloos, M.; Lane, T. J.; Légeret, B.; Legrand, P.; Li-Beisson, Y.; Moulin, S. L. Y.; Nurizzo, D.; Peltier, G.; Schirò, G.; Shoeman, R. L.; Sliwa, M.; Solinas, X.; Zhuang, B.; Barends, T. R. M.; Colletier, J.-P.; Joffre, M.; Royant, A.; Berthomieu, C.; Weik,

https://doi.org/10.1021/jacsau.4c00425
JACS Au 2024, 4, 2715−2745

M.; Domratcheva, T.; Brettel, K.; Vos, M. H.; Schlichting, I.; Arnoux, P.; Müller, P.; Beisson, F. Mechanism and Dynamics of Fatty Acid Photodecarboxylase. *Science* **2021**, *372* (6538), No. eabd5687.
(155) Wu, R.; Li, X.; Wang, L.; Zhong, D. Ultrafast Dynamics and Catalytic Mechanism of Fatty Acid Photodecarboxylase. *Angew. Chem., Int. Ed.* **2022**, *61* (50), No. e202209180.
(156) Huijbers, M. M. E.; Zhang, W.; Tonin, F.; Hollmann, F. Light-Driven Enzymatic Decarboxylation of Fatty Acids. *Angew. Chem., Int. Ed. Engl.* **2018**, *57* (41), 13648−13651.
(157) Mou, K.; Guo, Y.; Xu, W.; Li, D.; Wang, Z.; Wu, Q. Stereodivergent Protein Engineering of Fatty Acid Photodecarboxylase for Light-Driven Kinetic Resolution of Sec-Alcohol Oxalates. *Angew. Chem., Int. Ed.* **2024**, *63* (10), No. e202318374.
(158) Zheng, J.; Shen, Z.; Gao, J.-M.; Zhou, J.; Gu, Y. Enzymatic Photodecarboxylation on Secondary and Tertiary Carboxylic Acids. *Org. Lett.* **2023**, *25* (48), 8564−8569.
(159) Zhang, W.; Ma, M.; Huijbers, M. M. E.; Filonenko, G. A.; Pidko, E. A.; van Schie, M.; de Boer, S.; Burek, B. O.; Bloh, J. Z.; van Berkel, W. J. H.; Smith, W. A.; Hollmann, F. Hydrocarbon Synthesis via Photoenzymatic Decarboxylation of Carboxylic Acids. *J. Am. Chem. Soc.* **2019**, *141* (7), 3116−3120.
(160) Li, D.; Han, T.; Xue, J.; Xu, W.; Xu, J.; Wu, Q. Engineering Fatty Acid Photodecarboxylase to Enable Highly Selective Decarboxylation of trans Fatty Acids. *Angew. Chem., Int. Ed. Engl.* **2021**, *60* (38), 20695−20699.
(161) Benincá, L. A. D.; França, A. S.; Brêda, G. C.; Leão, R. A. C.; Almeida, R. V.; Hollmann, F.; de Souza, R. O. M. A. Continuous-flow CvFAP Photodecarboxylation of Palmitic Acid Under Environmentally Friendly Conditions. *Mol. Catal.* **2022**, *528*, 112469.
(162) Zhang, W.; Lee, J.-H.; Younes, S. H. H.; Tonin, F.; Hagedoorn, P.-L.; Pichler, H.; Baeg, Y.; Park, J.-B.; Kourist, R.; Hollmann, F. Photobiocatalytic Synthesis of Chiral Secondary Fatty Alcohols from Renewable Unsaturated Fatty Acids. *Nat. Commun.* **2020**, *11* (1), 2258.
(163) Qin, Z.; Zhou, Y.; Li, Z.; Höhne, M.; Bornscheuer, U. T.; Wu, S. Production of Biobased Ethylbenzene by Cascade Biocatalysis with an Engineered Photodecarboxylase. *Angew. Chem., Int. Ed.* **2024**, *63*, No. e202314566.
(164) Moulin, S.; Légeret, B.; Blangy, S.; Sorigué, D.; Burlacot, A.; Auroy, P.; Li-Beisson, Y.; Peltier, G.; Beisson, F. Continuous Photoproduction of Hydrocarbon Drop-in Fuel by Microbial Cell Factories. *Sci. Rep.* **2019**, *9* (1), 13713.
(165) Sui, Y.; Guo, X.; Zhou, R.; Fu, Z.; Chai, Y.; Xia, A.; Zhao, W. Photoenzymatic Decarboxylation to Produce Hydrocarbon Fuels: A Critical Review. *Mol. Biotechnol.* **2023**, DOI: 10.1007/s12033-023-00775-2.
(166) Bisang, C.; Long, P. F.; Cortés, J.; Westcott, J.; Crosby, J.; Matharu, A.-L.; Cox, R. J.; Simpson, T. J.; Staunton, J.; Leadlay, P. F. A Chain Initiation Factor Common to Both Modular and Aromatic Polyketide Synthases. *Nature* **1999**, *401* (6752), 502−505.
(167) Moore, B. S.; Hertweck, C. Biosynthesis and Attachment of Novel Bacterial Polyketide Synthase Starter Units. *Nat. Prod. Rep.* **2002**, *19* (1), 70−99.
(168) Chisuga, T.; Nagai, A.; Miyanaga, A.; Goto, E.; Kishikawa, K.; Kudo, F.; Eguchi, T. Structural Insight into the Reaction Mechanism of Ketosynthase-Like Decarboxylase in a Loading Module of Modular Polyketide Synthases. *ACS Chem. Biol.* **2022**, *17* (1), 198−206.
(169) Kudo, F.; Motegi, A.; Mizoue, K.; Eguchi, T. Cloning and Characterization of the Biosynthetic Gene Cluster of 16-Membered Macrolide Antibiotic FD-891: Involvement of a Dual Functional Cytochrome P450 Monooxygenase Catalyzing Epoxidation and Hydroxylation. *ChemBioChem* **2010**, *11* (11), 1574−1582.
(170) Amagai, K.; Takaku, R.; Kudo, F.; Eguchi, T. A Unique Amino Transfer Mechanism for Constructing the β-Amino Fatty Acid Starter Unit in the Biosynthesis of the Macrolactam Antibiotic Cremimycin. *ChemBioChem* **2013**, *14* (15), 1998−2006.
(171) Becerril, A.; Pérez-Victoria, I.; Ye, S.; Braña, A. F.; Martín, J.; Reyes, F.; Salas, J. A.; Méndez, C. Discovery of Cryptic Largimycins in Streptomyces Reveals Novel Biosynthetic Avenues Enriching the Structural Diversity of the Leinamycin Family. *ACS Chem. Biol.* **2020**, *15* (6), 1541−1553.
(172) Huang, Y.; Huang, S.-X.; Ju, J.; Tang, G.; Liu, T.; Shen, B. Characterization of the lnmKLM Genes Unveiling Key Intermediates for β-Alkylation in Leinamycin Biosynthesis. *Org. Lett.* **2011**, *13* (3), 498−501.
(173) Simunovic, V.; Zapp, J.; Rachid, S.; Krug, D.; Meiser, P.; Müller, R. Myxovirescin A Biosynthesis is Directed by Hybrid Polyketide Synthases/Nonribosomal Peptide Synthetase, 3-Hydroxy-3-Methylglutaryl-CoA Synthases, and trans-Acting Acyltransferases. *ChemBioChem* **2006**, *7* (8), 1206−1220.
(174) Sato, K.; Katsuyama, Y.; Yokota, K.; Awakawa, T.; Tezuka, T.; Ohnishi, Y. Involvement of β-Alkylation Machinery and Two Sets of Ketosynthase-Chain-Length Factors in the Biosynthesis of Fogacin Polyketides in *Actinoplanes missouriensis*. *ChemBioChem* **2019**, *20* (8), 1039−1050.
(175) Lohman, J. R.; Bingman, C. A.; Phillips, G. N., Jr; Shen, B. Structure of the Bifunctional Acyltransferase/Decarboxylase LnmK from the Leinamycin Biosynthetic Pathway Revealing Novel Activity for a Double-Hot-Dog Fold. *Biochemistry* **2013**, *52* (5), 902−911.
(176) Lohman, J. R.; Shen, B. The LnmK Bifunctional Acyltransferase/Decarboxylase Specifying (2R)-Methylmalonyl-CoA and Employing Substrate-Assisted Catalysis for Polyketide Biosynthesis. *Biochemistry* **2020**, *59* (43), 4143−4147.
(177) Geders, T. W.; Gu, L.; Mowers, J. C.; Liu, H.; Gerwick, W. H.; Håkansson, K.; Sherman, D. H.; Smith, J. L. Crystal Structure of the ECH2 Catalytic Domain of CurF from *Lyngbya majuscula*: Insights Into a Decarboxylase Involved in Polyketide Chain β-Branching. *J. Biol. Chem.* **2007**, *282* (49), 35954−35963.
(178) Nair, A. V.; Robson, A.; Ackrill, T. D.; Till, M.; Byrne, M. J.; Back, C. R.; Tiwari, K.; Davies, J. A.; Willis, C. L.; Race, P. R. Structure and Mechanism of a Dehydratase/Decarboxylase Enzyme Couple Involved in Polyketide β-methyl Branch Incorporation. *Sci. Rep.* **2020**, *10* (1), 15323.
(179) Qiu, M.; Shen, W.; Yan, X.; He, Q.; Cai, D.; Chen, S.; Wei, H.; Knoshaug, E. P.; Zhang, M.; Himmel, M. E.; Yang, S. Metabolic Engineering of *Zymomonas mobilis* for Anaerobic Isobutanol Production. *Biotechnol. Biofuels* **2020**, *13* (1), 15.
(180) Chen, G. S.; Siao, S. W.; Shen, C. R. Saturated Mutagenesis of Ketoisovalerate Decarboxylase V461 Enabled Specific Synthesis of 1-pentanol Via the Ketoacid Elongation Cycle. *Sci. Rep.* **2017**, *7* (1), 11284.
(181) Shen, X.; Xu, H.; Wang, T.; Zhang, R.; Sun, X.; Yuan, Q.; Wang, J. Rational Protein Engineering of a Ketoacids Decarboxylase for Efficient Production of 1,2,4-butanetriol from Arabinose. *Biotechnol. Biofuels Bioprod.* **2023**, *16* (1), 172.
(182) Chang, F.; Wang, Y.; Zhang, J.; Tu, T.; Luo, H.; Huang, H.; Bai, Y.; Qin, X.; Wang, Y.; Yao, B.; Wang, Y.; Wang, X. Efficient Production of γ-aminobutyric Acid Using Engineered *Escherichia coli* Whole-cell Catalyst. *Enzyme Microb. Technol.* **2024**, *174*, 110379.
(183) Gao, S.; Ma, D.; Wang, Y.; Zhang, A.; Wang, X.; Chen, K. Whole-cell Catalyze L-dopa to Dopamine Via Co-expression of Transport Protein AroP In *Escherichia Coli*. *BMC Biotechnol.* **2023**, *23* (1), 33.
(184) Xue, C.; Ng, I. S. A Direct Enzymatic Evaluation Platform (DEEP) to Fine-tuning Pyridoxal 5′-phosphate-dependent Proteins for Cadaverine Production. *Biotechnol. Bioeng.* **2023**, *120* (1), 272−283.
(185) Aleku, G. A.; Roberts, G. W.; Titchiner, G. R.; Leys, D. Synthetic Enzyme-Catalyzed CO(2) Fixation Reactions. *ChemSusChem* **2021**, *14* (8), 1781−1804.
(186) Martin, J.; Eisoldt, L.; Skerra, A. Fixation of Gaseous CO2 by Reversing a Decarboxylase for the Biocatalytic Synthesis of the Essential Amino Acid L-methionine. *Nat. Catal.* **2018**, *1* (7), 555−561.
(187) Payne, K. A. P.; Marshall, S. A.; Fisher, K.; Cliff, M. J.; Cannas, D. M.; Yan, C.; Heyes, D. J.; Parker, D. A.; Larrosa, I.; Leys, D. Enzymatic Carboxylation of 2-Furoic Acid Yields 2,5-Furandicarboxylic Acid (FDCA). *ACS Catal.* **2019**, *9* (4), 2854−2865.
(188) Saaret, A.; Villiers, B.; Stricher, F.; Anissimova, M.; Cadillon, M.; Spiess, R.; Hay, S.; Leys, D. Directed Evolution of Prenylated FMN-

dependent Fdc Supports Efficient *in vivo* Isobutene Production. *Nat. Commun.* **2021**, *12* (1), 5300.
(189) Nagy, E. Z. A.; Nagy, C. L.; Filip, A.; Nagy, K.; Gál, E.; Tőtős, R.; Poppe, L.; Paizs, C.; Bencze, L. C. Exploring the Substrate Scope of Ferulic Acid Decarboxylase (FDC1) from *Saccharomyces cerevisiae*. *Sci. Rep.* **2019**, *9* (1), 647.
(190) Payne, K. A. P.; Marshall, S. A.; Fisher, K.; Rigby, S. E. J.; Cliff, M. J.; Spiess, R.; Cannas, D. M.; Larrosa, I.; Hay, S.; Leys, D. Structure and Mechanism of *Pseudomonas aeruginosa* PA0254/HudA, a prFMN-Dependent Pyrrole-2-carboxylic Acid Decarboxylase Linked to Virulence. *ACS Catal.* **2021**, *11* (5), 2865−2878.
(191) Datar, P. M.; Marsh, E. N. G. Decarboxylation of Aromatic Carboxylic Acids by the Prenylated-FMN-dependent Enzyme Phenazine-1-carboxylic Acid Decarboxylase. *ACS Catal.* **2021**, *11* (18), 11723−11732.
(192) Christianson, D. W.; Lipscomb, W. N. Carboxypeptidase A. *Acc. Chem. Res.* **1989**, *22* (2), 62−69.
(193) Lee, M. F.; Poh, C. L. Strategies to Improve the Physicochemical Properties of Peptide-Based Drugs. *Pharm. Res.* **2023**, *40* (3), 617−632.
(194) Hetrick, K. J.; Walker, M. C.; van der Donk, W. A. Development and Application of Yeast and Phage Display of Diverse Lanthipeptides. *ACS Cent. Sci.* **2018**, *4* (4), 458−467.
(195) Urban, J. H.; Moosmeier, M. A.; Aumüller, T.; Thein, M.; Bosma, T.; Rink, R.; Groth, K.; Zulley, M.; Siegers, K.; Tissot, K.; Moll, G. N.; Prassler, J. Phage Display and Selection of Lanthipeptides on the Carboxy-terminus of the Gene-3 minor Coat Protein. *Nat. Commun.* **2017**, *8* (1), 1500.

https://doi.org/10.1021/jacsau.4c00425
JACS Au 2024, 4, 2715−2745